uOttawa

L'Université canadienne
Canada's university

**FACULTÉ DES ÉTUDES SUPÉRIEURES ET POSTOCTORALES**

uOttawa

L'Université canadienne
Canada's university

**FACULTY OF GRADUATE AND POSDOCTORAL STUDIES**

Sandra Ferreira
AUTEUR DE LA THÈSE / AUTHOR OF THESIS

M.Sc. (Chemistry)
GRADE / DEGREE

Department of Chemistry
FACULTÉ, ÉCOLE, DÉPARTEMENT / FACULTY, SCHOOL, DEPARTMENT

Improving the Rational Design of Antifreeze Glycoproteins Through Identification of the Parameters that Influence Ice Recrystallization Inhibition

TITRE DE LA THÈSE / TITLE OF THESIS

Robert Ben
DIRECTEUR (DIRECTRICE) DE LA THÈSE / THESIS SUPERVISOR

CO-DIRECTEUR (CO-DIRECTRICE) DE LA THÈSE / THESIS CO-SUPERVISOR

EXAMINATEURS (EXAMINATRICES) DE LA THÈSE / THESIS EXAMINERS

Keith Fagnou

Tony Durst

Gary W. Slater
Le Doyen de la Faculté des études supérieures et postdoctorales / Dean of the Faculty of Graduate and Postdoctoral Studies

# Improving the Rational Design of Antifreeze Glycoproteins Through Identification of the Parameters that Influence Ice Recrystallization Inhibition

Sandra S. Ferreira

Thesis submitted to the
Faculty of Graduate and Postdoctoral Studies
University of Ottawa
In partial fulfilment of the requirements for the degree of

Masters in Chemistry

Ottawa-Carleton Chemistry Institute
University of Ottawa
Ottawa, Ontario
Canada

*Your file Votre référence*
*ISBN:* 978-0-494-61204-0
*Our file Notre référence*
*ISBN:* 978-0-494-61204-0

# *Abstract*

Antifreeze glycoproteins (AFGPs) are a subclass of biological antifreezes isolated from Antarctic and Atlantic Teleost fish. These compounds have the ability to depress the freezing points of solutions as well inhibit ice crystal growth, thereby protecting fish from cryoinjury and death. Although native AFGPs have considerable promise as cryoprotectants, their limited bioavailability, cytotoxicity, biological instability and lengthy chemical syntheses have precluded their widespread use. Consequently, Ben et al. have designed non-cytotoxic stable C-linked AFGPs with comparable ice recrystalization inhibition (RI) to that of the natural compounds. This work also revealed that amongst glycopeptides with the same amino acid backbone, the overall recrystalization inhibition activity correlates to the hydration of the carbohydrate moiety. This interesting relationship lead to question if whether the hydration values of carbohydrates could be used to predict the activity of synthetic antifreeze glycoproteins. If true, it would greatly improve the rational design of synthetic analogues. Therefore the relationship between hydration and ice recrystalization inhibition was studied using small molecule carbohydrates. These results were also compared to the current standard in cryoprotection of tissues and cells, dimethyl sulfoxide, and C-linked carbohydrate derivatives. The study elucidates that there is a more accurate parameter then hydration to predict the ice recrystalization inhibition of carbohydrates, and it was defined as the *Hydration Index*.

Furthermore, the investigation of carbohydrates with respect to RI was extended to the disaccharide present in the native antifreeze glycoproteins, D-galactose-β(1-3)-N-acetyl-

galactosamine. Its vital importance in AFGPs is apparent as no synthetic AFGP (syAFGP) with a carbohydrate other then that found in the native disaccharide has been able to surpass the activity of the natural compounds. Yet the intrinsic properties of the disaccharide, separated from the peptide, have never been studied in terms of RI activity. Therefore, the synthesis of the native disaccharide and analysis of its RI activity would help to determine how much of a factor it is for the overall activity of the natural AFGP. This work also creates the opportunity to study how other aspects of D-galactose-β(1-3)-N-acetyl-galactosamine effects ice recrystalization inhibition, such as the C2 N-acetyl moiety and the regiochemistry of the glycosidic linkage.

Another key component in improving the rational design of syAFGPs as cryoprotectants is to distinguish between the structural motifs necessary for ice recrystalization inhibition and thermal hysteresis. In 2004, Nishimura et al. published such work on the essential components of AFGPs for thermal hysteresis. They reported that even small changes to the native AFGPs can cause a loss of thermal hysteresis, for example exchanging the naturally occurring threonine residues for serine. Unfortunately, they did not test any of their compounds for recrystallization inhibition. Opportunely, the synthesis towards an antifreeze glycoprotein which contains serine residues in place of threonine residues is presented, with the future goal of testing for its RI activity.

The overall objective of this dissertation is to probe the characteristics that dictate antifreeze glycoprotein activity in terms of ice recrystalization inhibition, with the goal of providing useful information towards the rational design of potent non-toxic cryoprotectants.

## *Acknowledgments*

I would like to start off by offering my gratitude to Professor Robert Ben for all the help, support and guidance that he has given me to write this paper. I would especially like to thank you for your encouragement and feedback on my work along the way.

I would like to thank all the people from the Ben Lab. Wendy and Gloria for the days we spend studying, laughing and helping each other. Jenn, I could not have asked for a better bench mate. Mathieu and John, for being pillars of knowledge and kindness. Taline, Jackie, Chantelle, Taz, and Mike, for always being the positive, funny and amazing people you are. Finally to Roger and Pawel, for being there for me whenever I needed it, thank you.

A special thanks to my family and friends in Vancouver, who have made me into the person I am. To the Melos, thank you for all the pictures and emails you send me, it helps me not feel so far away, I miss you. Erminia, for the gift of making everything better. To Marlene who never forgets her long distance sister, and always calls, I love you. Tina, my doll, you are always with me, you're my heart. To my parents, dad for your constant support and trust, and mom for teaching me how to be strong and determined, I love you, and would not be where I am today without you.

*Thank You !*

# *Table of Contents*

# *List of Figures*

## *CHAPTER 1*

## *CHAPTER 2*



## *CHAPTER 3*

# *List of Schemes*

## *CHAPTER 3*

# *List of Abbreviations*

| | |
|---|---|
| Ac | Acetyl |
| AFP | Antifreeze protein |
| AFGP | Antifreeze glycoprotein |
| Ala | Alanine |
| br | Broad |
| Bn | Benzyl |
| Bz | Benzoyl |
| °C | Degrees Celcius |
| $CH_2Cl_2$ | Dichloromethane |
| cm | Centimeter |
| d | Doublet |
| dd | Doublet of doublets |
| DIPEA | Diisopropylethylamine |
| DIS | Dynamic Ice-Shaping |
| DMF | *N,N*-dimethylformamide |
| DMAP | 4-dimethylamino pyridine |
| DMSO | Dimethylsulfoxide |
| dt | Doublet of triplets |
| eq | Equivalents |
| ESI | Electrospary ionization |
| Et | Ethyl |

| | |
|---|---|
| EtOAc | Ethyl acetate |
| $Et_2O$ | Diethyl ether |
| Fmoc | 9-Fluorenylmethoxycarbonyl |
| Gal | Galactose |
| GalNAc | N-acetyl-galactosamine |
| Glc | Glucose |
| Gly | Glycine |
| h | Hour |
| HI | Hydration index |
| Hz | Hertz |
| IR | Infrared |
| Lys | Lysine |
| m | multiplet |
| M+ | marent molecular ion |
| Man | Mannose |
| Me | Methyl |
| MeCN | Acetonitrile |
| MeOH | Methanol |
| MGS | Mean grain size |
| mL | Milliliters |
| MLGS | Mean largest grain size |
| MS | Molecular sieves |
| NaOMe | Sodium methoxide |
| NMR | Nuclear magnetic resonance |

| | |
|---|---|
| P | page |
| PBS | Phosphate buffered saline |
| Ph | Phenyl |
| Piv | Pivaloyl |
| PMC | Partial molar compressibility |
| pmm | Parts per million |
| PMV | Partial molar volume |
| Pro | Proline |
| q | Quartet |
| RI | Recrystallization inhibition |
| s | Singlet |
| SAR | Structure activity relationship |
| SEM | Standard error of mean |
| SPS | Solid phase synthesis |
| SPPS | Solid phase peptide synthesis |
| syAFGP | Synthetic antifreeze glycoprotein analogue |
| t | Triplet |
| TFA | Trifluoroacetic acid |
| TH | Thermal hysteresis |
| THF | Tetrahydrofuran |
| Thr | Threonine |
| TMS-OTf | Trimethylsilyltrifluoromethane sulphonate |
| $\delta$ | Chemical shift (in ppm) |
| v | Frequency (in $cm^{-1}$) |

# *CHAPTER 1*

## *Introduction to Biological Antifreezes*

### 1.1 Discovery of Biological

During winter months the oceans of the polar regions of the world, as well as near shore sub-arctic waters can reach temperatures as low as -1.9 °C, which is the freezing point of seawater. [1] Yet the typical freezing point of the blood serum of a marine Teleost fish is only -0.8 °C. This difference in temperature is enough to cause these fish to freeze, and subsequently die. [1] Therefore it was necessary for fish that inhabit these colder waters to evolve defensive mechanisms for survival.

DeVries and co-workers set out to discover what exactly protected these fish from freezing. In 1965, during the winter months they traveled to McMurdo Sound, Antarctica


**Figure 1.1** Map of Antarctica

(Figure 1.1), and collected three types of Antarctic toleost fish; *Trematomus borchgrevinki*, *Trematomus bernacchii* and *Trematomus hansoni*. [2] Immediately after catching the fish their blood serum was isolated and analysed, for the freezing point, and the concentrations of chloride ions, non-protein nitrogen content, free amino acids, urea, trichloroacetic acid (TCA) soluble proteins and total carbohydrate content. They found that the freezing point of the blood serum ranged from -1.87 ± 0.008 °C to -2.07 ± 0.008 °C, and that the freezing point depression due to the colligative properties of NaCl only accounted for 39-46 % of this activity.[2]

Further investigation of the blood serum fraction containing soluble TCA proteins, determined that the freezing point of this fraction alone was within 0.05 °C of that of the entire serum. Following extensive purification using Sephadex G-200 column chromatography and ion exchange chromatography the active compounds were identified as glycoproteins. In *Trematomus borchgrevinki*, this purified fraction of glycoproteins was responsible for over 30 percent of the freezing point depression. Also, to prove that the activity did not come from impurities within the fraction, they monitored the freezing point while degrading the protein with the enzyme Pronase. These experiments showed a gradual loss of activity over time, until complete abrogation of activity was observed to coincide with complete inactivation of the protein, thus demonstrating that the innate nature of the protein is necessary for its activity.

### 1.2 Purification and Chemical Properties of Antifreeze Glycoproteins

DeVries *et.* al began the purification process on *Trematomus borchgrevinki* serum with dialysis and diethylaminoethyl-cellulose chromatography. [3] This permitted separation into 5

different fractions of proteins (Figure 1.2A Fraction numbers 1-5). [3] Knowing that the active proteins were glycosidated they tested the fractions for carbohydrates (using α-napthanol and concentrated $H_2SO_4$), and found that only fractions 1-4 tested positively. These fractions were

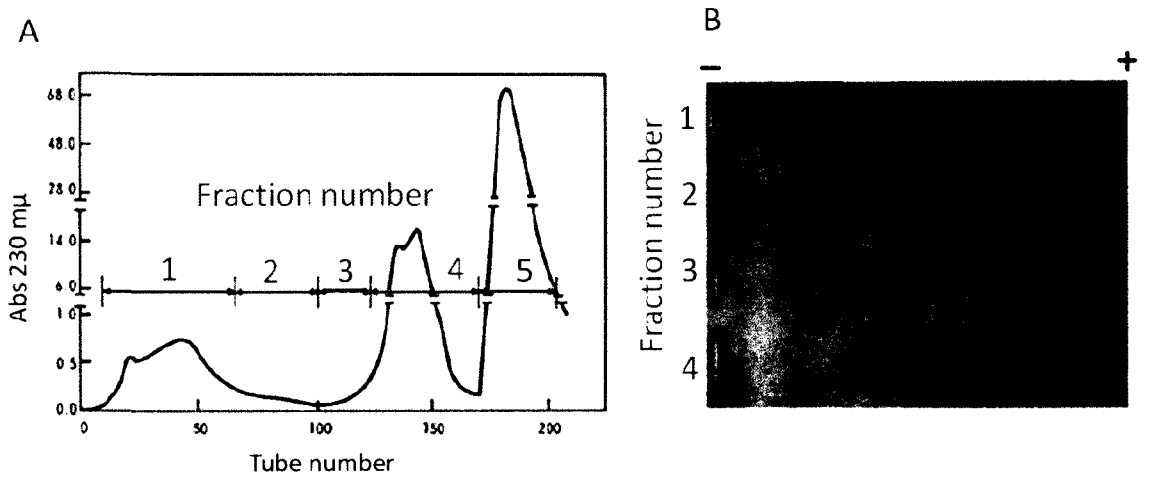


**Figure 1.2** A) Purification of Freezing point depressive glycoproteins using Diethylaminoethyl-cellulose column B) Acrylamide gel electrophoresis of glycoproteins isolated from diethylaminoethyl -cellulose column. [3]

subjected to acylamide gel electrophoresis which caused further separation, identifying 8 different glycoproteins (Figure 1.2B). [3] Consequently they were named AFGPs 1-8, nomeclature which is still used to date to refer to each group of antifreeze glycoproteins (AFGPs).

Over the next several years their structures were identified as glycoproteins containing three amino acid repeats, $H_2N$[Alanine- Alanine (β-galactosyl (1→3) α-N-acetylgalactosamine) Threonine]n Alanine- Alanine-COOH (Figure 1.3).[3],[4],[5],[6],[7],[8] The AFGPs 1-8 vary mostly in their molecular weight determined simply by the number of the repeating tripeptide units. For instance, where n represents the tripeptide unit, AFGPs 1-5 contain n= 55-17, and the smaller

AFGP 6-8 have n= 12, 6 and 4 respectively. An exception is in the lower molecular weight AFGPs 6-8, where these polymers can incorporate proline residues in place of alanine amino acids. The amount of incorporation is highly heterogeneous, for example, AFGP 8 (14 amino acids) of Arctic cod *Boreogadus saida*, incorporates proline at the 4th and the 10th position, while AFGP 8 of the Antarctic *Trematomus borchgrevinki*, incorporates them at positions 7th, 10th, and 13th.[6] Another variation, which occurs only in Arctic fish, is that threonine may be replaced by an arginine, leading to the loss of a carbohydrate unit (Figure 1.3). [9] However,

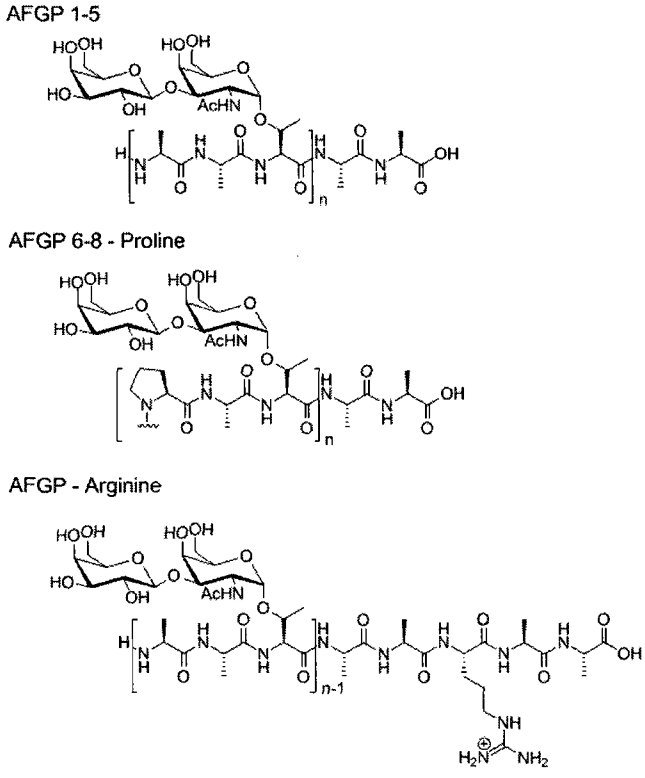


**Figure 1.3** Polymer of AFGP 1-5, AFGP 6-8 –Proline, and AFGP-Arginine

these changes in primary sequence occur in less than 5 % of all naturally occurring AFGPs and modifications to the carbohydrate moiety occur even less often. An example of these

modifications is the atypical type 1 AFGP from *Pleuragramma antarcticum* which contains N-Acetylglucosamine as the carbohydrate unit, and amino acids such as glycine, aspartic acid, and glutamic acid. [10]

### 1.3 Antifreeze Proteins

Antifreeze proteins (AFP), which lack a carbohydrate moiety, have not only been isolated from Teleost fish, but also from plants, insects, bacteria and fungi. [11], [12], [13] These life forms are exposed to much more extreme weather conditions than the Teleost infraclass as temperatures on land can reach far below the freezing point of the ocean (-2 °C). Therefore it is not surprising that AFP found in insects have shown freezing point depressions 3-4 times greater than the AF(G)Ps found in fish. [11] Their structural diversity also far exceeds that of antifreeze glycoproteins.

The antifreeze proteins are classified into four different groups, Type I-IV AFPs. Type I

| Characteristic | AFGP | Type I AFP | Type II AFP | Type III AFP | Type IV AFP |
|---|---|---|---|---|---|
| Mass (Da) | 2600 – 33000 | 3300 – 4500 | 11000 – 24000 | 6500 | 12000 |
| Key Properties | AAT repeat; disaccharide | Alanine-rich α-helix | Disulfide bonded | β-sandwich | Alanine rich; helical bundle |
| Representative Structure | 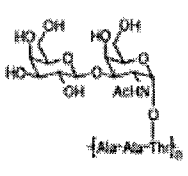 |  |  |  |  |
| Natural Source | Antarctic notothenioids; northern cods | Right-eyed flounders; sculpins | Sea raven; smelt; herring | Ocean pout; wolfish; eel pout | Longhorn sculpin |

**Figure 1.4** Antifreeze Proteins [9]

AFPs (Figure 1.4), are found in winter flounders, and sculpins. [14], [15] They are among the most studied of the AFPs due to their relatively small size of only 37 residues. [16] They are alanine rich (~65%) proteins, which have a predominately α-helix secondary structure. [17], [18] Type II AFPs are much larger then Type I AFPs; they are globular proteins with 130-150 amino acid residues containing five disulfide bonds. [16] Typically found in Atlantic herring, rainbow smelt and sea raven, they evolved from preexisting lectin proteins, and are homologous to the carbohydrate binding domains of these proteins. [19] Also, the Type II AFP from smelt and herring are $Ca^{2+}$ dependant and require it for their activity. [19], [16] Type III AFPs, are smaller than Type II AFPs, with 62-66 amino acid sequence, and are typically found in ocean pout, wolfish and eel pout. [20] They are compact, highly-organized, proteins that contain 9 short β-strands and several turns. [21] The strands make up two triple stranded sheets that are anti-parallel to each other and form a β sandwich. [22] Finally, Type IV AFPs are found in longhorn sculpins, and possess a high concentration of glutamine in comparison to the other types of AFP. They contain a high helical content, but unlike the Type I AFP, they are arranged in a four helix bundle. [23] All fish antifreezes fall into one of these categories, terrestrial AFPs (from winter rye, spruce budworm and the mealworm beetle) however, have evolved independently and so are classified separately. [24], [11], [25]

It is clear that many different antifreeze proteins and glycoproteins have been structurally identified. However there were simultaneous advances in elucidating their physical properties, including the assessment of antifreeze activity and their interactions with water and ice have also been made. It is known that both the antifreeze glycoproteins and proteins have

the same basic properties, yet the modes of these compounds have shown to include several differences.

## 1.4 Physical Properties of Antifreeze Glycoproteins

Once the antifreeze glycoproteins were isolated in the 1970's, scientists immediately began to probe their ability to depress the freezing point of water. They discovered that the freezing point of AFGPs from *Trematomus borchgrevinki* were up to ~ 500 times greater than would be expected colligatively. [26] However they only produced conventional colligative melting points. This difference between the equilibrium melting point due to colligative effects and the antifreeze influenced freezing point was termed the hysteretic gap. [27]

### 1.4.1 Dynamic Ice Shaping and Thermal Hysteresis

The behaviour of ice in the presence of biological antifreezes is very uncharacteristic. For example a seeded ice crystal does not grow within the hysteretic gap. This was demonstrated using the blood serum of T. *borchgrevinki*, where after 24 hours at -2.0 °C in the presence of an ice crystal seed, no ice growth was observed. [27] This falsified the hypothesis that antifreeze glycoproteins simply worked by slowing down ice crystal growth. Furthermore, when the temperature of the solution reached the thermal hysteretic freezing point, a seeded ice crystal grows very rapidly in a needle shape (Figure 1.5). [28], [29]

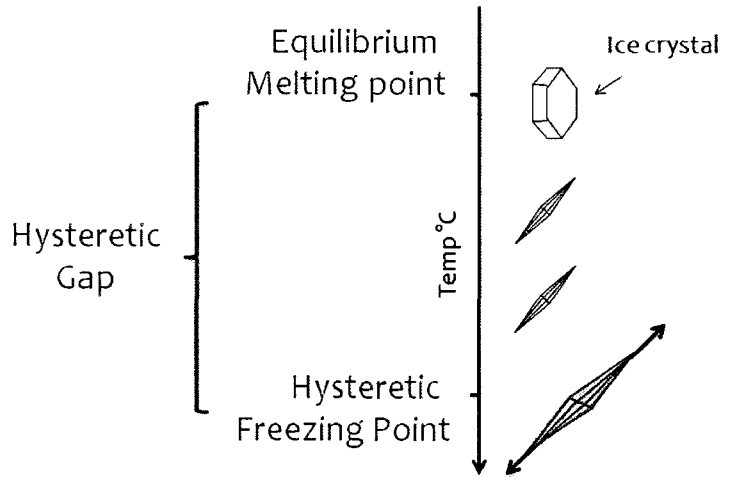


**Figure 1.5** Illustration of ice crystal behaviour within a solution containing AFGP [30]

Raymond and DeVries knew from previous studies of ice that changes in ice crystal morphology (or "habit") could be induced by adsorbents on the ice surface. [31] More specifically the adsorbents could retard crystal growth on the faces of the ice to which they absorb. In addition other experiments identified that ice growth in the presence of antifreeze glycoproteins occurs on the c-axis or the basal plane of the ice crystal. This is contrary to normal ice growth, which is perpendicular to the c-axis. This suggests that the antifreeze glycoproteins bind selectively to the a-axis of the ice crystal and forces it to grow on the basal planes, causing the observed dynamic ice shaping. [31]

Antifreeze binding to the surface of the ice crystal also affects the overall thermodynamics of ice growth. [31] As the AFGPs bind at intervals along the a-axis, growth along this face will be forced to grow between the adsorbed molecules, creating a convex curvature (Figure 1.6). This increases the surface area of the edge of the ice crystal containing

high-energy water molecules and causes a pressure build up between the two phases (ice and water). [30]

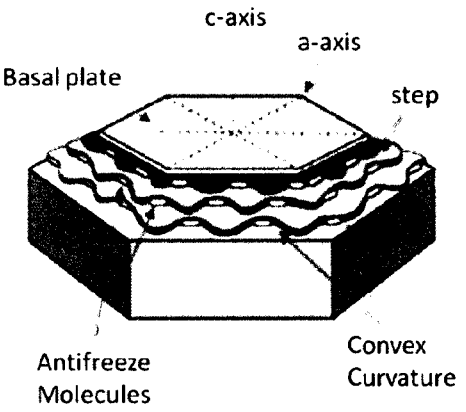


**Figure 1.6** Antifreeze glycoproteins bind to non-basal planes of ice [31]

Since a seeded ice crystal neither grows nor melts within the thermal hysteretic gap, the ice crystal must be in vapor pressure equilibrium with the solution. [30] The Kelvin-effect explains how vapor pressure changes occur at concave and convex surfaces. Specifically, a convex surface would increase the pressure beneath the surface, and increase the free energy of that phase, consequently the vapor pressure of the ice would increase. Since the ice phase is incompressible the change in vapor pressure would equal the $\Delta G_v$ (Equation 1). In other words increasing the convex curvature of ice, also increase its Gibbs free energy. This change in Gibbs free energy could then account for the observed difference between the melting point and the equilibrium freezing point. [30]

$$\Delta G_v = \frac{\Delta H \Delta T}{T_m}$$

Equation 1

$$\Delta P = \frac{2\sigma}{r}$$

Equation 2

$$\Delta G_v = \Delta P = \frac{2\sigma}{r} = \frac{\Delta H \Delta T}{T_m}$$

Equation 1 = Equation 2

$$r^* = \frac{2\sigma T_m}{\Delta H \Delta T}$$

Equation 3

**Equations 1-3** $\Delta G_v$ is the free energy per $cm^3$, $\Delta T$ is the degree of super cooling (K), $\Delta H$ is the heat of fusion of water, $T_m$ is the melting point of water (K), $\Delta P$ is the pressure difference that exists across a curved surface with radius r, $\sigma$ is the interfacial tension [30]

When the Gibbs free energy is equal to the vapor pressure of the ice, then equations 1 and 2 can be combined to give equation 3. This equation demonstrates the relationship between the radius curvature of ice and the degree of super cooling $\Delta T$. For example if there is an increasing $\Delta T$ then addition to the ice surface will cause a decreased $r$ (radius of curvature), and a decreasing $\Delta T$ will cause an increased $r$. But at a constant $\Delta T$ the localized curvature should have all the same radii along the entire surface of the ice (Figure 1.7). Therefore the ice crystals are able to adapt to different temperatures by changing radii of curvature between

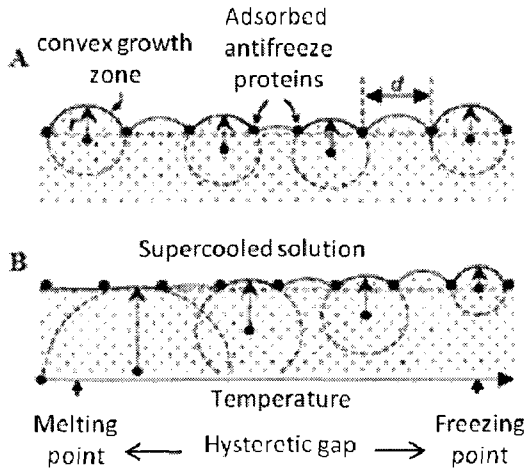


**Figure 1.7** Illustration of radius curvature between bound AF(G)Ps (A) At a constant temperature within the hysteretic gap the r should be equal across the surface of the ice crystal (B) The curvature of radius will change depending on the temperature of the system [30]

bound antifreeze molecules. The freezing point of the solution is reached when adding to the ice increasing the radius curvature instead of decreasing it. At this point the solution vapor pressure is lowered upon adding to the ice lattice and the ice will grow very rapidly.

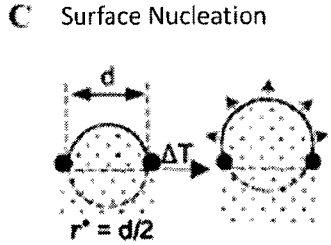


**Figure 1.8** Hysteretic Freezing point of the solution is reached when adding to the ice increases the radius of curvature [30]

This explanation of thermal hysteretic activity is known as the adsorption inhibition mechanism, and as its name implies works by inhibiting the growth of ice by adsorbing to specific surfaces. [32], [31] This theory assumes that the AFGP binding must occur irreversibly.

Supporters of irreversible binding theory believe that the AFGPs are hydrogen bonded to the ice surface and that the probability of all the hydrogen bonds disconnecting simultaneously is very low. [33] However, if it is true that AFGPs are permanently bound to ice then there should not be any AFGPs left in the solution phase, which is contradictory to what has been observed. [31], [34] Also, if the AFGPs were to irreversibly bind, then during melting the formation of concave melting curves will occur on the surface of the ice. If the same logic is applied to this opposite curvature then there should be localized superheating at these points, thereby increasing the melting temperature. However, the ice melts at the expected colligative temperatures suggesting that the AFGPs are no longer bound once the temperature of the system reaches the melting point. [2], [35] This amongst other arguments, suggests that there may be a dynamic relationship between the surface of the ice crystal and the AFGP molecules. [36], [37], [38] Others hypothesize a combination between a dynamic system at the melting point, but an irreversible system below the melting point. [39], [40]

### 1.4.2 Factors that Influence Ice Binding

It is well known that water dictates a large portion of proteins structure and function. [41] Bulk water molecules are dynamic and can adapt to form ideal interactions around antifreeze proteins to minimize potential energies using van der Waals, electrostatic and hydrogen bonding terms. [42] Ice is "rigid" and therefore is less likely to provide optimized interactions, especially the potential hydrogen bonds which require specific geometry. [42] Therefore, in terms of van der Waals, electrostatic and hydrogen bonding, the bulk water molecules

minimize the potential energy of antifreeze proteins better then ice does. This suggests that the preferred state of the glycoproteins should then be within bulk water rather than bound to ice, which is contrary to what is known. This leaves hydrophobic energy as the likely driving force towards AFP ice binding. [42] This is proposed to function via an entropically driven mechanism where water molecules form hydrogen bonded cages around hydrophobic groups of antifreeze proteins. This decreases the contact of the hydrophobic groups with the bulk water molecules. Then upon ice association these cages are released in an entropically favored process driving the interaction.

Further probing the interaction of water with antifreeze proteins Gallagher and Sharp studied the first hydration shell of AFPs. [41] The hydration shell being defined as of the network of tightly associated water molecules around the protein. They report that there are significant differences in hydration between the ice binding and the non-ice binding surfaces of antifreeze proteins. Specifically, the hydration of the ice binding surfaces is more uniform and is very hydrophobic. They state that first hydration shell of this surface is very similar to the surface of ice, and that this quality is imperative for ice recognition and the preference of ice association over water. [41], [43], [44] Nutt and Smith propose that as the protein approaches the ice crystal the ice-like water at the protein-water interface and the semi-ordered water of the ice-water interface overlap (Figure 1.9b). [45] Then localized ice growth incorporates the ice binding face of the antifreeze protein (Figure 1.9c). The rest of the protein is surrounded by more disrupted water molecules that protect it from being overgrown in turn.

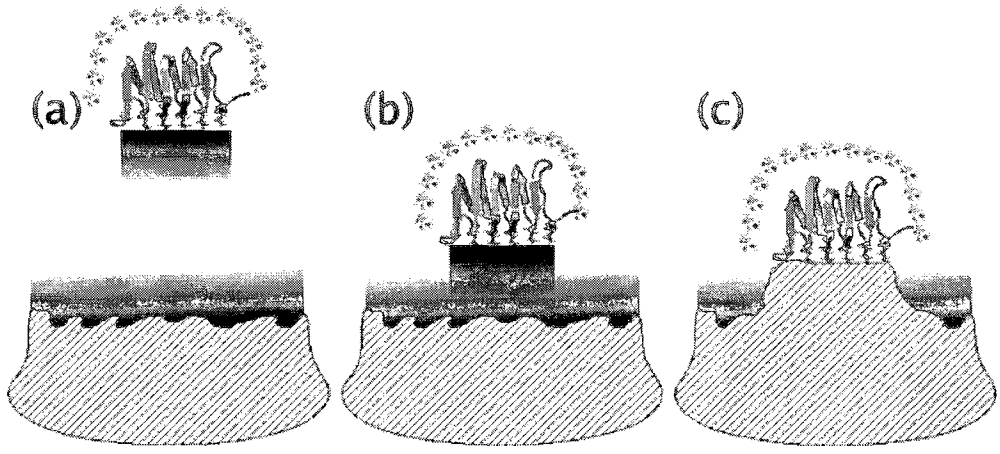


**Figure 1.9** Schematic of proposed ice-binding mechanism by Nutt and Smith [45]

This work demonstrates that the relationship between antifreeze proteins and water is equally important as the relationship between the proteins and ice. Since, in order to achieve ice binding there must first be a driving force to favour association with the ice crystal over solvation in the bulk water phase.

### 1.4.3 Ice Recrystalization Inhibition

The second property of antifreeze glycoproteins is ice recrystalization inhibition (RI). [26] This is the ability of AFGPs to stop the natural conversion to a few large ice crystals at the expense of many small ice crystals, if the solution is held at a constant temperature below the freezing point. As demonstrated in Figure 1.10A, when a sucrose solution is flash frozen (t = 0 min) the initial crystal size is relatively small. [46] Yet, when kept at a constant temperature (-6 °C) over a period of 30 min, the crystal size visibly increases. This process is argued to occur in two ways. The first mechanism is Oswalt ripening where larger crystals grow at the expensive of smaller crystals via a diffusion of water molecules from one crystal to the next. [46] The second

is by agglomeration, which occurs when the boundaries between contacting crystals collapse to form larger crystals. Either way, they are both thermodynamically driven in order to reduce the interfacial energy of the system. [46] Figure 1.10B demonstrates how when a solution containing AFGP 8 is flash frozen and kept at a constant temperature (-6 °C), after 30 min of annealing time the crystal size remains small relative to the negative PBS control (right side of 1.9B, same magnification).

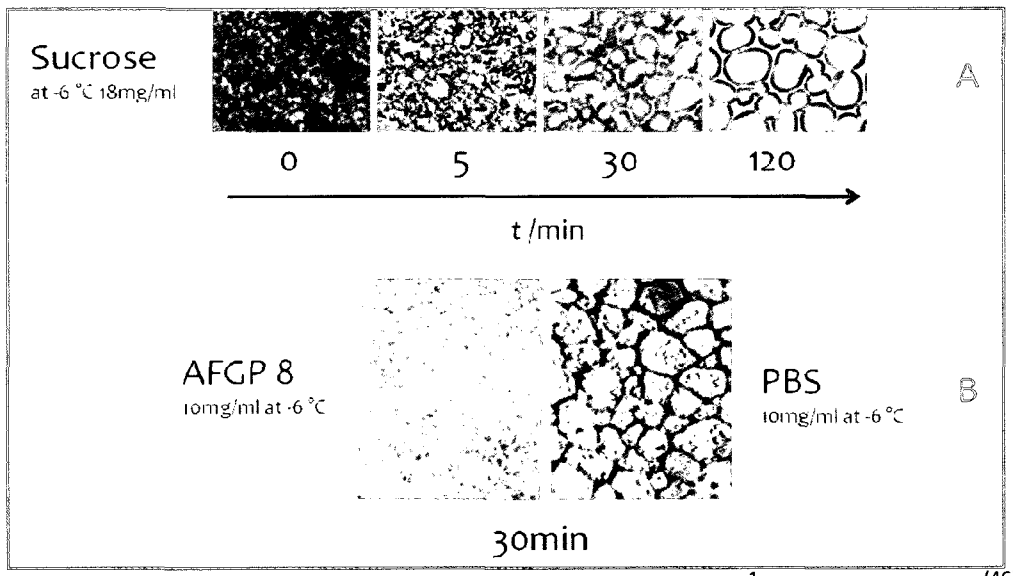


**Figure 1.10** (A) Recrystalization of ice within an 18 $mgmL^{-1}$ sucrose solution [46] (B) Recrystalization inhibition of ice with a positive control (10 $mgmL^{-1}$ AFGP8) and negative control (10 $mgmL^{-1}$ phosphate buffered solution)

Antifreeze glycoproteins can inhibit the growth of ice by decreasing diffusion and by changing the interfacial energy properties, and both of these mechanisms are significant during flash freezing, or splat cooling to -80 °C. [20] This is because during this type of freezing the ice grains exclude the majority of the impurities to the boundaries between the ice crystals. [47]

Therefore even when dilute solutions containing antifreeze glycoproteins are splat cooled, they will contain high concentrations of AFGPs in the ice grain boundaries. These higher boundary concentrations make it easy to understand how large molecules such as glycoproteins can inhibit diffusion of water molecules, or decrease the contact between adjacent ice crystals. But this method of splat cooling is not designed to determine if the antifreeze compounds are also functioning by binding to the surface of the ice crystal. Also because AFGPs bind to ice in a specific orientation, the splat cooling method might or might not allow enough time for these compounds to bind to ice. Therefore, the additions of salts are used to widen the ice grain boundary and to give these compounds more mobility so that they can orient properly to facilitate adsorption. [46] This should therefore provide conditions to maximize activity of these compounds if the binding is partially responsible for RI activity. But further studies that probe the modes of action of the AFGPs are needed in order to fully understand how they function as recrystallization inhibitors.

### 1.5 Carbohydrates as Cryoprotectants

There are other complex cryoprotection systems present in nature to fulfill requirements unsatisfied by either antifreeze proteins or glycoproteins. These cyroprotectants work under completely different modes of action. For example, freeze tolerant frogs, can endure the conversion of 50 % or more of their total body water into extracellular ice, then thaw and revive. [48] When extracellular ice begins to form, the osmolality of the system changes, and there is a drastic efflux of intercellular water to compensate for the loss of

extracellular water. This causes desiccation of the cells and has lethal consequences, such as stress to cell membranes and increasing intracellular ion concentrations. [48] Eventually the frogs' cells will reach their freezing point, which will halt vital functions such as breathing, smooth muscle movement and heart beat. Even if the organism survives these effects, upon thawing the rapid reintroduction of oxygen can produce a burst of free radicals, which can further damage the cells. [48] Consequently, the frogs have evolved a remarkable system to be able to protect themselves from osmotic shock and cell damage. As a part of their complex protection system they recruit simple carbohydrates.

Winter frogs and spring frogs use glucose, while the chorus frog will produce glucose as well as trehalose as cryoprotectants. [49], [50], [51] These frogs are able to store glucose in the form of glycogen in their livers. Once the temperature surrounding the frog falls below its freezing point and an ice nucleation event occurs, the frog will begin to freeze over a period of several hours. Meanwhile glucose pours out of the liver, and is transported via the blood to all the major organs, functioning to limit cell desiccation through colligative properties. Upon thawing, the glucose is returned to the liver to restore the glycogen stock. [48] Trehalose functions differently then glucose: it interacts directly with the polar head group of the cell membrane to support the lipid bilayer during extreme temperatures. Therefore it is not surprising that chorus frogs upregulate trehalose during the winter months. [48] Both of these carbohydrates are very small molecules in comparison the AF(G)Ps seen in the previous sections; nevertheless they still have a large impact on the protection of these frogs. This further demonstrates the diversity that nature has evolved to help cryoprotect all different forms of life. It also suggests

the possibility of small carbohydrates being used as cryoprotectants for human cells and tissues.

### 1.6 Application of AF(G)Ps

Antifreeze glycoproteins and antifreeze proteins have unique properties that have been explored for medical, commercial, and industrial applications. Cryosurgery is one of the many research areas that have looked at the potential of AFPs. During routine cryosurgery, a cryogenic probe is brought into contact with undesired tissue and held -20 °C, for several minutes. This procedure needs to be repeated several times, to ensure that the tissues not in direct contact with the probe will also undergo apoptosis upon thawing. [52] The sharp spicule formation caused by freezing AFP solutions, combined with cancer cells promiscuous uptake habits has been shown to aid in the destruction of tumour cells, during cryosurgery. [52] Also, AFPs have shown to be excellent inhibitors of recrystallization, which is important during the cryopreservation of cells. This is because even if cells can withstand the cooling process, they acquire lethal damage by ice crystal growth during warming. [53] Initial studies demonstrated how AFPs from winter flounder decrease the amount of extracellular ice formed during prolonged time periods, below the freezing point of red blood cells. Later, scientists assessed that AFP I-III decreased the amount of hemolysis of red blood cells by ~30 % after the cells were frozen and warmed. [54] Also, AFGPs 1-8 have been shown to improve cell viability during the cryopreservation of pig oocytes, and liposomes. [9] However, these are only a few of the many examples of the research exploring the different AF(G)Ps cryopreservation abilities on several

cell lines. Despite these reports, the current method of cryoprotection of cells and tissues for bone marrow and organ transplantation is still dimethyl sulfoxide (DMSO), even though it has been found to be highly cytotoxic. [55] Recent studies by Faber et al. further demonstrated that DMSO causes widespread apoptosis to the central nervous system in mice at concentrations as low as 0.3 $mLkg^{-1}$. [55] It is speculated that children who undergo bone marrow transplantations, who are thus routinely exposed to DMSO concentrations greater then 0.3 $mLkg^{-1}$ might be undergoing similar neuronal damage. [55] This adds to the urgency of developing improved and less toxic cryoprotectants, which in turn requires a better understanding of the properties that dictate cryoprotectant activity. This leads to the basic goal of this dissertation, which is to probe the characteristics that dictate antifreeze glycoprotein activity in terms of ice recrystalization inhibition, and use the information to rationally design potent non-toxic cryoprotectants.

## 1.7 References


1. DeVries, A. L., *Annual Review of Physiology*, **1983**, *45*, 245
2. DeVries, A. L.; Wohlschlag, D. E., *Science,* **1969**, *163*,1073.
3. DeVries, A.L.; Komatsu, S.K.; Feeney, R. E., *The Journal of Biological Chemistry,* **1970**, *245*, 2901.
4. DeVries ,A. L.; Vandenheede, J.; Feeney, R. E., *The Journal of Biological Chemistry*, **1971**, *246*, 305.
5. Komatsu, S. K.; DeVries, A. L.; Feeney, R. E,. *The Journal of Biological Chemistry,* **1970**, *245*, 2909.
6. Osuga, D. T.; Feeney, R. E., *The Journal of Biological Chemistry,* **1978**, *253*, 5338.
7. Vanderheed, J.; Ahmed, A. I.; Feeney, R. E., *The Journal of Biological Chemistry*, **1972**, *247*, 7885.
8. Feeney, R. E.; Burcham, T. S., *Annual Review of Biophysics and Biomolecular Chemistry,* **1986**, *15*, 59.
9. Harding, M. M.; Anderberg, P. I.; Haymet, A. D. J., *The journal of European Chemsitry,* **2003**, *270*, 1381.
10. Wohrmann, A. P. A.; Hagen, W.; Kunzmann, A., *Marine Biology Progress Series*, **1997**, *151*, 205.
11. Graether, S. P.; Kuiper, M. J.; Gagne, S. M.; Walker, V. K.; Jia, Z.; Skyes, B. D.; Davies, P. L., *Nature*, **2000**, *406*, 325.
12. Griffith, M.; Ala, P.; Yang, D. S. C.; Hon, W.; Moffatt, B. A., *Plant Pysiology,* **1992**, *100*, 593.
13. Duman, J. G.; Olsen, T. M., *Cryobiology*, **1993**, *30*, 322.
14. Duman, J. G.; DeVries A. L., *Nature,* **1974**, *247*, 237.

15. Kwan, A. H.; Fairley, K.; Anderberg, P. I.; Liew, C. W., Harding, M. M., Mackay, J. P., *Biochemistry*, **2005**, *44*, 1980.

16. Ewart, K. V.; Lin, Q.; Hew, C. L., *Cell and Molecular Life Sicence,* **1999,** *55*, 271.

17. Ananthanarayanan, V. S.; Hew, C. L., *Biochemical and Biophysical Research Communications*, **1977,** *74*, 685.

18. Raymond, J. A.; Radding, W.; DeVries, A. L., *Biopolymers*, **1977**, *16*, 2575.

19. Ewart, K. V.; Rubinsky, B.; Fletcher, G. L., *Biochemical and Biophysical Research and Communications*, **1992**, *185*, 335.

20. Yeh, Y.; Feeney, R. E., *Chemical Reviews,* **1996**, *96*, 601.

21. Sonnichsen, F. D.; Skyes, B. D.; Chao H.; Davies, P. L., *Science,* **1993**, *259*, 1154

22. Chao, H.; Sonnichsen, F. D.; DeLuca, C. I.; Sykes, B. D.; Davies, P. L., *Protein Science*, **1994**, *3*, 1760.

23. Deng, G.; Andrews, D. W.; Laursen, R. A., *Federation of European Biochemical Society*, **1997**, *402*, 17.

24. Hon, W.; Griffith, M.; Mlynarz, A.; Kwok, Y. C.; Yang, D. S. C., Plant Physiology, **1995**, *109*, 879.

25. Graham, L. A.; Liou, Y. C.; Walker ,V. K.; Davies, P. L., *Nature*, **1997,** *388*, 727.

26. Knight, C. A.; DeVries, A. L.; Oolman, L. D., *Nature*, 1984, *308*, 295.

27. DeVries, A. L, *Science*, **1971**, *172*, 1152.

28. Lin, Y.; Raymond, J. A.; Duman, J. G.; DeVries A. L., *Cryobiology*, **1976**, *13*, 334.

29. Raymond, J. A.; DeVries, A. L., *Journal of Colloid and Interface Science*, **1975**, *52*, 406.

30. Kristiansen, E.; Zachariassen, K. E., *Cryobiology*, **2005**, *51*, 262.

31. Raymond, J. A.; DeVries, A. L., *Proceedings of the National Academy of Science,* **1977**, *74*, 2589.

32. Raymond, J. A.; DeVries, A. L., *Cryobiology*, **1972**, *9*, 541.

33. Knight, C. A.; Driggers, E.; DeVries, A. L., *Philosophical Transactions of the Royal Society of London. Series B, Biological sciences*, **1993**, *64*, 252.

34. Grandum, S.; Yabe, A.; Nakagomi, K.; Tanaka, M.; Takemura, F.; Kobayashi, Y.; Frivik, P., *Journal of Crystal Growth*, **1999**, *205*, 382.

35. Knight, C. A., *Nature*, **2000**, *406*, 249.

36. Burcham, T. S.; Osuga, D. T.; Yeh, Y.; Feeney, R. E., *Journal of Biological Chemistry*, **1986**, *261*, 6390.

37. Li, Q.; Luo, L., *Chemical Physical Letters*, **1993**, *216*, 453.

38. Hall, D. G.; Lips, A., *Langmuir*, **1999**, *15*, 1905.

39. Jia, Z.; DeLuca ,C. I.; Chao H.; Davies, P. L., *Nature*, **1996**, *384*, 285.

40. Houston, M. E.; Chao, H.; Hodges, R. S.; Sykes, B. D.; Kay, C. M.; Sonnichsen, F. D.; Loewen, M. C.; Davies, P. L., *Journal of Biological Chemistry,* **1998**, *273*, 11714.

41. Gallagher, K. R.; Sharp, K. A. *Biophysical Chemistry,* **2003**, *105*, 295.

42. Jorov, A., Zhorov, B. S., Yang, D. S. C. s.l. : Protein Science, 2004, Vol. 13, p. 1524.

43. Smolin, N., Daggett, *Journal of Physical Chemistry*, **2008**, *112*, 6193.

44. Yang, C.; Sharp, K. A. *Proteins: Structure, Function, and Bioinformatics*, **2005**, *59*, 266.

45. Nutt, D. R.; Smith, J. C. *Journal of the American Chemical Society*, **2008**, *130*, 13066.

46. Budke, C.; Koop, T., *The European Journal of Chemical Physics and Physical Chemistry*, **2006**, *7*, 2601.

47. Knight, C. A.; Hallet, J.; DeVries, A. L., *Cryobiology*, **1988**, *25*, 55.

48. Storey, K. B.; Storey, J. M., *Annual Review of Ecology and Systematics*, **1996**, *27*, 375.

49. Storey, J. M.; Storey, K. B., *Journal of Comparative Physiology B*, **1985**, *156*, 191.

50. Churchill, T. A.; Storey, K. B., *Copeia,* **1996,** *3*, 517.

51. Edwards, J. R.; Jenkins, J. L.; Swanson, D. L., *Journal of Experimental Zoology*, **2004**, *301A*, 521

52. Rubinsky, B., *Annual Review of Biomedical Engineering*, **2000**, *2*, 157.

53. Carpenter, J. F.; Hansen, T. N., *Proceedings of the National Acadamy of Science*, **1992**, 89, 8953.

54. Chao, H.; Davies, P. L.; Carpenter, J. F., *The Journal of Experimental Biology*, **1996**, *199*, 2071.

55. Hanslick, J. L.; Lau, K.; Noguchi, K. K.; Olney, J. W.; Zorumski, C. F.; Mennerick, S.; Faber, N. B., *Neurobiology of Disease*, **2009**, *34*, 1.

56. Lane, A. N.; Hays, L. M.; Tsvetkova, N.; Feeney, R. E.; Crowe, L. M.;Crowe, J. H *Biophysical Journal,* **2000**, Vol. *78,* pp. 3195-3207.

# *CHAPTER 2*

# *Goals and Objectives*

## 2.1 Introduction to Antifreeze Glycoprotein Analogues

Although the properties of antifreeze glycoproteins are promising for various applications, there are many restrictions holding back the widespread commercial, medical, and industrial use of these macromolecules. The first problem is that acquiring large quantities of these compounds is very challenging. Isolation of large amounts from Antarctic fish would be extremely labor intensive as it would require a commercial fishery in Antarctica followed by the economically prohibitive purification of their blood serum to isolate the AFGPs (Chapter 1). Synthetic production of these compounds would appear to be far more feasible, but this approach has its own set of problems. The traditional synthetic procedures towards glycoproteins are long and time consuming. [(1) (2)] Not only do they require the use of solid phase peptide synthesis but they also need to be purified through high performance liquid chromatography, which produces low yields of the isolated peptides. This makes them very expensive to manufacture, making this approach inappropriate for large-scale production. Another issue prohibiting the use the native AFGPs in applications with biological systems is that they are cytotoxic to both human embryonic liver and human embryonic kidney cells. [(3)] This disappointingly makes them unusable as cryoprotectants for human cells and tissues.

Finally, AFGPs have two intrinsic properties, RI and TH; the former is essential for cryoprotection, yet the second property, TH, causes the formation of needle like crystals which damages cells instead of protecting them. [4], [5] Fortunately, even though both of these properties are present in the native compounds, they function by separate mechanisms. [6], [7] Theoretically this should make it possible to custom design synthetic AFGP analogues (syAFGP), with excellent RI and no TH. But to function as feasible cryoprotectants, syAFGP must be benign, biologically stable, and synthetically simple.

Antifreeze glycoproteins contain three different structural components or moieties, each of which can be strategically modified to produce an optimized syAFGP (Figure 2.1). The first is the carbohydrate component. The native system contains β-D-galactopyranosyl-(1→3)-2-

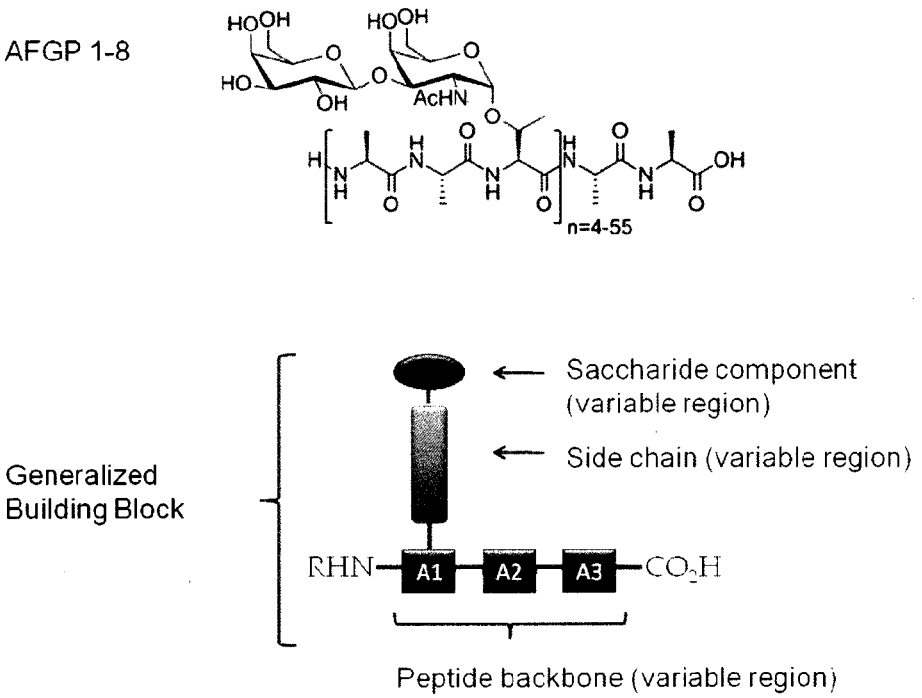


**Figure 2.1** AFGPs 1-8 and Generalized Building Block

acetamido-2-deoxy-D- galactopyranoside disaccharide, which requires a prodigious number of steps to synthesize. This can be modified to a less complex structure such as a commercially available disaccharide or monosaccharide. Secondly, the native linker region between the carbohydrate and the peptide backbone is susceptible to both chemical and biological degradation. Changing the anomeric C-O bond to a *C*-linked system has shown to overcome these problems with minimal effect on substrate binding or sugar conformation. [8] The last piece is the peptide backbone, which is the threonine-alanine-alanine tripeptide, repeated from 4 to 55 times. This can be simplified by designing peptides which contain the smallest length, of four repeating tripeptides and switching alanines for glycines which eliminates the complication of epimerization of the methyl groups on the alanine residues during synthesis. By incorporating all these changes Ben et al. have synthesized potent inhibitors of recrystallization that lack any detectable thermal hysteretic activity. [9], [10]

The most potent inhibitors, as defined by RI activity, discovered by Ben and coworkers are both *C*-linked to a galactose unit and contain a glycine-glycine peptide backbone, but differ in the side chain component (Figure 2.2). [9], [10] Based on their side chain they are named the

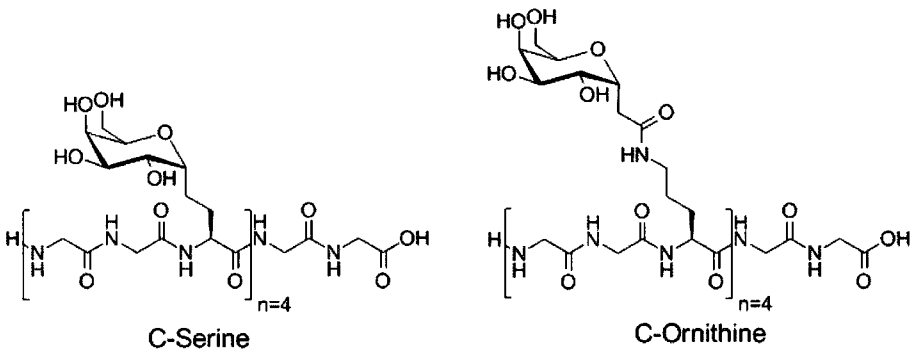


**Figure 2.2** Potent *C*-linked AFGPs Recrystallization Inhibitors

C-Serine analogue and the OGG-Gal analogue (where OGG represents ornithine-glycine-glycine). The RI activity was measured using the splat cooling method as previously described by Knight and DeVries. [11] Briefly, it requires obtaining a very thin frozen wafer. This is achieved by dropping a 10 µL sample drop through a 2 m long tube onto a polished aluminum block cooled to -78 °C. The sample is instantly frozen and transferred onto a similarly cooled glass slide. This is then quickly placed into a refrigerated microscope stage that is set to the annealing temperature (-6 °C) and allowed to recrystallize over thirty minutes. For each sample including PBS, three drops were performed and three images were taken from the middle of each wafer. Image analysis of the ice wafers was performed using novel domain recognition software or DRS, (for more detail refer to section 4.5.1). The mean grain size is calculated, and compared

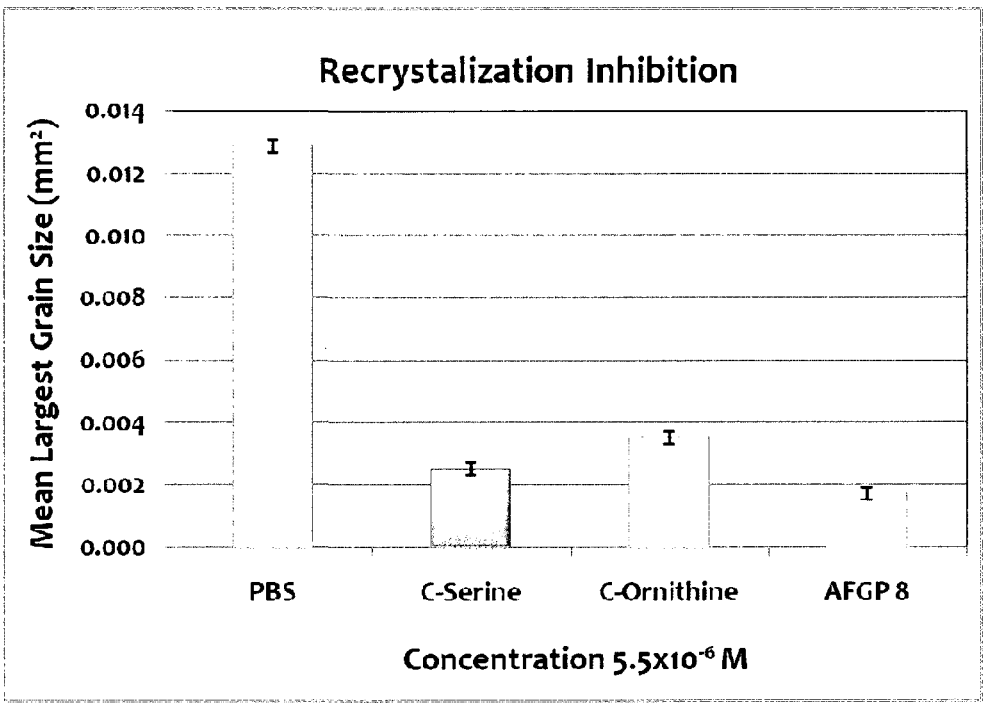


**Figure 2.3** RI Activities of Potent Recrystallization Inhibitors

to a negative control, phosphate buffered saline (PBS) solution. [12], [13] As can be seen in Figure 2.3, the RI activity of the *C*-Serine and the OGG-Gal analogues are comparable to AFGP 8. This was a great advance in the rational design of syAFGP as cryoprotectants, as they do not contain the disadvantages of cytotoxicity, *O*-linkages, or long synthetic procedures. [3] Both of these analogues were discovered during the SAR studies involved in the side chain component, but more recent efforts have focused on the carbohydrate domain and its effect on RI activity.

## 2.2 Hydration and Recrystallization Inhibition

In 2008 Ben and coworkers investigated how modifying the carbohydrate unit on their OGG-Gal syAFGP affected the recrystallization inhibition activity. [10] They tested D-glucose, D-mannose and D-talose in addition to the previously prepared D-galactose. Finding that these

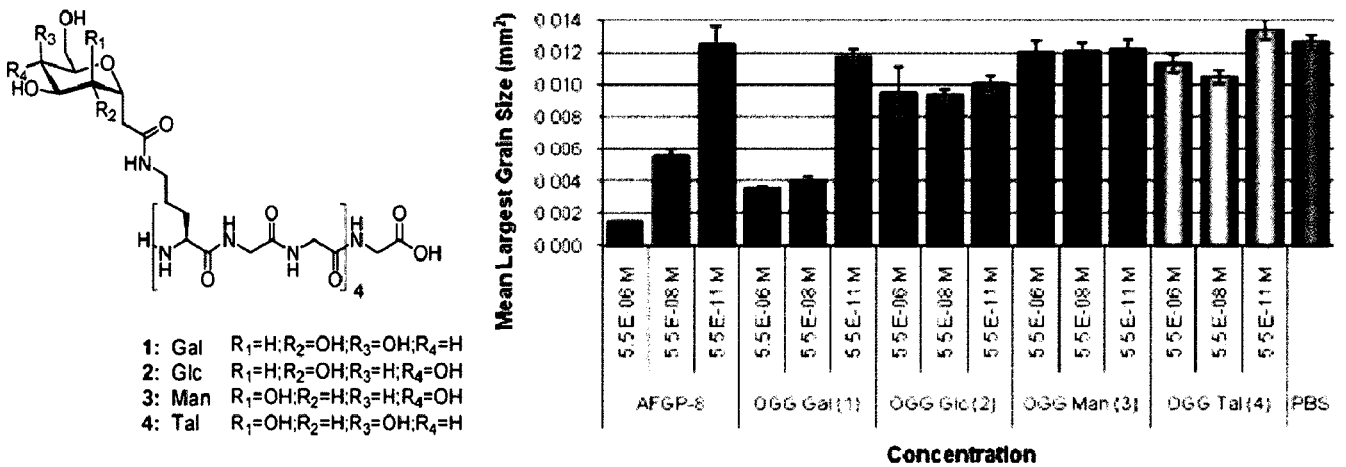


**Figure 2.4** RI activities of OGG-Carbohydrate Analogues [10]

changes had a drastic effect on the RI activity, they demonstrated that the carbohydrate configuration is very important for activity (Figure 2.4).[10] This led them to work by Galema et al., which examines the compatibilities of various carbohydrates in aqueous solutions.[14] The most relevant properties are partial molar volumes, the contribution that a carbohydrate makes to the overall volume within a solution, and isentropic partial molar compressibility, the ability of a molecule to be compacted or compressed. Galema and coworkers then used these values to calculate the corresponding hydration number, defined as the number of tightly bound water molecules surrounding the given carbohydrate. As one can imagine these values are highly interrelated, as they quantify the "compatibility" of the sugar within the three dimensional hydrogen bonded network of bulk water. For example as the stereochemistry of

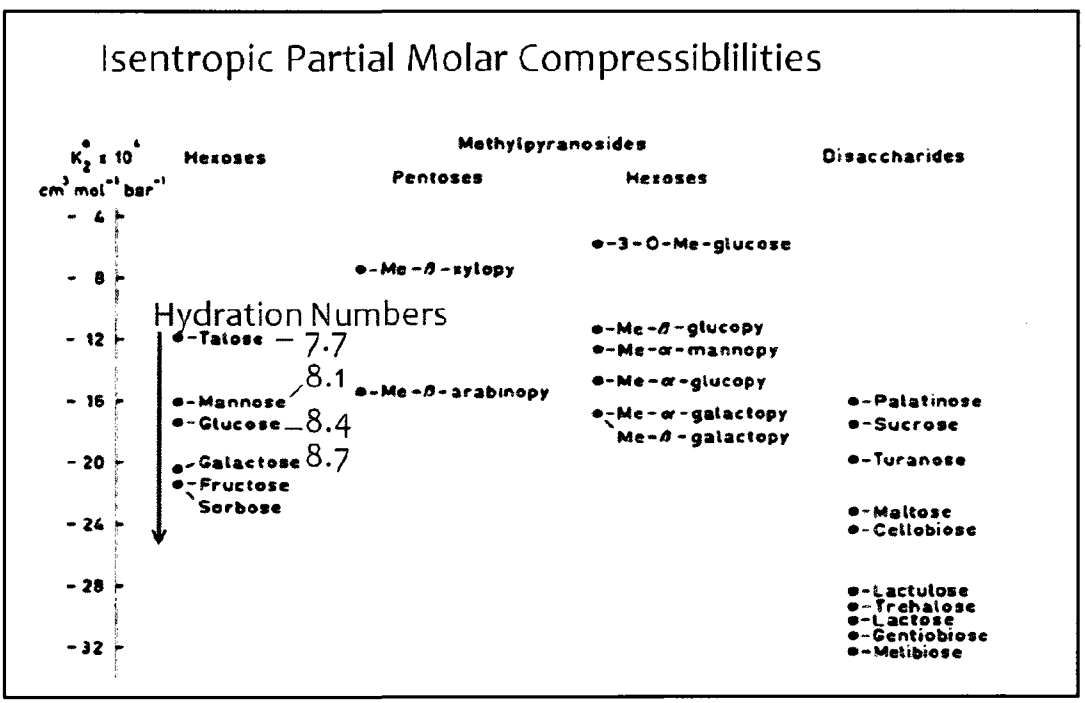


**Figure 2.5** Measured isentropic molar compressibilities and calculated hydration numbers[14]

of the carbohydrate changes so does its fit within the bulk water. For the carbohydrates examined by Ben et al. in the OGG-Carbohydrate syAFGPs (Figure 2.4) the fit or compressibility of the carbohydrate decreases from talose, through mannose and glucose to galactose (Figure 2.5). The hydration of these carbohydrates also increases from talose to galactose, due to the fact that hydration is inversely related to molar compressibility. Remarkably, Ben et al. reported that RI activity had a direct relationship to partial molar compressibility and therefore inverse relationship to hydration number. [10] They postulate that the increased ability to disturb water molecules increases the energy associated with adding bulk water molecules to ice crystals, which would slow down the growth of the ice crystals over time.

Although the biological importance of hydration and carbohydrates is well known, their significance in recrystallization inhibition is newly discovered and is far from being fully understood. [15] But it is clear, as shown by Ben et al. that as the hydration of the carbohydrate increases so does the recrystallization inhibition activity of the entire C-ornithine syAFGP. This led to speculation over whether one could use the RI activity of simple carbohydrates to predict the activity of their syAFGP analogues. Therefore the first objective of this thesis is to explore the relationship between hydration and ice recrystalization inhibition using small molecule carbohydrates. These results were also compared to the current standard in cryoprotection of tissues and cells, dimethyl sulfoxide, and C-linked carbohydrate derivatives. The final goal of this research would be to provide a model able to accurately predict the RI activity of a theoretical syAFGP for applications in cryomedicine or industry.

## 2.3 Determining the relationship between RI activity and changing regiochemistry of the terminal carbohydrate on the native AFGP disaccharide

The special properties of the D-galactose-β(1-3)-N-acetyl-galactoseamine disaccharide is evident in the vital role it plays in many human biological processes. [16], [17], [18] For example it is part of the T-antigen, D-Gal-β(1-3)-GalNAc-Serine/Threonine which is present in over 85 % of human carcinomas. [19] Its importance in AFGPs is also apparent as no syAFGP with a carbohydrate other then that found in the native disaccharide has been able to surpass the activity of the natural compounds. Efforts into studying the carbohydrate portion of syAFGPs have been done by Ben et al. which demonstrated that even small changes of the carbohydrate component can drastically curtail the syAFGP's RI activity. [10] But these studies were not performed using the native disaccharide. In fact the recrystalization inhibition ability of the native disaccharide, released from the peptide support, has never been studied in terms of RI activity.

There are two questions pertaining D-galactose-β(1-3)-N-acetyl-galactoseamine disaccharide. The first is whether or not it has superior RI activity in comparison to other carbohydrates, and therefore is a major factor as to why the natural AFGPs are more active then syAFGP. The second is how important is the beta 1-3 glycosidic linkage in terms of the RI activity and would a change to the regiochemistry affect RI?

To address these questions would require the synthesis of the native disaccharide analogue Allyl-β-D-galactopyranosyl-(1→3)-2-acetamido-2-deoxy-β-D-galacto pyranoside, and a comparison of its RI activity to that of several other carbohydrate derivatives. This would include a comparison of the native disaccharides to the individual monosaccharides, galactose

and N-acetyl galactoseamine, both of which have been synthesize by Ben et al. as the corresponding α-O-linked-threonine-alanine-alanine glycopeptides and had significantly diminished activity ($(Gal-\alpha-O-TAA)_4$ MLGS = 0.0083±0.0002 $mm^2$ and $(Gal-NAc-\alpha-O-TAA)_4$ MLGS = 0.0049±0.0003 $mm^2$ at $5.5x10^{-6}$ M in PBS, C-serine MLGS = 0.0025±0.0002 $mm^2$, and PBS MLGS = 0.0129 $mm^2$) compared to AFGP 8. If the disaccharide is in fact is a better inhibitor then the monosaccharides this would demonstrate that the increased activity of the native AFGP 8 is most likely due to the intrinsic nature of the disaccharide. However if the opposite is true, if disaccharide demonstrates worse or equal RI activity then the monosaccharides, then this would suggest that it is not the carbohydrate that dictates the activity between glycopeptides with the same backbone, but the wholistic structure of the glycopeptide. The argument would be the same with respect to galactose and N-acteylgalactoseamine. In addition, this project would also create an opportunity to study the importance of the C2 substituent of galactose, and compare how changing between C2 hydroxyl, N-Acetyl, C2 amine, azide and C2 deoxy affects the RI activity.

Furthermore to investigate the RI activity of changing the regiochemistry of the glycosidic linkage of Gal-GalNAc would require the synthesis of the regioisomers Allyl-β-D-galactopyranosyl-(1→4)-2-acetamido-2-deoxy-β-D-galactopyranoside and Allyl-β-D-galacto pyranosyl-(1→6)-2-acetamido-2-deoxy-β-D-galactopyranoside (Figure 2.6). This novel study would lead to a better understanding of the native system, and determine if nature has chosen the best inhibitor amongst the three compounds. Examining the RI activity of these compounds will give insight into which of the hydroxyl groups of the GalNAc are the most

important for RI activity, and whether adding a terminal galactose to each position enhances or reduces this activity.

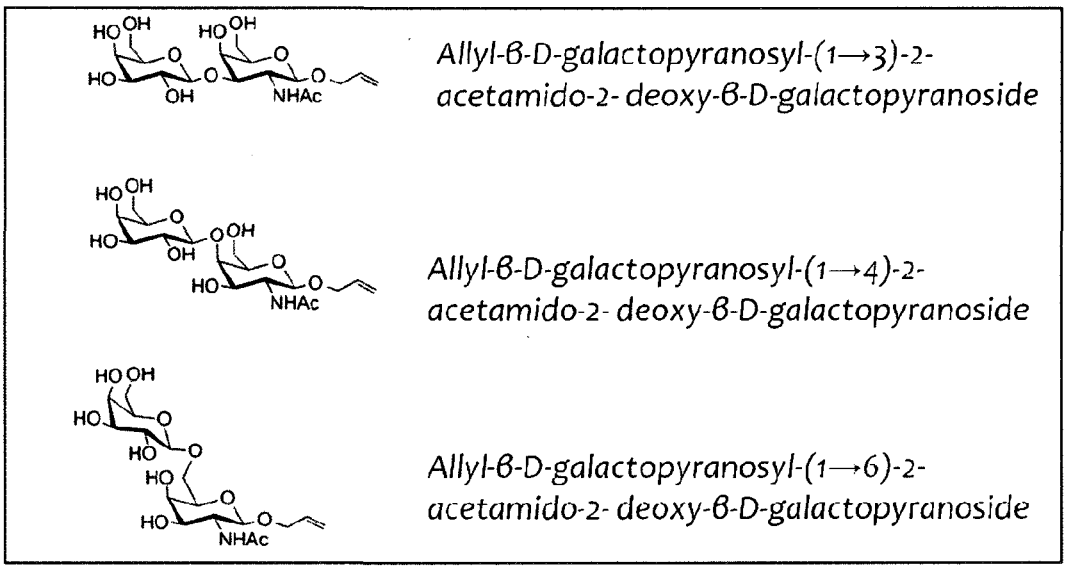


**Figure 2.6** β-O-Allyl-Gal-GalNAc synthetic targets

Collectively, this study will probe several components of the native disaccharide, and their importance for RI activity. This will potentially lead to a better understanding of the properties that dictate antifreeze glycoproteins activity, and therefore improve the rational design of future synthetic analogues.

## 2.4 Synthesis of syAFGP (β-Gal-(1-3)-Gal-NAc-α-O-TAA)$_4$

Another important step in the development of a commercially viable syAFGP cryoprotectant is to distinguish between which structural features are necessary for RI, and

which are necessary for TH. In 2004 Nishimura et al. published work exploring the essential components of AFGPs required for thermal hysteresis.[20] They began by analyzing the minimum size of the repeating glycosylated tripeptide that was necessary for dynamic ice shaping, and found that even the monomer was capable of some interaction with ice. Next, they synthesized several AFGP analogues and assessed the resulting ice crystal morphology (Figure 2.7). They reported that even small changes to the natural AFGP can cause a loss of thermal hysteresis, for example changing to a β-O linked glycoprotein (Figure 2.7 A), replacing the disaccharide with either lactose or galactose (Figure 2.7 B-C), or exchanging the threonine residue for a serine (Figure 2.7 D) all caused loss of all thermal hysteretic activity. This work

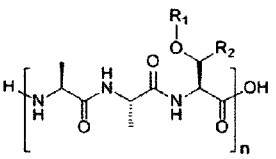

| | $R_1$ | $R_2$ | Average Mw (Da) | DIS |
|---|---|---|---|---|
| PolyAFGP | 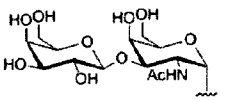 | $CH_3$ | 6600 |  |
| A | 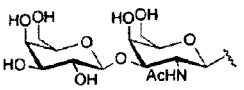 | $CH_3$ | 6620 |  |
| B | 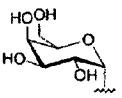 | $CH_3$ | 4230 |  |
| C | 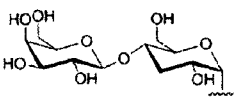 | $CH_3$ | 7000 | |
| D | 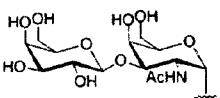 | H | 6590 |  |

**Figure 2.7** AFGP derivatives synthesized by Nishimura et al. including TH lacking entries A-D [20]

demonstrated that the glycosidic linkage, carbohydrate stereochemistry, C2 N-acetyl moiety and the γ methyl group of the threonine are all preconditions for ice binding.

In terms of designing syAFGP cryoprotectants, abrogation of thermal hysteresis is beneficial, but further analysis of these synthetic analogues needs to be carried out to determine if the RI properties of the AFGPs have been conserved. Unfortunately, Nishimura et al. did not test any of these analogues in terms of recrystallization inhibition. Opportunely, the synthesis of these syAFGP and their variants has been an on-going focus in the Ben research group. A previous synthesis of Nishimura's TH lacking gal-α-O-threonine-alanine-alanine (Figure 2.7 B), demonstrated a moderate RI activity of 0.0056 ±0.0002 $mm^2$ (at 5.5 x $10^{-6}$ mM), demonstrating that the original disaccharide is also an important component for RI activity. However, the remaining TH lacking glycoproteins Figure 2.7 C-D have not been synthesized and tested for RI activity. To address this concern, the last objective of this dissertation is the synthesis and RI testing of the serine derivative (Figure 2.7 D). This study will provide new information on whether the γ methyl group of threonine has such drastic effects on RI as it does with the binding to ice and will lead to improved understanding of what could lead to an improved syAFGP.

Overall this thesis hopes to investigate various structural elements of carbohydrates and glycoproteins and how they effect recrystallization inhibition. It involves studying the basic properties of carbohydrates that contribute to activity, probing the native disaccharide, exploring the effects of changing its glycosidic bond regiochemistry and finally exploring the structural motifs that are important for only RI acitivity. However all of these different areas of

research have the same goal, which is to acquire the information necessary to design and synthesize potent recrystallization inhibitors as cryoprotectants.

## 2.5 References


1. Herzner, H.; Reipen, T.; Schultz, M.; Kunz, H. *Chemical Reviews*, **2000,** *12*, 4495.
2. Tachibana, Y.; Matsubara, N.; Nakajima, F.; Tsuda, T.; Tsudo, S.; Monde, K.; Nishimura, S.; *Tetrahedron*, **2002**, *58*, 10213.
3. Liu, S.; Wang, W.; Von Moos, E.; Jackman, J.; Mealing, G.; Monette, R.; Ben, R. N., *Biomacromolecules*, **2007**, *8*, 1456.
4. Carpenter, J. F.; Hansen, T. N. *Proceedings of the National Academy of Science*, **1992**, *89*, 8953.
5. Rubinsky, B. *Annual Review of Biomedical Engineering*, **2000**, *2*,157.
6. Knight, C A. *Nature*, **2000**, *406*, 249.
7. Sidebottom, C.; Buckley, S.; Pudney, P.; Twigg, S.; Jarman, C.; Holt, C.; Telford, J.; McArthur, A.; Warrall, D.; Hubbard, R.; Lillford, P. *Nature*, **2000**, *406*, 256.
8. Wanga, J.; Kovac, P.; Sinay, P.; Glaudemans, C. P. J. *Carbohydrate Research*, **1998**, *308*, 191.
9. Liu, S.; Ben, R. N. *Organic Letters*, **2005**, *7*, 2385.
10. Czechura, P.; Tam, R. Y.; Dimitrijevic, E.; Murphy, A. V.; Ben, R. N. *Journal of American Chemical Society*, **2008**, *130*, 2928.
11. Knight, C. A.; Hallett, J.; DeVries, A. L. *Cryobiology*, **1988,** *25*, 55.
12. Eniade, A.; Purushotham, M,; Wang, J. B.; Horwath, K.; Ben, R. N. *Cell Biochemistry and Biophysics*, **2003**, *38*, 115.
13. Jackman, J.; Noestheden, M.; Moffat, D.; Pezacki, J. P.; Findlay, S.; Ben, R. N. *Biochemical and Biophysical Research Communications*, **2007**, *354*, 340.

14. Galema, S.; Hoiland, A. *The Journal of Physical Chemistry*, **1991**, *95*, 5321.

15. Frank, F. *Pure and Applied Chemistry*, **1987**, *59*, 1189.

16. Hang, C. H.; Bertozzi, C. R. *Bioorganic and Medicinal Chemistry*, **2005,** *13*, 5021.

17. Hanisch, F. *Biological Chemistry*, **2001**, *382*, 143.

18. Hounsell, E. F.; Davies, M. J.; Renouf, D. V. *Glycoconjugate Journal*, **1996**, *13*, 19.

19. Van Den Akker, F.; Steensma, E.; Hol, W. G. J. *Protein Science*, **1996**, *5*, 1184.

20. Tachibana, Y, et al. *Angewandte*, **2004**, *119*, 874.

# *CHAPTER 3*

# *Results and Discussion*

## 3.1 Hydration Index

The first objective of this thesis was to explore the relationship between the hydration of carbohydrates and recrystallization inhibition, and determine whether their activities could be used to predict that of corresponding synthetic antifreeze glycopeptides. However, this study extended beyond the simple monosaccharides used in the OGG-carbohydrate peptide series (galactose, glucose, mannose and talose) to include a comparison of hydration and RI activity of several commercially available disaccharides. [1] In addition the RI activities of these mono- and di-saccharides were compared to the RI activities of several allyl C-linked pyranoses, and the industrial standard cryoprotectant: dimethyl sulfoxide (DMSO). [2]

First, an optimal working concentration for the RI assay was required as carbohydrates separated from a peptide backbone have never analyzed for their RI activities. However, the addition of trehalose at concentrations of 0.2 M to DMSO solutions (ranging from 1-10 (v/v) %) has demonstrated to improve the cryopreservation of human hepaocytes over solutions with DMSO alone. [3] Thus a concentration scan of galactose in PBS solution starting from 0.22 M and ranging to 0.00022 M (Figure 3.1) was performed. Overall, this scan demonstrated that there is a logarithmic relationship between the galactose concentration and RI activity. The minimum

effective concentration for recrystallization inhibition is 0.00022 M, when the crystals approach the size of those of the PBS solution (the negative control). This non-linear relationship suggests that the activity is not colligative, supporting what has been previously observed for biological antifreezes[4], [5] Moreover, this scan demonstrated that a high concentration of

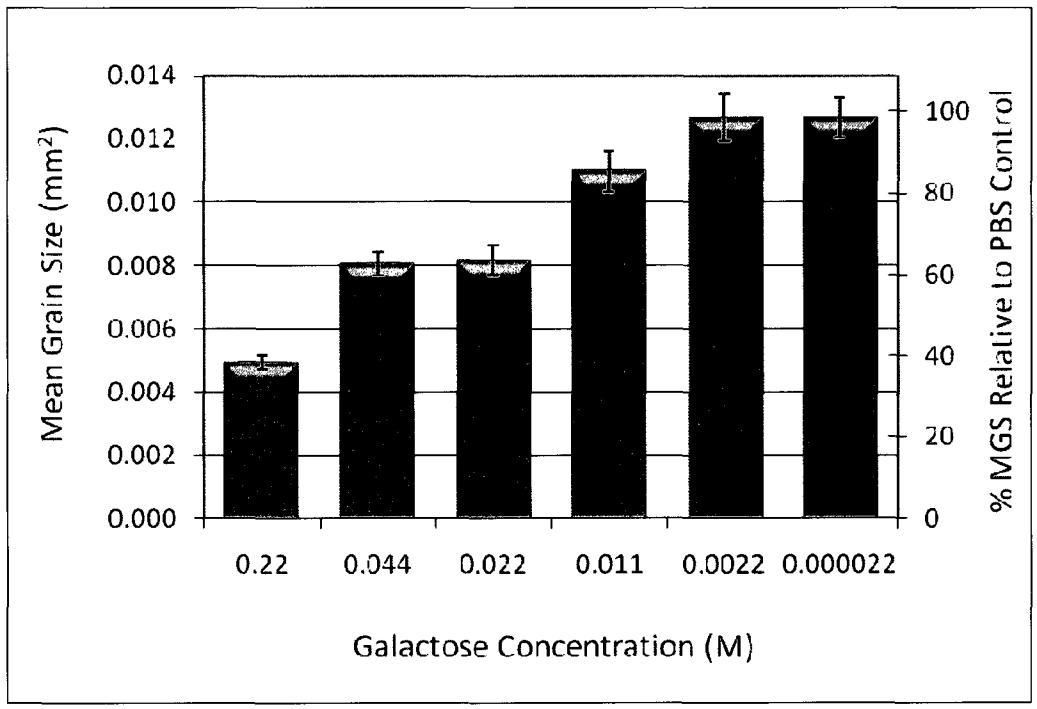


**Figure 3.1** Recrystallization-inhibition (RI) activities of various concentrations of D-galactose solutions in PBS solution

0.22 M galactose solution in PBS is an effective inhibitor of recrystalization, but due to its high viscosity it posed technical difficulties during the RI assay. Alternatively, concentrations of 0.044 M and 0.022 M showed moderate inhibition but did not lead to the technical problems associated with the higher concentration; consequently, a concentration of 0.022 M was employed for all the saccharides.

The initial carbohydrates chosen for the study were four monosaccharides and five disaccharides, all of which were studied by Galema et al.. These included the monosaccharides employed in the synthesis of the OGG-saccharide series (galactose, glucose, manose and talose) and the commercially available disaccharides sucrose, maltose, trehalose, lactose, and melibiose (Figure 3.2). [1] We selected these particular carbohydrates because they displayed a

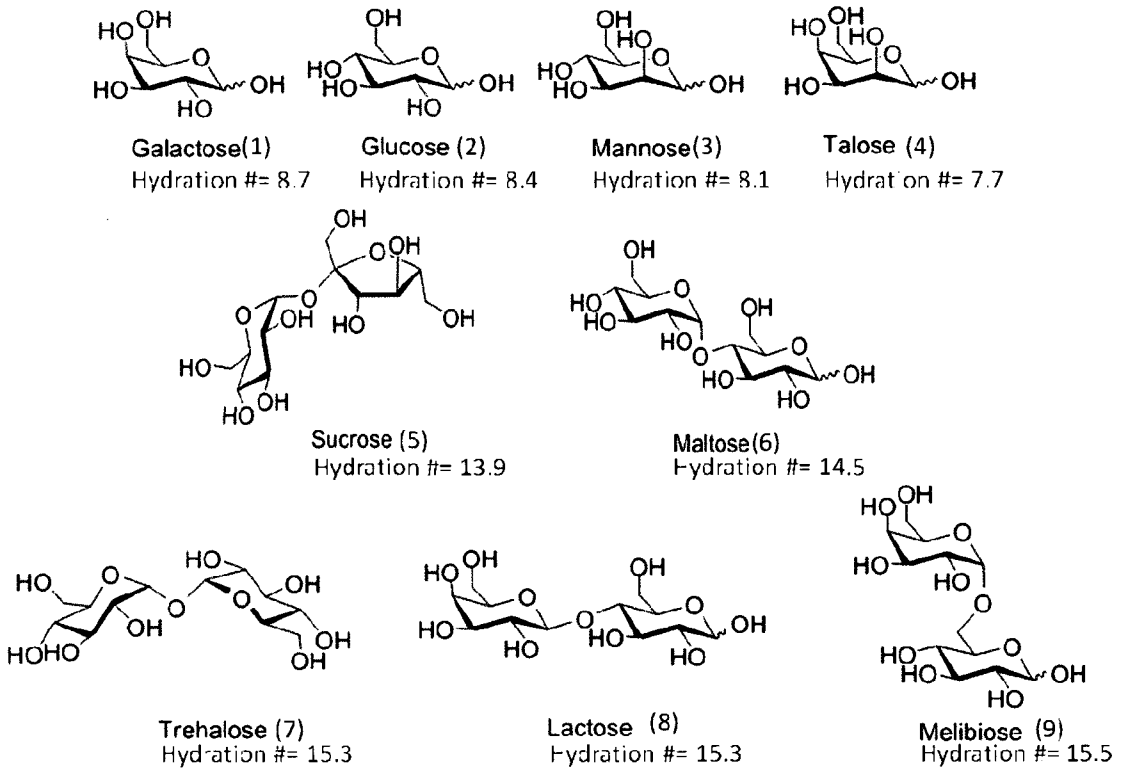


**Figure 3.2** Hydration numbers of Monosaccharides (**1-4**) and Disaccharides (**5-9**) [6]

wide variety of hydration numbers. [6] Their RI activities were then plotted as a function of hydration numbers from Galema et al. (Figure 3.2). Their hydration numbers were calculated

based on molar compressibility values which were computed using ultrasound density measurements, and are widely regarded as an accurate measure of hydration. [6]

As evident from Figure 3.2, each series (mono- and disaccharides) shows a strong linear trend between the hydration number and their respective RI activity. However, it was expected based on hydration numbers that the disaccharides would have RI activity that was nearly twice that of the monosaccharides and therefore demonstrate one single trend, but this was not the

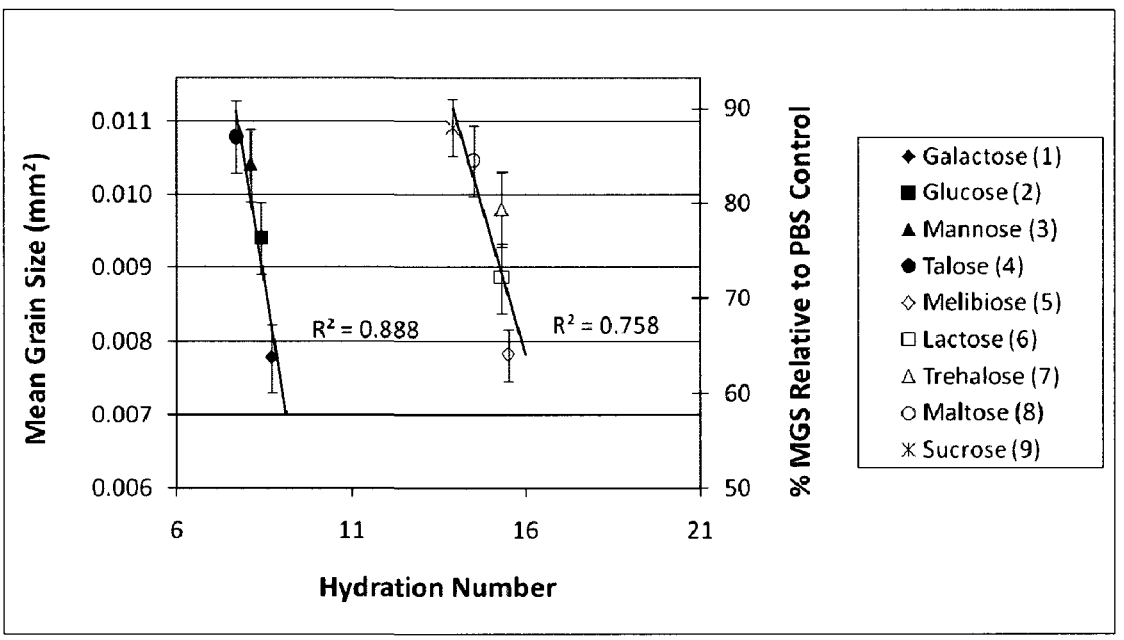


**Figure 3.3** RI activity of various monosaccharides (**1-4**) and disaccharides (**1-9**) at 0.022 M in PBS solution, plotted against their respective hydration numbers [2]

case. For example the hydration number of galactose is 8.7 while melibioses is 15.5, yet their RI activity is very similar (0.6 % difference). Even more surprisingly, was the fact that the remaining disaccharides (sucrose, maltose, lactose and trehalose) all had activity that was less then galactose, even though the corresponding hydration numbers (13.9-15.3) were much

higher then galactose (8.7). This data clearly demonstrated that there are other properties of carbohydrates besides their hydration that influence RI activity.

The most striking observation is the fact that the disaccharides have approximately half the expected RI activity in comparison to the monosaccharides, and physically they are twice their volume. These observations led to the definition of the *Hydration Index* which takes the steric bulk of the solute (carbohydrate) into consideration, and is believed to account for the unexpected deviation of the recrystallization inhibition activity in the disaccharides series. The definition of the *Hydration Index* begins with the hydration numbers, $n_h$, which were calculated

$$n_h = (n_w / n_s)(1 - \beta_s/\beta_{so}) \qquad \textbf{Equation 3.1}$$

$$\beta = 1/u_2 d \qquad \textbf{Equation 3.2}$$

by Galema et al. using Passynsky's equation (equation 3.1). In this equation $n_w$ and $n_s$ represent the mole fractions of water and the solute, respectively and $\beta_s$ and $\beta_{so}$ are the isentropic coefficients of compressibility of the solute and water. [6] These molar compressibility coefficients can be further described as shown in Equation 3.2 where $u$ is the speed of sound and $d$ is the density of solution. [6] Dividing the $n_h$ by the partial molar volume, results in a description of the number of tightly bound water molecules per given volume, which was termed the *Hydration Index* (HI) by Tam et al.[2] The importance of this calculation has also been demonstrated by Parke et al., who compared the taste properties of several different compounds, including salts, carbohydrates, acids and alcohols, to their hydration per unit volume of solute. [7] However, our study was the first that correlated solute volume to

recrystallization inhibition activity. As shown in Figure 3.4, when the RI activity was plotted against the corresponding *Hydration Indices,* it gave a good linear fit ($R^2$ = 0.791) for both the mono- and di- saccharides, whereas hydration number alone led to two isolated series. This is

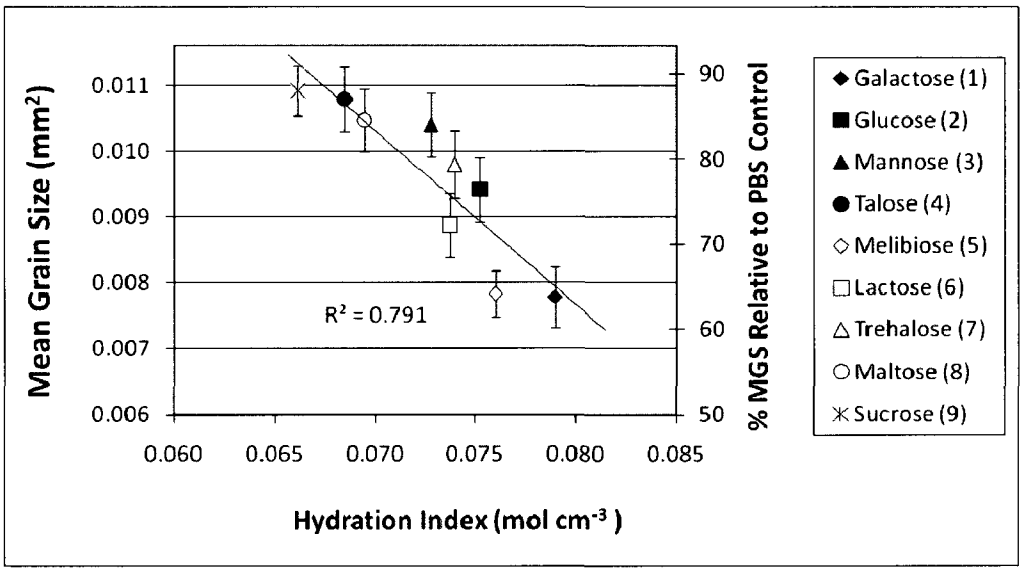


**Figure 3.4** RI activities of carbohydrates (**1-9**), plotted against their respective hydration index ($molcm^{-3}$)

significant because while the number of water molecules is important for predicting RI activity, how highly concentrated they are around the given solute is equally important, and gives new insight into the modes of action of carbohydrate as RI inhibitors.

Understanding the mechanisms of action of these compounds requires a better understanding of how they interact with ice. First, the possibility that the saccharides were functioning by binding to ice could be eliminated as a possible mode of action by analyzing their ice crystal morphology. This was done using Nanoliter osmometry as described by Chakrabartty and Hew (and in more detail in section 4.5.2). [8] As can be seen in Figure 3.5, there was no dynamic ice shaping (DIS) observed for any of the carbohydrates tested (D-Galactose, D-

Glucose, D-Talose, D-Melibiose, D-Trehalose, and D-Sucrose). This eliminates the possibility that the observed RI activity is due to the carbohydrates binding to the ice surface. But also removes the possibility that the carbohydrates contain any thermal hysteresis which requires

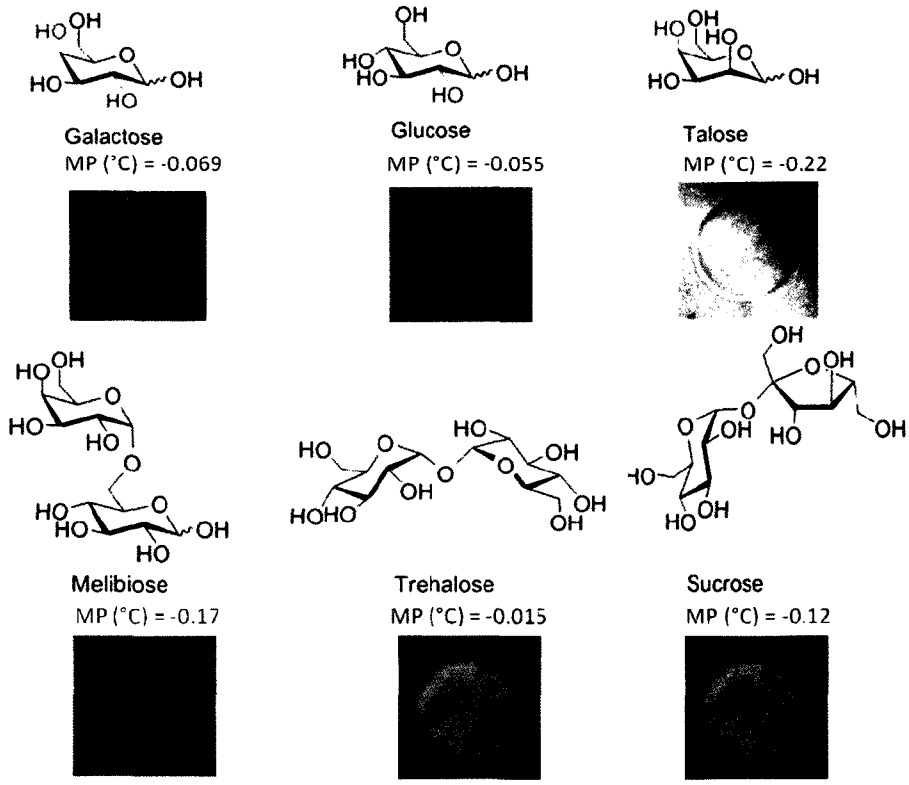


**Figure 3.5** Ice Crystal Morphology and Melting Points of 10 mg/mL Solutions of D-Galactose, D-Glucose, D-Talose, D-Melibiose, D-Trehalose, and D-Sucrose in Double-Distilled Water, Determined Using Nanoliter Osmometry [2], [8]

ice binding. Further supporting the lack of TH was the fact that the observed melting points and freezing points were the same, and that this temperature was only slightly below zero, which is to be expected based on the colligative properties of the carbohydrates. This contradicts previous literature, which reports that the thermal hysteresis activity of simple mono- and disaccharides is based on complimentarity of hydroxyl groups with the ice lattice. [9],

[10], [11] In addition Madura et al. propose that the quasi liquid layer (QLL) of water molecules (which exists between the ice crystal and the bulk water) also plays a key role in biological antifreeze binding. [12]

Therefore with respect to the present study, since there was no DIS observed it is unlikely that the carbohydrates interact at the ice-QLL interface, but this does not exclude the possibility of an interaction at the QLL-bulk water interface. In the splat-cooling RI assay, the wafer is frozen and contains very little unfrozen water. Furthermore, as solutes are excluded from the ice lattice, the carbohydrate will be concentrated at the interface between two adjacent ice crystals and their QLLs, which are 3-10 Å thick. [13] Exactly where the carbohydrate is positioned with respect to the QLL is hard to determine based on the difficulty associated with studying the layer (Figure 3.6). But there are two possibilities, first is that the

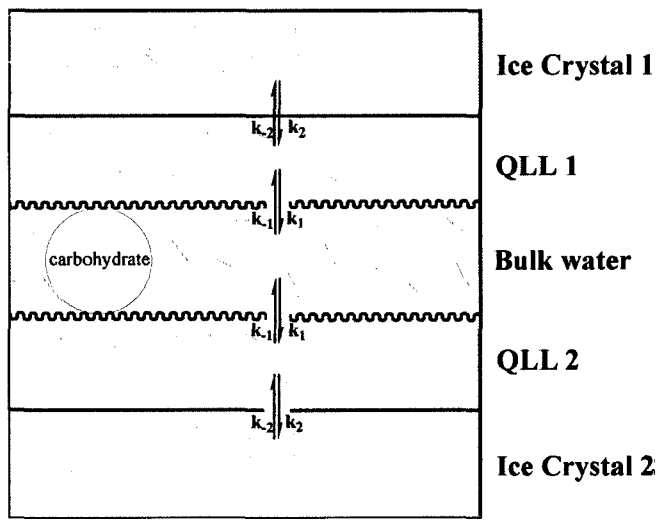


**Figure 3.6** Proposed mechanism for inhibition of ice recrystallization. Carbohydrates reside at the QLL–bulk water interface between two adjacent ice crystals. The area shaded red represents hydrated solute, QLL (quasi-liquid layer) [2]

carbohydrates would be fully incorporated within the QLL, and the second is that it is at the QLL-bulk water interface. The first possibility is unlikely as there is no known precedence of this occurring. However there is experimental evidence reported by Uchida and co-workers using TEM and trehalose solutions that the second possibility is likely. [5] The TEM images revealed that there were two distinct areas of the ice: a smooth surface which represented ice and an area that included homogeneously distributed trehalose precipitates with a minimum size of ~10 nm. [5] Since the QLL are only between 3-10 Å thick, these precipitates would therefore be too large to be fully incorporated into these layers. [13] Furthermore, they did not report any observed contact between the smooth surface (representing ice) and these precipitates, as a result it was concluded that the carbohydrates concentrate at the QLL- bulk water interface.

Consequently we proposed that carbohydrates with higher *Hydration Indicies* (hydration number per molar volume of carbohydrate) positioned at the QLL-water interface will cause a greater disruption on the ordering of bulk water and the surrounding hydration shell. In addition it is known that the disruption of the first hydration shell can extent out to the third hydration shell, causing a significant energy difference. [14] This long-range effect on the motion of bulk water is therefore proposed to increases the energy associated with adding bulk water molecules to the QLL. This will in turn cause a decreased in the addition of bulk water to the QLL, and consequently to the ice lattice, inhibiting the growth of ice crystals over time. We propose the reason that the hydration number is insufficient at predicting the recrystalization inhibition is because it does not take into account the disruption of extended hydration shells.

### 3.2 RI Activity Comparison between C-Glycosides and O-Glycosides

Previous syAFGPs synthesized by Ben et al. have been C-linked glycopeptides designed to reduce chemical and biological degradation. [1] Although studies report that changing from *O*-linked carbohydrates to *C*-linked carbohydrates has little effect of the on the conformation of the glycopeptides, this change has not been investigated systematically in terms of recrystallization inhibition. [15], [16], [17] This was achieved by synthesizing several C-allyl derivatives of galactose, glucose, mannose and talose (compounds **10-15** Figure 3.7). Unfortunately, there are no known hydration numbers for these compounds. But, it is generally accepted that hydration is largely dictated by the stereochemistry of the hydroxyl groups at the C2 and C4 positions of the pyranose, and that the anomeric position is not as important. [18] To test this, several C-allylated derivatives were analyzed for their recrystallization inhibition and compared to their native O-linked carbohydrates.

The results demonstrated that the α-C-allyl galactose had statistically identical RI activity as D-galactose. [2] In fact the, the entire α-C-allyl series demonstrated the same trend as that of the native carbohydrates, confirming that the anomeric hydroxyl group has little effect on hydration, or recrystallization inhibition. The results for the β-C-allyl series were not as straightforward. The β-C-allyl galactose demonstrated a marked loss in RI activity in comparison to D-galactose, yet there was no change in activity between β-C-allyl glucose and D-glucose (Figure 3.7). This suggests that the β-C-allyl group on galactose might affect the hydration of this compound, which is then reflected in the RI activity. However in order to make confident conclusions on the effects of the β-C-allyl group, the remaining compounds (mannose and talose) need to be synthesized and tested for their corresponding RI activities.

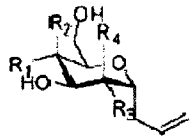

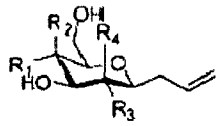

**10** (Gal), $R_1$=H, $R_2$=OH, $R_3$=OH, $R_4$=H
**11** (Glc), $R_1$=OH, $R_2$=H, $R_3$=OH, $R_4$=H
**12** (Man), $R_1$=OH, $R_2$=H, $R_3$=H, $R_4$=OH
**13** (Tal), $R_1$=H, $R_2$=OH, $R_3$=H, $R_4$=OH

**14** (Gal), $R_1$=H, $R_2$=OH, $R_3$=OH, $R_4$=H
**15** (Glc), $R_1$=OH, $R_2$=H, $R_3$=OH, $R_4$=H

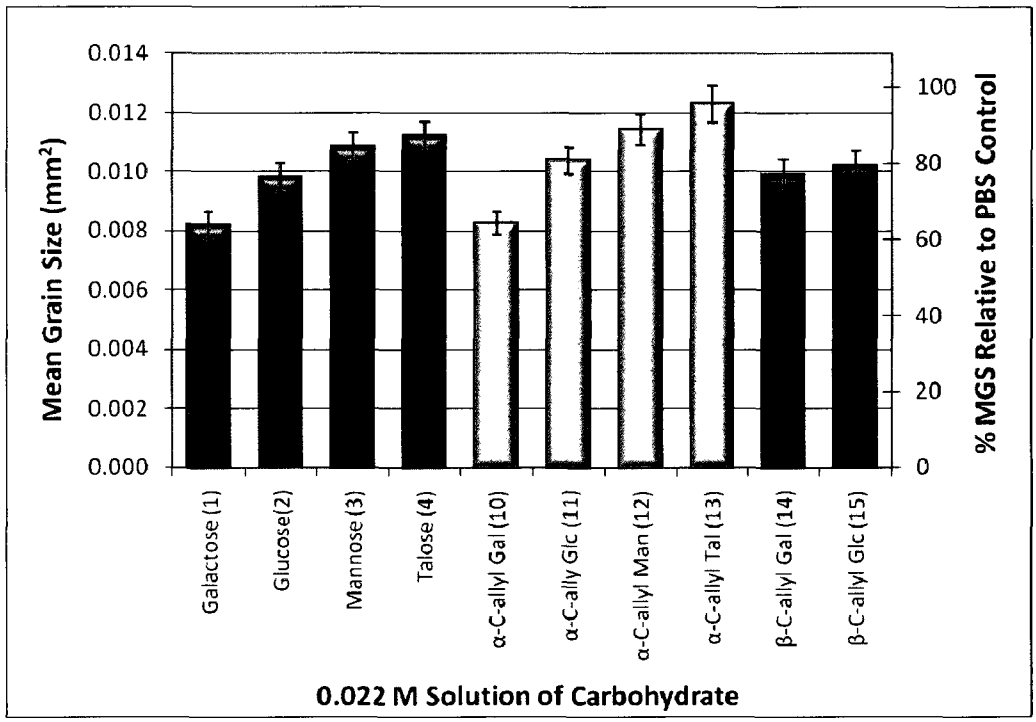


**Figure 3.7** RI activity of native O-linked monosaccharides (**1-4**) and their C-glycoside derivatives (**10-15**) at 0.022 M in PBS solution

### 3.3 Comparing the RI activity of D-galactose and α-C-allyl galactose derivatives to DMSO

The ability of D-galactose and α-C-allyl galactose to serve as cryoprotectants was explored by comparing their RI activities to the industrial standard, dimethyl sulfoxide (DMSO). As mentioned previously DMSO is regularly used as an additive prior to freezing of tissues and cells. [19], [20] It is known that DMSO functions as a cryoprotectant in two ways: firstly, it protects

cell membranes against fractionation by replacing water within the membrane during thermatropic phase transitions. [21], [22] Secondly, it facilitates the transport of water in and out of the cell to relieve osmotic stress during freezing, and helps to prevent dehydration. [21], [22] Regardless of the mechanism of action, it results in improved viability of many cell types post freezing and thawing in comparison to many other methods. The fact that DMSO is well known to be quite cytotoxic, yet seems to be the best available industrial cryoprotectant, demonstrates the infancy of this field and the vast room for improvement. It also makes DMSO and its properties very interesting to study. For example it is not known if DMSO can inhibit the growth of ice. Therefore a concentration scan was preformed based on the typical

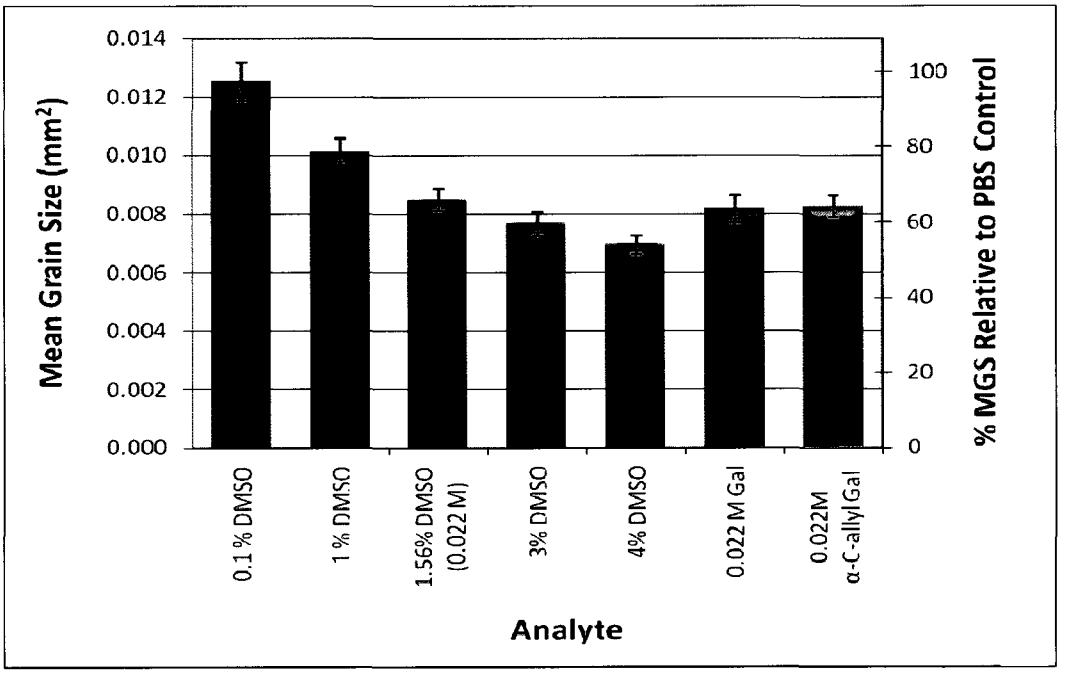


**Figure 3.8** RI activities of various concentrations of DMSO and 0.022 M solutions of compounds **1** and **10** in PBS solution [2]

concentrations of DMSO that are used commercially (Figure 3.8). These can range anywhere between 1-20 %, but studies have shown that very little additional cryoprotective benefit is obtained by surpassing 5 % volume by volume. [23] Concentrations larger then 6 % resulted in large amounts of unfrozen water and therefore could not be used to measure the ice crystal size. The tested concentrations are shown in Figure 3.8, and range from 0.1 % to 4 % (v/v) in PBS solutions. The results demonstrate that low concentrations of 0.1 % DMSO have no recrystallization inhibition activity and have a mean crystal size which is the same as solutions of PBS alone. However, the RI activity gradually increases as the concentration of DMSO increases, with a 4 % DMSO solution containing the most RI activity (54 % mean grain size relative to PBS). Interestingly, a 3 % (v/v) of DMSO had the same activity as a 0.022 M solution of D-galactose. This suggests that DMSO may also function as a cryoprotectant by inhibiting the recrystallization of ice, and that galactose may also be a suitable cryoprotectant. If true this could represent a significant advance in the field of cryoprotection as natural carbohydrates are not as toxic as DMSO.

The investigation of the carbohydrate and carbohydrate derivatives has expanded the knowledge of the how they function as recrystallization inhibitors and their possible use as cryoprotectants. Originally the study began with the promise that hydration numbers could be used to predict RI activity of the entire syAFGPs analogues. But it was discovered that the *Hydration Index* is a much better predictor because it takes the steric bulk of the carbohydrate into consideration. Also, when the *O*-linked native saccharides were substituted with *C*-linked allyl carbohydrates it did not have a large effect on the RI activity of the carbohydrate. There was an exception with the fact that β-allyl galactose lost activity in comparison to the native

carbohydrate. Finally it was discovered that 0.022 M D-galactose was as good as a recrystallization inhibitor as a 3 % (v/v) solution of DMSO, suggesting that it could function as a possible cryoprotectant.

### 3.4 Determining the relationship between RI activity and changing regiochemistry of the terminal carbohydrate on the native AFGP disaccharide

The next objective of this thesis was to investigate the special properties of the native disaccharide, and the importance of the glycosidic linkage to regiochemistry. More specifically, we were interested in whether attachment of the terminal galactose at other positions on the N-acetyl galactose amine would have an effect upon RI activity. This would involve the synthesis of a derivative of native disaccharide and its regioisomers, followed by the determination of their recyrstalization inhibition activities and a comparative analysis between these disaccharides.

The retrosynthetic analysis of the three disaccharides envisions a route where all three disaccharides can be synthesized from an orthogonally protected N-Acetyl glucosamine derivative **2**. Then upon inversion of the C4 stereocentre to the axial conformation, would yield the correct stereochemistry for the galactose carbohydrate. The reasoning behind starting with the N-acetyl glucosamine instead of N-acetyl-D-galactosamine is because of the costs associated with these compounds. The price of N-acetyl-D-glucosamine is ~ $1 per gram where as N-acetyl galactosamine is ~ $230 per gram. That being said, upon inversion of the glucose C4 center, either the C3 or the C4 position can have the unprotected hydroxyl group, depending on

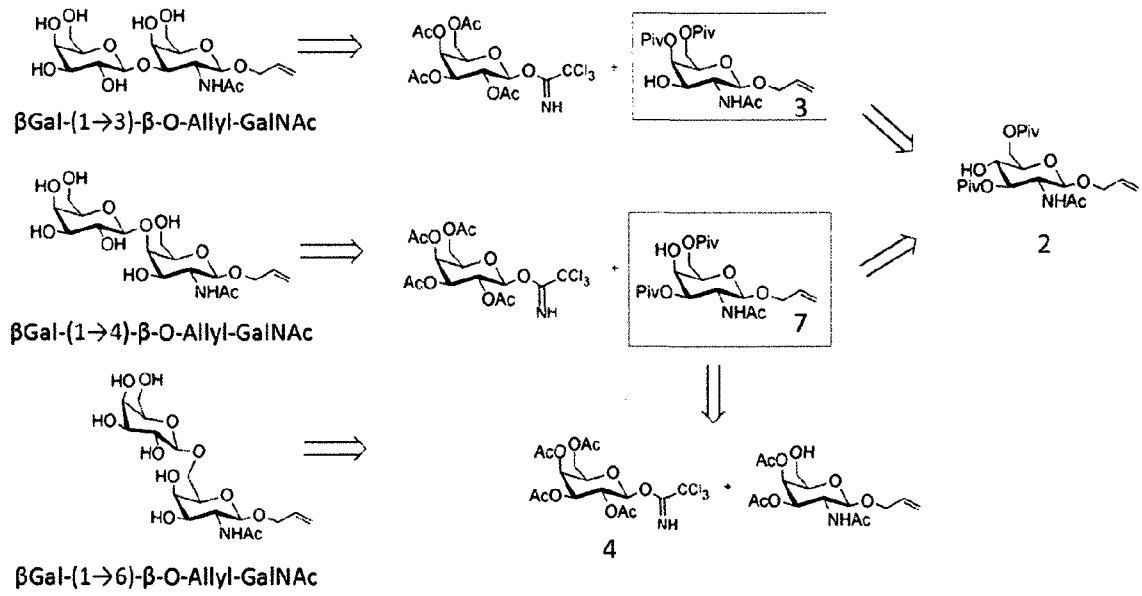


the conditions used for the inversion. This produces the orthogonally protected glycosyl acceptors **3** and **7**, ready for coupling to a glycosyl donor **4**, to produce both the protected β-Gal-(1-3)-GalNAc and β-Gal-(1-4)-GalNAc. The remaining steps would involve selectively deprotecting the disaccharides to achieve the desired compounds. The synthesis of the final regioisomer would have to undergo protecting group manipulation, starting from either compound **3** or **7,** to obtain the free hydroxyl group at the C6 position. Then coupling to the galactopyranoside glycosyl donor **4** to give the protected β-Gal-(1-6)-GalNAc, and selective deprotection would yield the final 1-6 disaccharide.

The synthesis of β-Gal-(1-3)-GalNAc (**6**) disaccharide began with commercially available N-acteyl glucosamine. The anomeric position was allyl protected under kinetic conditions, as shown in Scheme 3.1, to produce an α:β mixture which was then separated via column chromatography to produce **1** in a 75 % yield. [24] The next step involved selectively pivaloylating at C2 and C6 to produce **2**. The following reaction accomplishes two purposes: first it inverts the

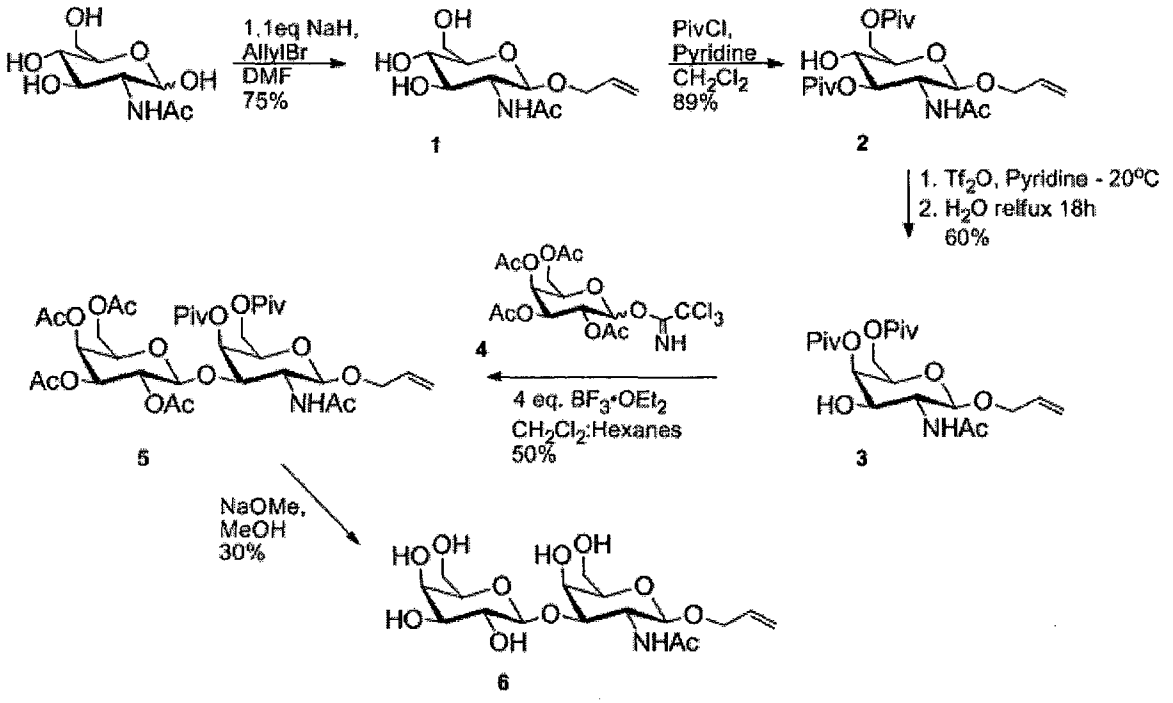


**Reaction Scheme 3.1** Synthesis of Allyl-β-D-galactopyranosyl-(1→3)-2-acetamido-2-deoxy-β-D-galactopyranoside **6**

stereochemistry at C3 to the axial position which is the correct stereochemistry for galactose and the second is that it frees up the hydroxyl group at C3. [25] This was carried out by first triflating the C3 hydroxyl group of compound **2**, then adding water and refluxing overnight. [25] Mechanistically, as seen in Figure 3.9, there is an intramolecular displacement of the triflate by the carbonyl oxygen of the pivaloyl group at C3 which produces the dioxolenium ion (**A**). [26] Then water attacks from the least hindered side to give the hemi-ortho ester **B** after a proton transfer. This intermediate then collapses with the assistance of two primary stereoelectronic effects and forms the axial ester compound **3**. Although **C** could theoretically exist, it is not observed due to the high degree of steric hindrance between the ring and the pivaloyl group.

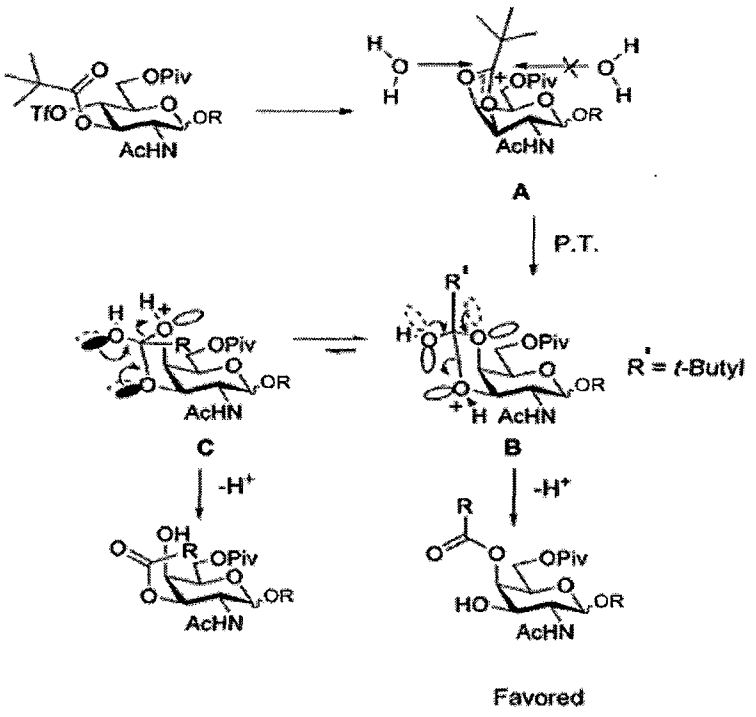


**Figure 3.9** Stereoselectivity in the Ring Opening of Hemiortho ester Intermediates **B** and **C** [26]

[26] This produces the glycosyl acceptor that is fully prepared for coupling to a glycosyl acceptor.

There are many different ways to form *O*-glycosidic bonds yet they all consist of the same basic principles. First, there is a sufficiently protected glycosyl donor equipped with a leaving group (LG), and that activation of the leaving group by a suitable promoter will create a highly reactive intermediate that will readily undergo nucleophilic attack from an appropriately functionalised glycosyl acceptor. This process can give simple disaccharides, but it can also lead

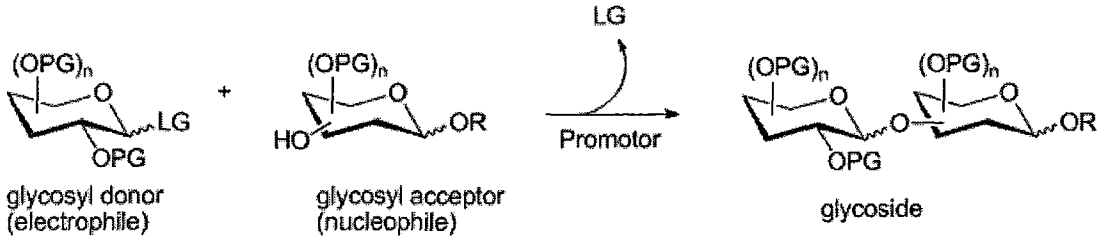

to the synthesis of complex oligosaccharides. There is also a vast variety of glycosyl donors and glycosylation methods available, but there are three main kinds which have been used to synthesize most oligosaccharides. They are the *Koenigs-Knorr* type reaction which uses glycosyl halides, the *trichloroacetimidate* method, and the use of *thioglycosides* and *n-pentenyl glycosides* as glycosyl donors. There is no superior method, the synthesis of disaccharides or oligosaccharides are individual problems which depend on the substrates used, in this case the use of trichloroacetimidates was determined to be successful. [27] These glycosyl donors are relatively straight forward to synthesize in two steps. First, the anomeric acetate group of pentaacetyl–D-galactose is selectively deprotected using either hydrazine acetate or benzyl amine. The liberated hydroxyl group is then functionalized as its trichloroacetimidate (TCA) using trichloroacetonitrile and base (typically NaH, $K_2CO_3$, or DBU). [28], [29], [30] The choice of base determines the anomeric stereochemistry of the resulting TCA glycoside synthesized. In this case, whether the TCA glycoside is α or β is irrelevant, as there is a C2 participating ester

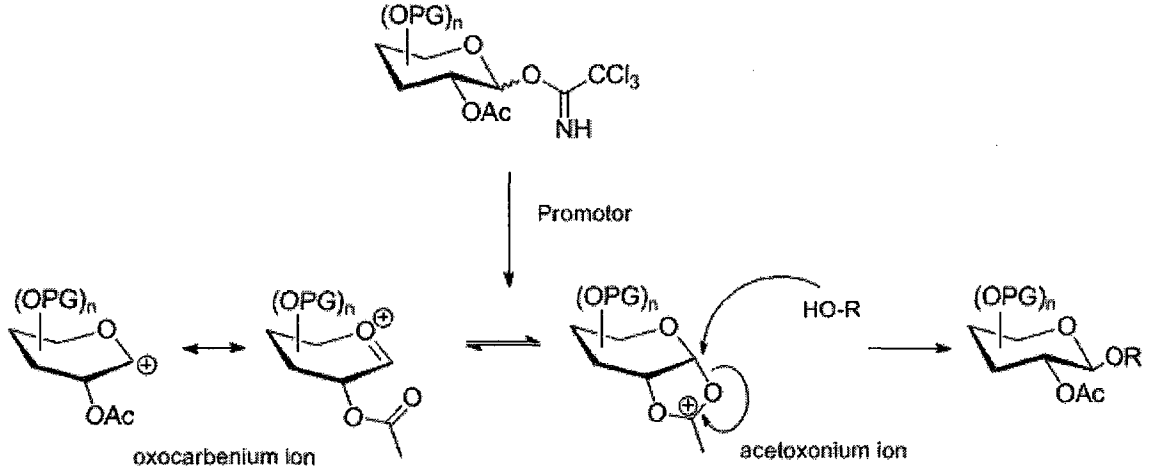

they both will result in the β disaccharide. For example the typical promotors of trichloroacetimidates are either TMS-OTf or $BF_3 \bullet OEt_2$ lewis acids. If TMS-OTf is used to promote the α –TCA donor then an oxocarbenium intermediate will be produced, and the C-2 ester group (acetate) will exert an anchimeric effect leading to the acetoxonium ion intermediate. Nucleophilic attack of this ring will then form the desired β product. If $BF_3 \bullet OEt_2$ used to promote activation of the α –TCA donor then direct displacement of the TCA leaving group, would result the β product. However if either TMS-OTf or $BF_3 \bullet OEt_2$ are used to promote β-TCA donor, the TCA leaving group will be displaced with by the C2 acetate to produce the acetoxonium ion intermediate, which upon nucleophilic attack will produce β product. In this case $BF_3 \bullet OEt_2$ was chosen as the promoter, and desired β disaccharide (**5**) was obtained in an acceptable 50 % yield. The next steps would then involve allyl deprotection and removal of the pivaloyl and acetate protecting groups. However, this proved to be a difficult accomplishment. For example, the anomeric allyl group was removed by first isomerizing the double bond with hydrogen activated Wilkinson-type catalyst, $[Ir(COD)(Ph_2MeP)_2]PF_6$, followed by electrophilic cleavage with $I_2$, in THF. But unfortunately several attempts to selectively deprotect the pivaloyl and acetate groups with catalytic amounts of NaOMe solution in methanol also deacetylated the N-acetyl moiety, producing the amine. Furthermore, the reversal of the deprotection steps creates another set of challenges. For instance, once the pivaloyl and acetate groups are deprotected as previously described, this produces a very polar compound with 6 free hydroxyl groups. This limits the solvents that are able to dissolve this disaccharide and several attempts to deallylate in MeOH, $H_2O$ or ACN, with activated Wilkinson-type catalyst failed. Also, deallylation with $PdCl_2$ and NaOAc in acetic acid : $H_20$ (20 : 1), is reported to form oxazoline ring

byproducts (where the N-Acetyl group eliminates the an isomerized allyl group). [31] Never the less this method of deallylation was attempted, and as reported formed mixtures of products by thin layer chromatography. However, it was reported by Dashnau et al. that an anomeric substituent has little effect on hydration and that positions C2 and C4 are most important. [18] This implies that the anomeric allyl group will have little effect on hydration and therefore should have a small effect on recrystallization inhibition activity. This was supported by previous work done by Ben et al. who reported only small changes in RI activity between monosaccharides as reducing sugars and their C-allylated derivatives. [2] Hence it was decided to leave the anomeric allyl group and deprotect only the acetate and pivaloyl groups, which would leave a compound polar enough to perform the RI assay in PBS solution.

The synthesis of β-Gal-(1-4)-GalNAc is very similar to the previous disaccharide and varies mainly in the inversion of stereochemistry reaction. Beginning with orthogonally protected glucose shown in scheme 3.2 below, the free hydroxyl group was triflated as before,

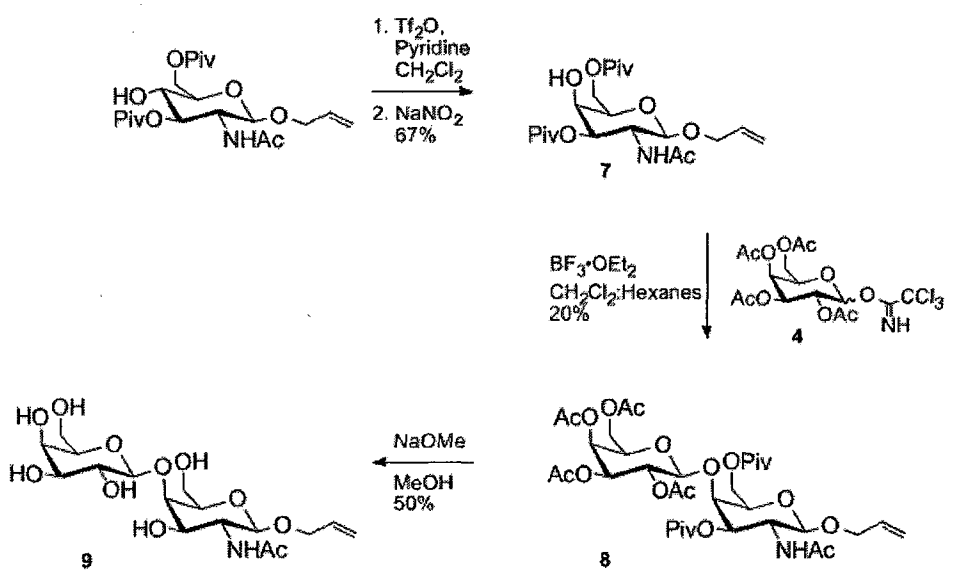


**Reaction Scheme 3.2** Synthesis of Allyl-β-D-galactopyranosyl-(1→3)-2-acetamido-2-deoxy-β-D-galactopyranoside **9**

however the next step involves a $S_N2$ reaction. The triflate is displace by nitrite which is hydrolyzed by an acid catalyzed reaction during workup, to yield the galactose derivative **7** with a hydroxyl group at C4. This glycosyl acceptor was then coupled using the trichloroacetimidate method with **4**, under the same conditions previously described, to yield **8** in a 20 % unoptimized yield. This was then selectively deprotected with NaOMe in methanol to achieve the desired final disaccharide **9**. Unfortunately, do to time constraints the third disaccharide was not completed. Nonetheless the two completed disaccharides were tested for their recrystallization inhibition activity and evaluated against the RI activities of a number of monosaccharides.

The RI activity of several monosaccharides including galactose, galactosamine, N-acetyl galactosamine, and C2-deoxy galactose were analyzed and compared. As a result, some interesting trends were observed between the monosaccharides. For instance, upon changing the C2 position of D-galactose to an azide or amine demonstrated only moderate losses in activity, but changing to either the deoxy or N-acetyl moiety caused a significant decrease (Figure 3.10). This difference could be attributed to the varying degrees of hydration of the C2 substituents. For example, the azide would exist as a zwitter ion and the amine as $NH_3^+$, under the conditions used during the RI assay, and thus they would be highly solvated. This increases their ability to hydrate over the deoxy or acetate substituents which would be both neutral. This is significant as changes in the carbohydrates substituents hydration have been shown to change the overall hydration. [32] This scan of monosaccharides also re-affirms the importance of the C2 position in recrystallization inhibition activities, as was previously reported. [1]

A second observation was the difference between the RI activity of carbohydrates (galactose and N-acetyl galactose) and their corresponding syAFGPs analogues. For instance the N-acetyl-galactose is a worse recrystallization inhibitor then D-galactose as the free carbohydrate but better as the bound the α-O-TAA peptide ($(Gal-\alpha-O-TAA)_4$ MLGS= $0.0083\pm0.0002mm^2$ and $(Gal-NAc-\alpha-O-TAA)_4$ MLGS= $0.0049\pm0.0003mm^2$ at $5.5x10^{-6}M$ in PBS solution). This increased antifreeze glycoprotein activity was also reported in terms of TH by

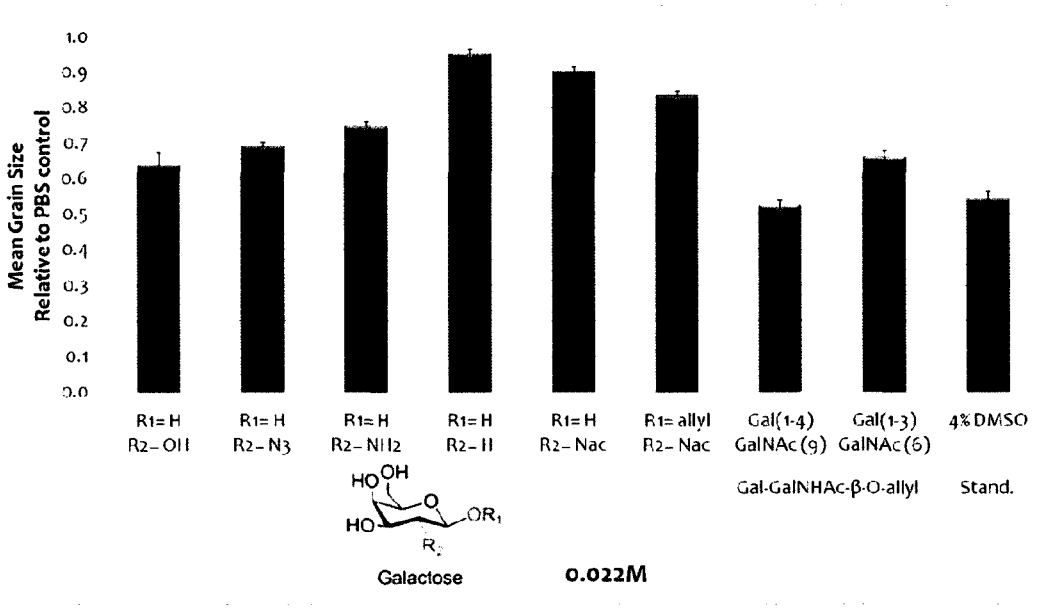


**Figure 3.10** RI activities of various analogues of D-galactose derivatives and compounds **6** and **9** at 0.022 M solutions in PBS solution

Nishimura et al. where $(Gal-\alpha-O-TAA)_4$ had no TH and $(Gal-NAc-\alpha-O-TAA)_4$ demonstrated dynamic ice shaping. [33] This difference could arise from a known interaction between the N-acetyl moiety and the peptide backbone, which was reported by Corzana et al. to occur via a hydrogen bonded water molecule bridge. [32] This effects the overall hydration of the syAFGPs, and therefore could account for the increase RI activity. However, the synthesis of more syAFGP

analogues containing the GalNAc carbohydrate and then testing of their RI activities would be needed to verify this hypothesis.

The final observation from the monosaccharides series was that there was only a slight increase in RI activity between N-acetyl galactosamine and its β-O allylated derivative. This however was not surprising as anomerically substituted carbohydrates are reported to have only small differences in hydration in comparison to their reducing carbohydrates. [18] However in order to fully validate this, more synthetic analogues containing various substituents at the anomeric center would have to be synthesized.

Next, the recrystallization inhibition activity of Allyl-β-D-galactopyranosyl-(1→3)-2-acetamido-2-deoxy-β-D-galactopyranoside demonstrated a distinct increase in RI activity in comparison to the β-O allylated N-acteyl galactosamine. This supports the hypothesis that the increased activity between (Gal-NAc-α-O-TAA)$_4$ and AFGP 8 is largely in part due to the native disaccharide. Unfortunately, the ability of this disaccharide is not fully appreciated simply by testing the RI activity on its own, as the activity of both β-Gal-(1-3)-GalNAc and N-acetyl glucosamine are both greatly enhanced as the α-O-TAA peptides.

Finally, the RI activity of Allyl-β-D-galactopyranosyl-(1→4)-2-acetamido-2-deoxy-β-D-galactopyranoside was found to exceed that of Allyl-β-D-galactopyranosyl-(1→3)-2-acetamido-2-deoxy-β-D-galactopyranoside as shown in Figure 3.10. This was an exciting result, as it was the first time that a small carbohydrate demonstrated better activity then D-galactose. However, the fact that there was a difference in RI activity between the disaccharides was expected as different hydroxyl groups of carbohydrates are known to have varying levels of importance on hydration. [18], [6]

Also, like the galactose derivatives there are no known comparative hydration numbers for either of these disaccharides, making it difficult to justify increased RI activity based on their *Hydration Indicies.* Nonetheless, when taking a closer look at the hydration numbers published by Galema et al. there are some basic trends observed. [6] For instance 1-4 linked carbohydrates have lower hydration numbers then 1-6 linked disaccharides (Figure 3.11). Also considering the large hydration number difference between cellobiose and gentibiose, which only differ in the regiochemistry of the glycosidic linkage, the hydration difference is more likely attributed to hydration changes of the ``reducing`` end glucose carbohydrate, which undergoes a larger structural modification.

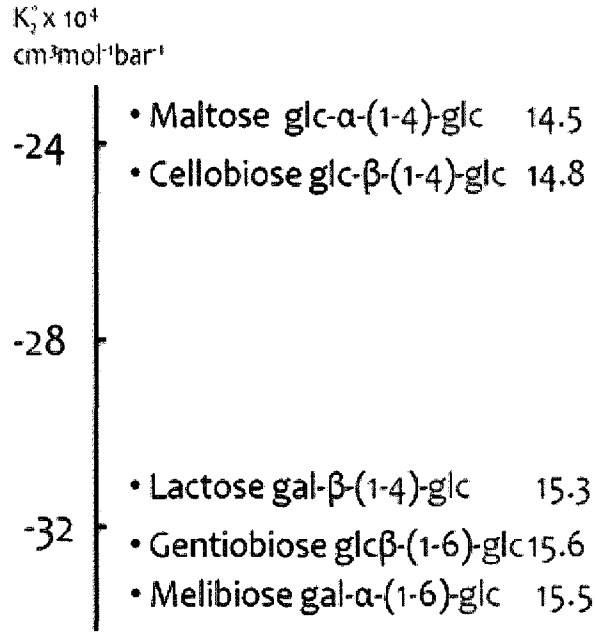


**Figure 3.11** Partial Molar Compressibility Values and Hydration numbers of several disaccharides as calculated by Galema et al. [6]

The gas phase hydration of both glucose and galactose derivatives were extensively studies with DFT calculations and near-IR by Simons et al. [34] They reported that the carbohydrates have intricate *Intra*-molecular hydrogen bonding networks (Figures 3.12 and 3.13). Specifically studying the hydrates of phenyl β-D-glucopyranoside and phenyl β-D-galactopyranoside, they found that water inserts into the weakest intramolecular hydrogen bond and takes part in these networks. In the glucose derivative, the most stable hydrate confirmation occurs when water inserts between the C4 and C6 hydroxyl groups and in the galactose derivative the most stable hydrate forms when water inserts between C6 hydroxyl group and the ring oxygen. [34]

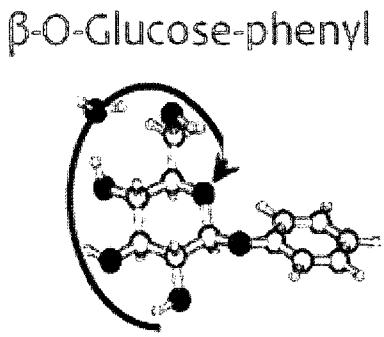


**Figure 3.12** Molecular modeling of hydrated phenyl β-D-glucopyranoside using DFT calculations by Simons et al. [34]

Unfortunately, these intramolecular hydrogen bonds decrease the number of hydrogen bond donors and acceptors available to hydrogen bond to bulk water molecules, and therefore decrease the carbohydrates ability to hydrate. A disturbance in these networks could then free up hydrogen bond donors and acceptors to hydrogen bond to bulk water and thereby increase hydration. Thus it is proposed that the difference in hydration between the 1-4 linked

disaccharides and 1-6 linked disaccharides (reported by Galema et al. Figure 3.11) is due to the increasing ability to disturb the intramolecular bonding network of the ``reducing`` end glucose carbohydrate.

The fact that the hydration of glucose changes upon glycosylation was exemplified in the DFT calculations made for the monohydrate of methyl β-D-lactoside. [34] For instance, the most stable hydrate of glucose is now formed when water inserts between the C6 hydroxyl group and the oxygen ring (Figure 3.13), where as before it was between C4 and C6 hydroxyl groups. Also a noteworthy observation of the methyl β-D-lactoside hydrogen bonding network, is that there are hydrogen bonds connecting the two carbohydrates, such as between the terminal galactose C6 hydroxyl group and the ``reducing`` end glucose C6 hydroxyl group . This suggests that the hydration of disaccharides is also affected by the ability to form these types of intramolecular hydrogen bonds.

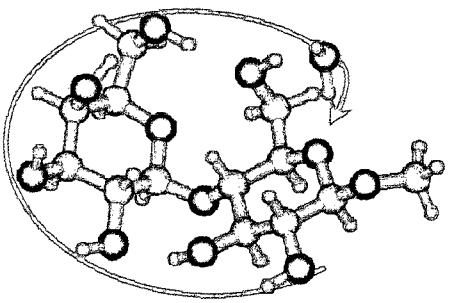

**Figure 3.13** Molecular modeling of hydrated methyl β-D-lactoside using DFT calculations by Simons et al.[22]

Consequently, the marked difference in recrystallization inhibition between Allyl-β-D-Gal-(1→4)-GalNAc and Allyl-β-D-Gal-(1→3)-GalNAc is proposed to be due to hydration differences, which arise from the varying degrees of disruption of the intramolecular hydrogen bonding networks of the ``reducing`` end N-acetyl galactosamine. In this case that would mean

the disruption of intramolecular hydrogen bonding of the ``reducing`` end N-acetyl galactosamine and thus the hydration would increase from Allyl-β-D-Gal-(1→3)-GalNAc to Allyl-β-D-Gal-(1→4)-GalNAc. Also, the volume change between these two dissacharides is likely to be small, as is the volume change between cellobiose and gentiobiose (which only differ in regiochemistry of their glycosydic linkage Figure 3.11). [6] This would then create a higher

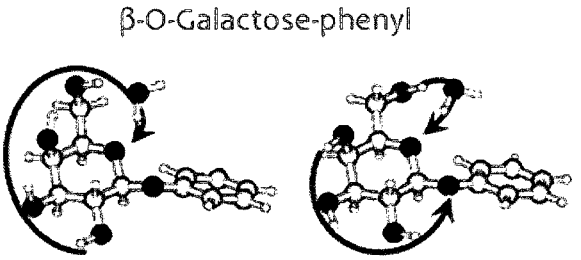


**Figure 3.14** Molecular modeling of hydrated phenyl β-D-galactopyranoside using DFT calculations by Simons et al.[22]

*Hydration Index* (hydration number per molar volume of carbohydrate) for the 1-4 linked disaccharide, and therefore account for its increased RI activity over the 1-3 linked disaccharide. [2]

In conclusion, it is clear the hydration models of disaccharides are very complex, and in turn little is known on how changing the regiochemistry of glycosidic bonds between disaccharides effects hydration. Yet this study demonstrated that changing regiochemistry has large effects on these compounds ability to inhibit ice recrystalization, which could be attributed to the capacity to disturb intramolecular hydrogen bonding networks and therefore their hydration. However, the determination of the disaccharides hydration numbers would be imperative to make more clear conclusions. Also the synthesis of Allyl-β-D-Gal-(1→6)-GalNAc

and testing for its RI activity would give further insight into the hydration of these disaccharides, and the importance of the individual hydroxyl groups of β-O-allyl GalNAc. These are important inquiries as increasing the knowledge of saccharides with respect to hydration and recrystalization improves the ability to rationally design small carbohydrate cyroprotectants that are urgently needed to replace the toxic dimethyl sulfoxide.

### 3.5 Synthesis of syAFGP (β-Gal-(1-3)-Gal-NAc-α-O-TAA)$_4$

Although small carbohydrates are promising cyroprotectants, they do not nearly approach the recrystalization inhibition activity of the glycopeptides. Hence the last objective of this thesis was to synthesize the TH-lacking synthetic AFGP analogue, previously reported by Nishimura and coworkers and test for its recrystallization inhibition. [33] The target differed from the native AFGPs by incorporating a serine in exchange of threonine, which causes a loss in the γ methyl group (Figure 3.15).

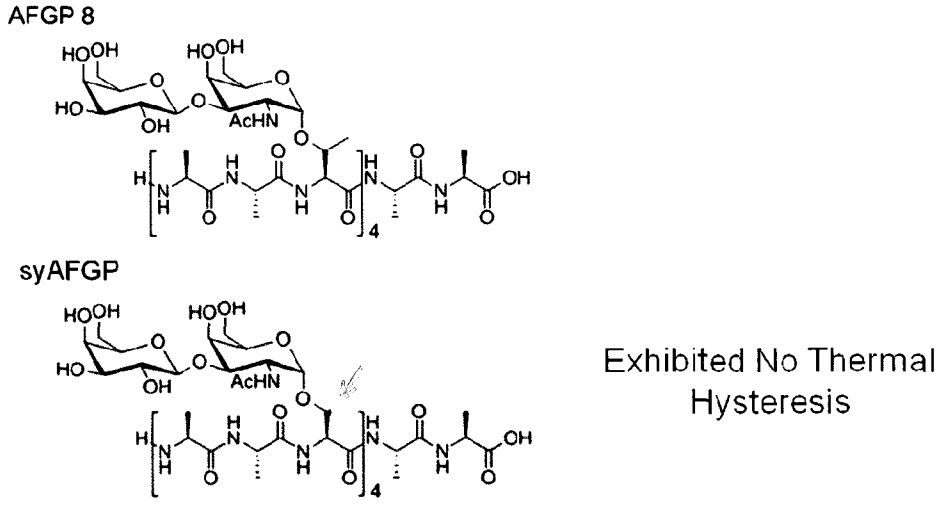


**Figure 3.15** AFGP 8 and synthetic Target, syAFGP (β-Gal-(1-3)-Gal-NAc-α-O-TAA)

There are many different approaches to synthesizing C2 participating O-linked glycopeptides. The first decision is whether to synthesize the peptide backbone and then attach the orthogonally protected disaccharide, or the second option is to fully synthesize the glycoconjugate building block and then subject it to solid phase peptide synthesis. Since the second option is known to result in better yields of glycopeptides it was the logical choice.

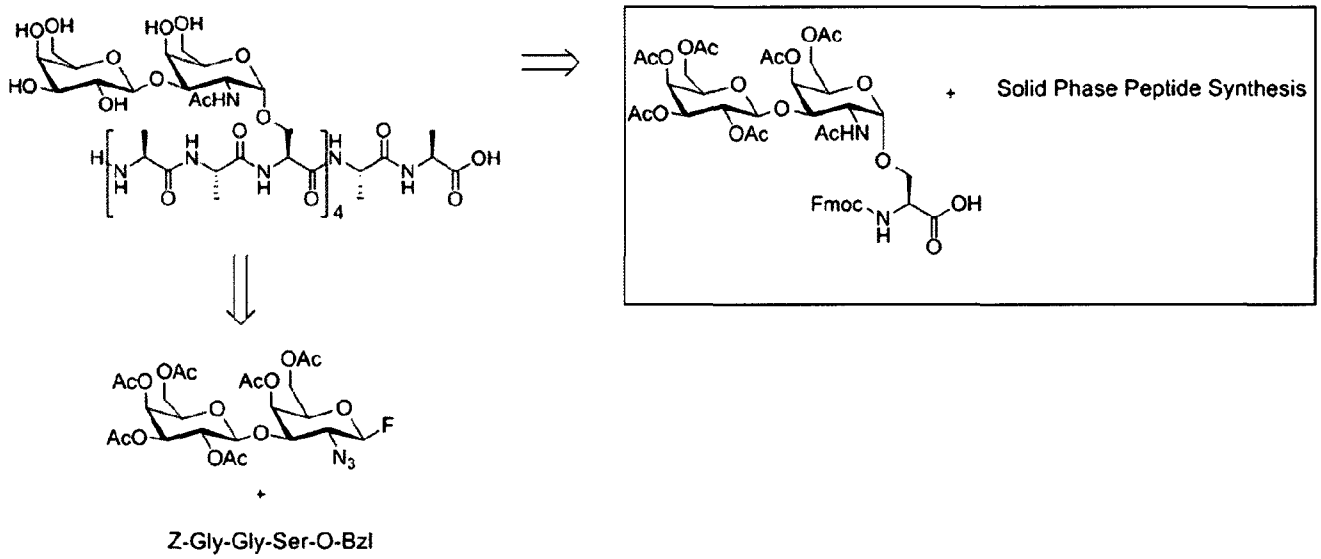


The synthesis of the glycoconjugate building block contains many challenges. First large amounts (~300 mgs) of the final glycoconjugates are needed for solid phase peptide synthesis. This is largely in part due to the loss of compound during high performance liquid chromatography purification. Secondly, which unfortunately adds to the first challenge is that these glycoconjugates require several steps to synthesize. They are *O*-linked to a serine amino acid, yet contain a C2 participating N-acetyl group. As a result the synthesis must involve a precursor to and N-acetyl moiety in the C2 position during coupling to serine. This is typically

achieved with the use of an azide acting as a masking group for the acetylated amine. Next, the disaccharide needs to be synthesized since commercially they are very expensive, ~ $245 per 5 mgs. As a result the primary synthesis would be that of an orthogonally protected galactose glycosyl acceptor containing a C2 azide.

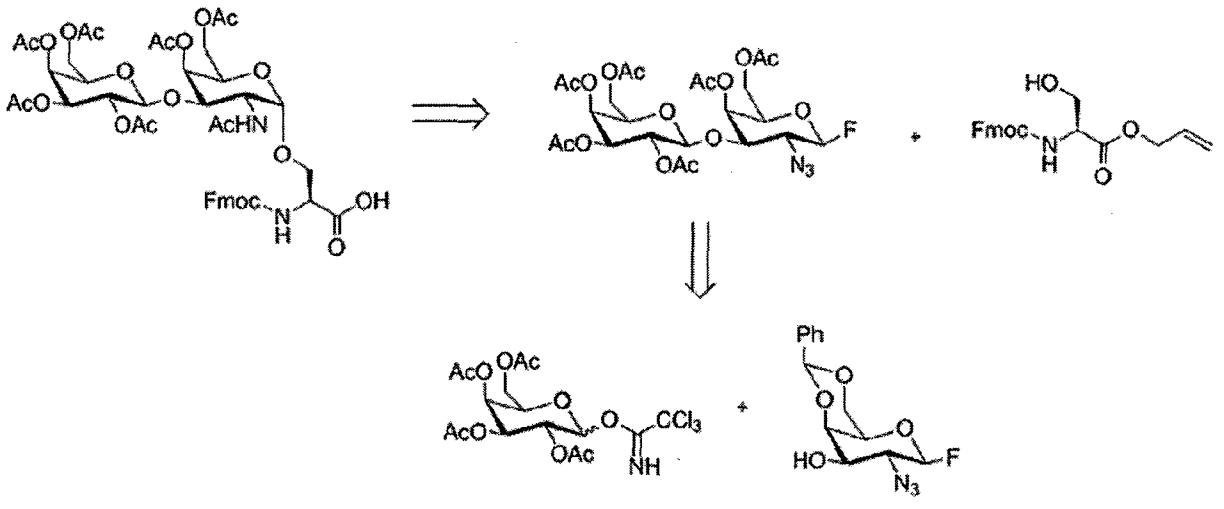


The synthesis begins with petaacetylated galactose which is α-brominated using 30 % HBr in acetic acid, which is obtained quantitatively (Scheme 3.3). To this bromosugar intermediate, zinc powder and 1-methyl imidazole were added and the solution was refluxed in ethyl acetate to produce the desired galactal in an 85 % yield. The next step involves an azido nitration step which requires sodium azide and cerium ammonium nitrate (CAN). [35] Azido nitration proceeds through a radical mechanism where first the azide ion is oxidized by cerium (IV), which is consequently reduced to cerium (III). The azide radical then attacks the double bond of the galactal, and a single electron transfer reduces another molecule of cerium (IV) to cerium (III) producing an oxocarbenium ion. A nitrate anion then adds to give a mixture of products, **11** below. This reaction also yields trace amounts of the talose derivative, which

produces an inseparable mixture of compounds until the conversion of the anomeric nitrate to

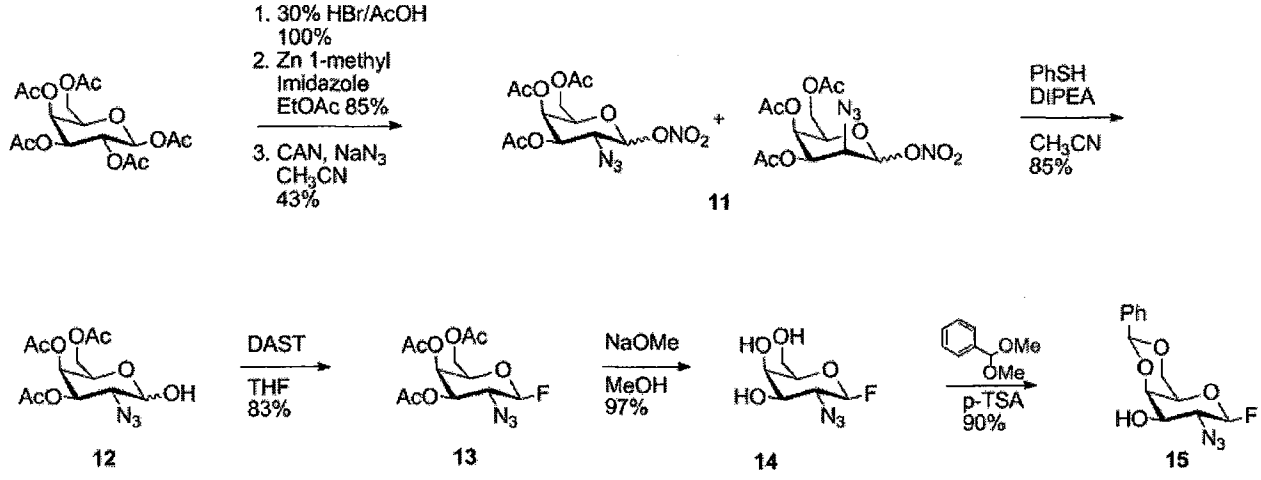


**Reaction Scheme 3.3** Synthesis of glycosyl acceptor 2-Azide-4,6-O-benzylidene-2-deoxy- D-galactopyranosyl fluoride **15**

the hydroxyl group. This is obtained in an 83 % yield using thiophenol and diisopropylethyamine (DIPEA) in acetonitrile. The following step uses diethyl amino sulphur trifluoride in tertrahydrofuran (THF) to fluorinate the anomeric position. This creates a functional group that is useful during the coupling to serine, but also orthogonally protects the anomeric centre during the remaining synthesis. The final two steps involve deacetlyation of C3, C4 and C6 using catalytic sodium in methanol, then selectively reprotecting with a 4,6-O-benzylidene group, producing the glycosyl acceptor **15** shown in Scheme 3.3.

The following key step was the coupling of the glycosyl acceptor **15** to a suitable galactose glycosyl donor. As before the type of glycosylation used was the trichloroacetimidate method. But here the initial choice of promoter was trimethylsilyl trifluoromethanesulfone or TMS-OTf. This method however, is quite sensitive, and requires rigorous attention to the

reaction conditions. For example if the TMS-OTf is not freshly distilled, it can decompose to produce traces of triflic acid. This will remove the acid-labile 4,6-O-benzylidene group, exposing a primary alcohol that will preferentially couple over the desired C3 hydroxyl group. Furthermore, if there are even trace amounts of water present, it will hydrolyze molecules of activated trichloroacetimidate acceptor, producing a hydroxyl group that can dimerize. These

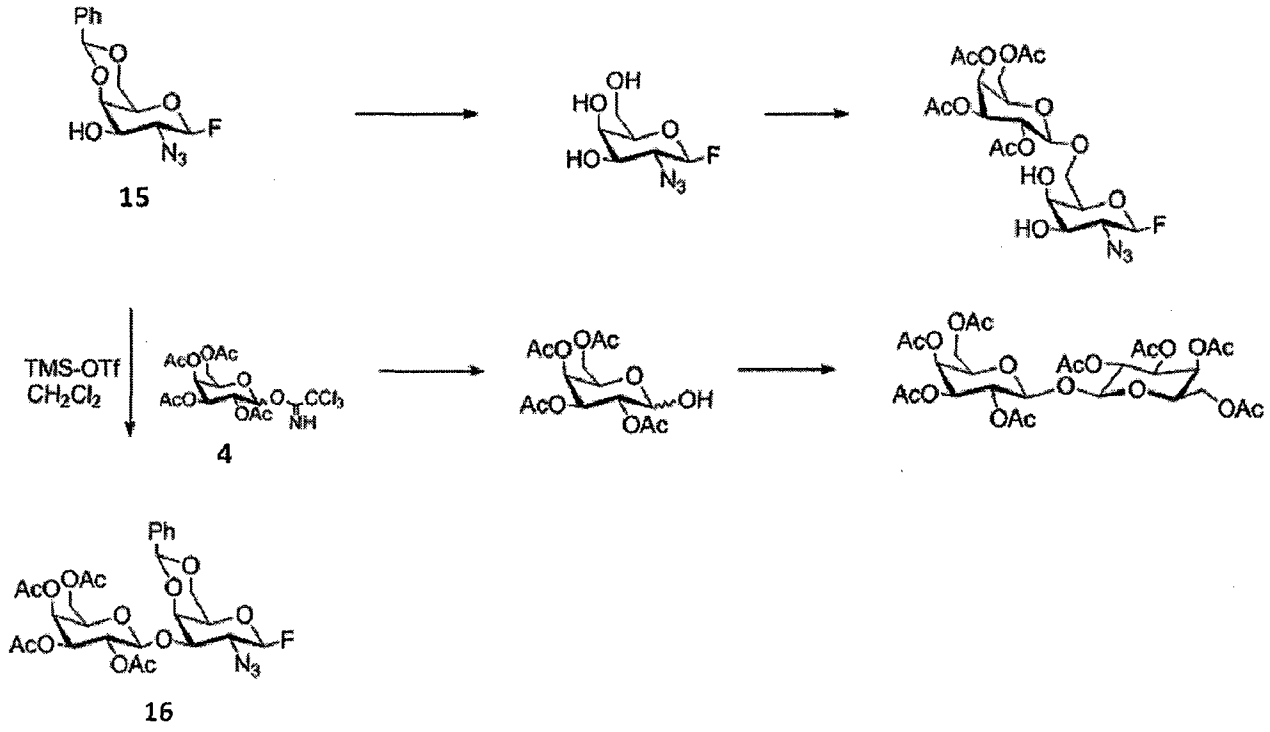


**Figure 3.16** Side Reactions during the glycosylation reaction between **15** and **4**

side reactions, along with the hydrolyzed TCA-sugar and the desired disaccharide produce a mixture of carbohydrates that is extremely difficult to separate via silica gel column chromatography. Therefore different reaction conditions and glycosyl donors were tested in attempts to increase the original isolated yield of 7 % (first entry Table 3.1). All the reactions

were preformed in flame dried glassware with 4 Å molecular sieves, under argon. The glycosyl acceptors and donors were dried under high vacuum for a minimum of 16 hours, and the promoters were all freshly distilled immediately prior to the reaction. First the glycosyl donor was changed to the bromosugar, using AgOTf as a promoter resulted in no isolated product. This was also the case when promoter $Pd(CH_3CN)_4(BF_4)_2$, was used in place of TMS-OTf, and when all three reaction conditions were preformed with benzoylated glycosyl donors.

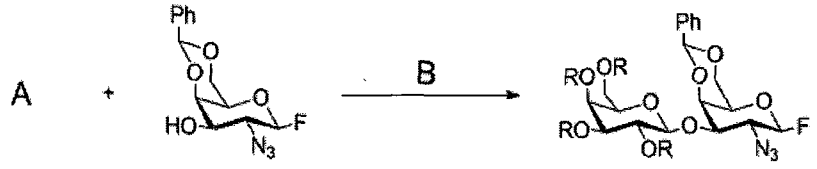


| A | B | %Yeild |
|---|---|---|
| 1.2 eq 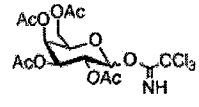 | TMS-OTf 0.1eq<br>$CH_2Cl_2$<br>-15 °C | 7% product<br>(1-6) byproduct<br>(1-1) dimer<br>Hydrolyzed TCA sugar |
| 1.4 eq 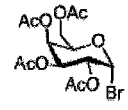 | AgOTf 1.5eq<br>2,6 Lutidine<br>$CH_2Cl_2$<br>RT 24h | Hydrolyzed Bromosugar |
| 1.3eq 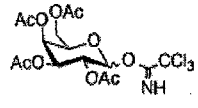 | $Pd(CH_3CN)_4(BF_4)_2$<br>0.05eq<br>$CH_2Cl_2$ | (1-1) Dimer and<br>Hydrolysed TCA sugar |
| 1.3eq 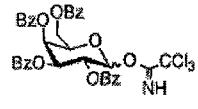 | $Pd(CH_3CN)_4(BF_4)_2$<br>0.05eq<br>$CH_2Cl_2$ | (1-1) Dimer and<br>Hydrolysed TCA sugar |
| 1.4eq 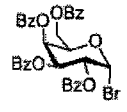 | AgOTf 1.5eq<br>2,6 Lutidine<br>$CH_2Cl_2$<br>RT 24h | Hydrolyzed Bromosugar |
| 1.3eq 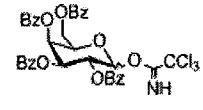 | TMS-OTf 0.1eq<br>$CH_2Cl_2$<br>-15 °C | (1-1) Dimer and<br>Hydrolysed TCA sugar |
| 2.0eq 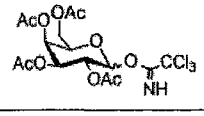 | TMS-OTf 0.1eq<br>$CH_2Cl_2$<br>-78 °C | 46% product<br>(1-6) byproduct<br>(1-1) dimer<br>Hydrolyzed TCA sugar |

**Table 3.1** Various glycosylation reaction conditions

This caused a reassessment the original reaction condition which led to increasing the trichloroacetimidate glycosyl donor equivalents to two and running the reaction at -78°C, resulting in a 50 % yield of product **16**. Although there was sufficient enough material to carry forward to the next step in the synthesis, the following steps produced low unoptimized yields. These were the removal of the 4,6-O-benzylidene group, re-protection with acetates and

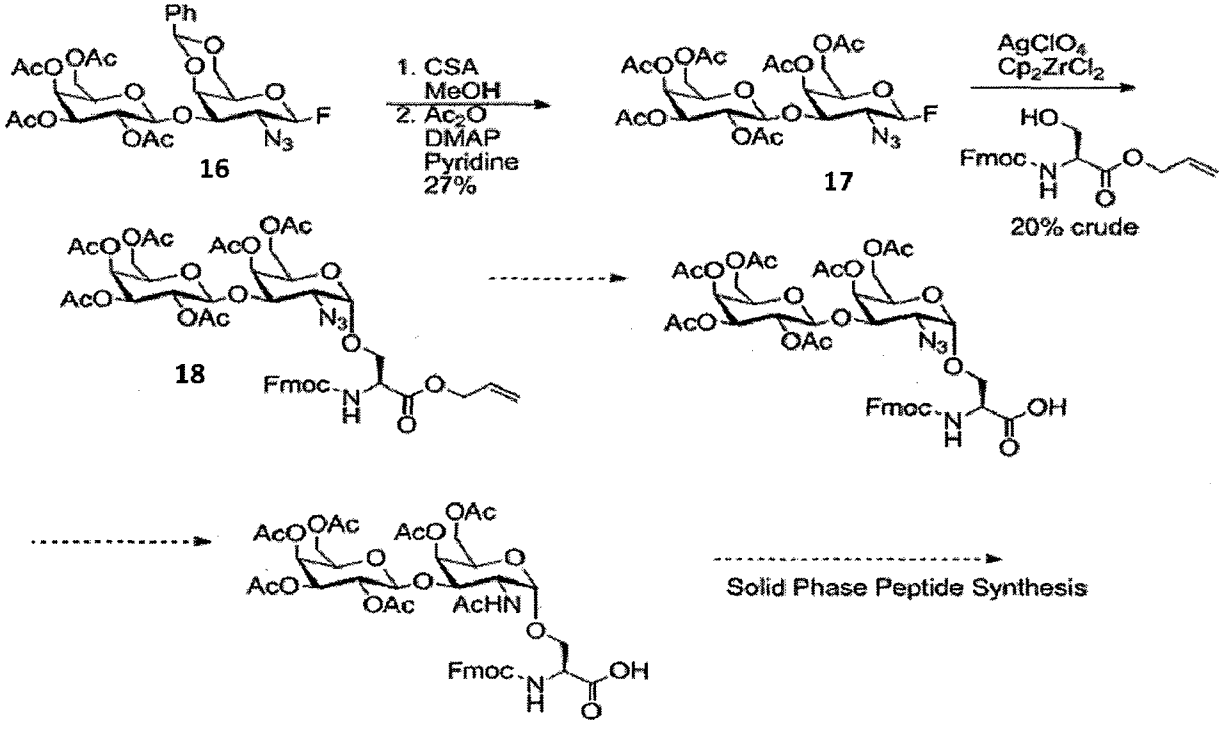


**Figure 3.16** Projected Synthesis of Glycoconjugate

the glycosydation to orthogonally protected serine amino acid (Figure 3.16). Unfortunately, due to time constraints the optimization of the final reactions remains incomplete. Yet, with new insight into the reaction conditions required to facilitate the glycosylation future attempts to synthesize this syAFGP should be successful.

**References 3.6**


1. Czechura, P.; Tam, R. Y.; Dimitrijevic, E.; Murphy, A. V.; Ben, R. N., *Journal of American Chemical Society*, **2008**, *130*, 2928.
2. Tam, R.Y.; Ferreira, S. S.; Czechura, P.; Chaytor, J. L.; Ben, R. N., *Journal of American Chemical Society*, **2008**, *130*, 17494.
3. Katenz, E., Vondran, F. W. R., Schwartlander, R., Pless, G., *Liver Transplantation*, **2007**, *13*, 38.
4. Bouvet, V. R. Lorello, G.R.; Ben, R. N., *Biomacromolecules*, **2006**, *7*, 565.
5. Uchida, T.; Nagayama, M.; Shibayama, T.; Gohara, K., *Journal of Crystal Growth*, **2007**, *299*, 125.
6. Galema, S. A.; Hoiland, H., *The Journal of Physical Chemistry*, **1991**, *95*, 5321.
7. Parke, S. A.; Birch, G. G.; Dijk, R., *Chemical Senses*, **1999**, *24*, 271.
8. Chakrabartty, A.; Hew, C. L., *European Journal of Biochemistry*, **1991**, *202*, 1057.
9. Baruch, E.; Belostotskii, A. M.; Mastai, Y. J., *Journal of Molecular Structure*, **2008**, *874*, 170.
10. Leinala, E. K.; Davies, P. L.; Jia, Z., *Structure*, **2002**, *10*, 619.
11. Baardsnes, J.; Davies, P. L., *Biochimica et Biophysica Acta*, **2002**, *1601*, 49.
12. Madura, J. D.; Baran, K.; Wierzbicki, A., *Journal of Molecular Recognition*, **2000**, *13*, 101.
13. Karim, O. A.; Haymet, A. D. J., *Journal of Chemical Physics Letters*, **1987**, *138*, 531.
14. Heyden, M.; Bründermann, E.; Heugen, U.; Niehues, G.; Leitner, D. M.; Havenith, M., *Journal of the American Chemical Society*, **2008**, *130*, 5773.

15. Wanga, J., *Carbohydrate Research*, **1998**, *308*, 191.

16. Espinosa, J. F.; Montero, E.; Vian, A.; Garcia, J. L.; Dietrich A. L.; Schmidt, R. R.; Martin-Lomas, M.; Imberty, A.; Canada, F. J.; Jimenez-Barbero, J., *Journal of American Chemical Society*, **1998**, *120,* 1309.

17. Ravishankar, R.; Surolia,A.; Vijayan, M.; Lim, S.; Kishi, Y., *Journal of the American Chemical Society*, **1998**, *120*, 11297.

18. Dashnau, J. L.; Sharp, K. A.; Vanderkooi, J. M., *Journal of Physical Chemistry*, **2005**, *109*, 24152.

19. Heng, B. C.; Ye, C. P.; Liu, H.; Toh, W. S.; Rufiahah, A. J.; Yang, Z.; Bay, B. H.; Ge, Z.; Ouyang, H. W.; Lee, E. H.; Cao, T. J., *Journal of Biomedical Science*, **2006**, *13,* 433.

20. Hanslick, J. L.; Lau, K.; Noguchi, K.K.; Olney, J. W.; Zorumski, C. F.; Mennerick, S.; Faber, N. B., *Neurobiology of Disease*, **2009**, 34, p. 1.

21. Gurtovenko, A. A.; Anwar, J., *The Journal of Physical Chemistry*, **2007**, *111*, 10453.

22. Notman, R.; Noro, M.; O'Malley, B.; Anwar, J., *Journal of the American Chemical Society*, **2006**, *128*, 13982.

23. Leseth, K.; Abrahamsen, J. F.; Bjorsvik, S.; Grottebo, K.; Bruserud, O., *Cryotherapy*, **2005**, *4*, 328.

24. Huang, G. L., et al. *Journal Bioorganic Medicinal Chemistry Letters*, **2006**, *16,* 2042.

25. H. Amer et al., Carbohydrate Research, **2003**, *338*, 35.

26. Bouvet, R. V.; Ben, N. B., *Journal of Organic Chemistry*, **2006**, *71*, 3619.

27. Kinzy, W.; Schmidt R. R., *Advances in Carbohydrate Chemistry and Biochemistry*, **1994**,

*50*, 21.

28. Ritter, T. K.; Mong, K. T.; Liu, H.; Nakatani, T.; Wong, C., *Angewandte Chemie. International Edition in English*, **2003**, *42*, 4657.

29. Dubber, M.; Soerling, O.; Lindhorst, Th. K., *Organic Biomolecular Chemistry*, **2006**, *50*, 21.

31. Ross, A. J.; Sizova, O.; Nikolaev, A. V., *Carbohydrate Research*, **2006**, *341*, 1954.

31. Guibe, F., *Tetrahedron*, **1997**, *53*, 13509.

32. Corzana, F.; Busto, J. H.; Jimenez-Oses, G.; Asensio,J. L.; Barbero, J. J.; Peregrina, J. M.; Avenoza, A., *Journal of American Chemical Society*, **2006**, *128*, 14640.

33. Tachibana, Y. et al. *Angewandte*, **2004**, *119*, 874.

34. Simons, J. P.; Jockusch, R. A.; Carcabal, P.; Hunig, I.; Kroemer, R. T.; MacLeod, N. A.; Snoek, L. C., *International Reviews in Physical Chemistry*, **2005**, *24*, 489.

35. Lemieux, R. U.; Ratcliffe, R. M., *Canadian Journal of Chemistry*, **1979**, *57*, 1244.

# *CHAPTER 4*

# *Experimental Procedures*

## 4.1 General Procedures

Unless otherwise stated all anhydrous reactions were performed in flame-dried or oven-dried glassware under a positive pressure of dry argon or nitrogen. Air or moisture-sensitive reagents and anhydrous solvents were transferred with oven-dried syringes or cannulae. All flash chromatography was performed with E. Merck silica gel 60 (230-400 mesh). All solution phase reactions were monitored using analytical thin layer chromatography (TLC) with 0.2 mm pre-coated silica gel aluminum plates 60 F254 (E. Merck). Components were visualized by illumination with a short-wavelength (254 nm) ultra-violet light and/or staining (ceric ammonium molybdate, potassium permanganate, phosphomolybdate stain, or orcinol stain solution).

## 4.2 Solvents

All solvents used for anhydrous reactions were distilled. Tetrahydrofuran (THF) and diethyl ether were distilled from sodium/benzophenone under nitrogen atmosphere. Dichloromethane, acetonitrile, triethylamine, benzene and diisopropylethylamine (DIPEA) were distilled from calcium hydride. Methanol was distilled from calcium sulfate. Hexanes were

distilled from phosphorus pentoxide. *N,N*-dimethylformamide (DMF) and acetone were stored over activated 4Å molecular sieves under argon atmosphere.

All deuterated solvents ($CDCl_3$, $CD_3OD$ and $D_2O$) were obtained from Cambridge Isotope Laboratories Ltd. and $CDCl_3$ was stored over Linde 4Å molecular sieves.

**4.3 Instrumentation**

$^1H$ (300, 360, 400, or 500 MHz) and $^{13}C$ NMR (75, 90, 100 or 125 MHz) spectra were recorded at ambient temperature on a Bruker Avance 300, Bruker AM 360, Bruker Avance 400, Bruker Avance 500, or INOVA 500 spectrometer. Chemical shifts are reported in ppm downfield from TMS and corrected using the solvent residual peak or TMS as an internal standard. Splitting patterns are designated as follows: s, singlet; d, doublet; t, triplet; q, quartet; m, multiplet and br, broad. Low resolution mass spectrometry (LRMS) was performed on a Micromass Quatro-LC Electrospray spectrometer with a pump rate of 20μL/min using electrospray ionization (ESI) or a Voyager DE-Pro matrix-assisted desorption ionization-time of flight (MALDI-TOF), (Applied Biosystem, Foster City, CA) mass spectrometer operated in the reflectron/positive-ion mode with DHB in 20 % EtOH/$H_2O$ as the MALDI matrix. High resolution mass spectrometry (HRMS) data was acquired on Applied Biosystems/Sciex QStar (Concord, ON). Samples in $CH_2Cl_2$/MeOH 1:1 were mixed with Agilent ES tuning mix for internal calibration, and infused into the mass spectrometer at 5 μL/min. Infrared absorption spectra (IR) were recorded on a Shimadzu FTIR-8400S spectrometer as a neat film from 4000 $cm^{-1}$ to 650 $cm^{-1}$. Analytical and preparatory scale RP-HPLC were carried out with C-18 columns on a

Varian Dynomax HPLC system equipped with a variable wavelength detector (ProStar 330 PDA) or a Waters Delta 600E HPLC system equipped with a variable wavelength detector.

## 4.4 Synthetic Procedures

### 4.4.1 Reaction Scheme 1, Synthesis of Allyl-β-D-galactopyranosyl-(1→3)-2-acetamido-2-deoxy-β-D-galactopyranoside

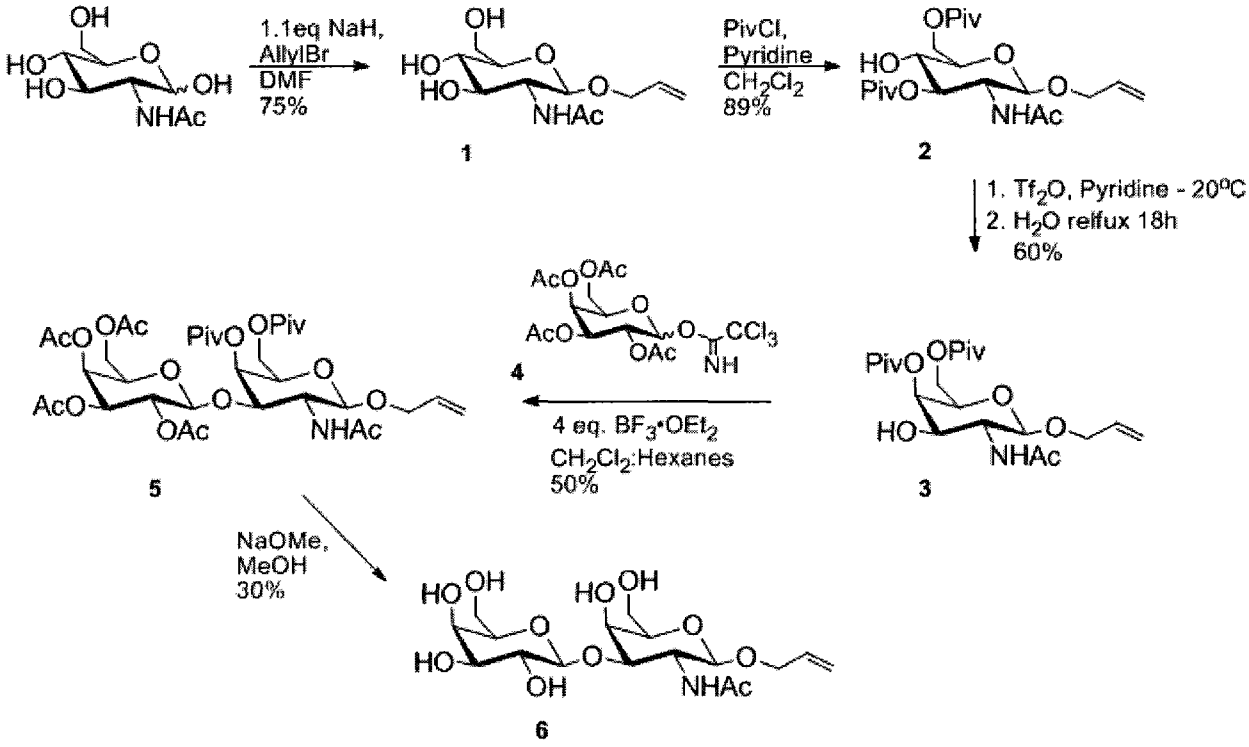


#### 4.4.1.1 Synthesis of allyl 2-acetamido-2-deoxy- $\beta$ -D-glucopyranoside (1)

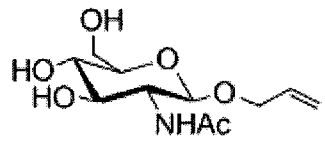

2-acetamido-2-deoxy-β-D-glucopyranoside (4.42 g, 0.020mol) was suspended in DMF (30 mL) under nitrogen. Cool to 0°C, after which 60 % sodium hydride (0.88 g, 0.022mol) and allyl bromide (5.19 mL, 0.060mol) were added. The crude product, was an α:β mixture of 1:2.5 and was purified by flash column chromatography (4:1 EtOAc-MeOH), and 2.53 g of β-allyl glycoside **1** as a solid was obtained in 48 % yield. [1]

$^1$H NMR (400 MHz, $D_2O$) δ ppm 5.98–5.88 (m, 1H), 5.35–5.26 (m, 2H), 4.59 (d, *J* = 8.5Hz, 1H), 1H NMR 4.59 (d, *J* = 8.50 Hz, 1H), 4.36 (dddd, *J* = 13.2, 5.2, 1.4, 1.4 Hz, 1H), 4.18 (dddd, *J* = 13.2, 6.3, 1.3, 1.3 Hz, 1H), 3.94 (dd, *J* = 12.3, 1.6 Hz, 1H), 3.79-3.71 (m, 2H), 3.59-3.54 (m, 1H), 3.48-3.44 (m, 2H), 2.06 (s, 3H). [1]

*Spectral Data in accordance with reference 1*

### 4.4.1.2 Synthesis of allyl 2-acetamido-2-deoxy-3,6-di-O-pivaloyl- $\beta$ -D-glucopyranoside (2)

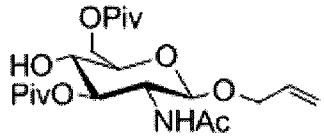


A mixture of **1** (1.7 g, 6.5 mmol), pyridine (2 mL) and $CH_2Cl_2$ (25 mL) was cooled to 0°C. Pivaloyl chloride (2.09 mL, 17.0 mmol), was added dropwise. The solution was stirred and allowed to warm to room temperature overnight. The solution was further diluted with $CH_2Cl_2$ (100 mL), extracted twice with saturated $CuSO_4$ solution, twice with water, dried ($MgSO_4$), and concentrated under reduced pressure. The residue was purified by flash column chromatography (7:3 Ethyl Acetate: Hexanes), to yield compound **2** (2.40 g, 86 %). [2]

$^{1}$H NMR (400 MHz, $CDCl_3$) δ ppm 5.85 (dddd, *J* = 17.0, 10.5, 6.4, 4.9 Hz, 1H), 5.57 (d, *J* = 9.27 Hz, 1H), 5.26 (ddd, J = 17.3, 3.2, 1.6, Hz, 1H), 5.18 (ddd, J = 10.4, 2.8, 1.3 Hz, 1H), 5.03 (dd, J = 10.7, 8.8 Hz, 1H), 4.52 (d, J = 8.3 Hz, 1H), 4.41-4.38 (m, 1H), 4.31 (dddd, *J* = 13.1, 4.8, 1.5, 1.5 Hz, 1H), 4.07 (dddd, *J* = 13.1, 6.4, 1.3, 1.3 Hz, 1H), 3.98 (ddd, *J* = 10.7, 9.2, 8.5 Hz, 1H), 3.55-3.50 (m, 1H), 2.95 (d, *J* = 4.3, 1H), 1.93 (s, 3H), 1.24 (s, 9H), 1.20 (s, 9H). [2]

$^{13}$C NMR (100 MHz, $CDCl_3$) δ 179.8, 179.2, 169.9 ,133.8, 117.6, 100.0, 74.9, 74.3, 69.5, 69.5, 63.2, 53.9, 39.0, 39.0, 27.2, 27.1, 23.3. [2]

Spectral Data in accordance with reference 2

**4.4.1.3 Synthesis of allyl 2-acetamido-2-deoxy-4,6-di-O-pivaloyl- β -D-galacopyranoside (3)**

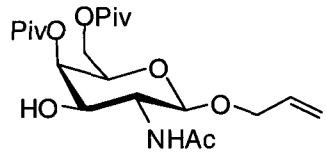


Compound 2 (2.4 g, 5.6 mmols) was dissolved in $CH_2Cl_2$ (20 mL) and Pyridine (1 mL). The solution was cooled to -35°C and triflic acid anhydride (1.13 mL, 6.7 mmols) was added dropwise. The solution was allowed to stir to room temperature over a period of 3 h. Water (0.24 mL, 13.4 mmols) was added and the solution was heated to reflux over 16 h. The solution was diluted with $CH_2Cl_2$ (50 mL), extracted with saturated $CuSO_4$ solution, water, dried over $MgSO_4$, and concentrated. The residue was purified by flash column chromatography (Ethyl Acetate), to yield compound **3** (1.4 g, 60 %). [2]

$^1$H NMR (400 MHz, $CDCl_3$) δ 5.91 (dddd, *J* = 17.1, 10.4, 6.6, 5.2 Hz, 1H), 5.70 (d, *J* = 4.8 Hz, 1H), 5.35-5.24 (m, 3H), 4.58 (d, *J* = 8.3 Hz, 1H), 4.40-4.32 (m, 2H), 4.21-3.97 (m, 4H), 3.88 (ddd, *J* = 7.3, 6.1, 1.2 Hz, 1H), 3.68 (ddd, *J* = 10.4, 8.3, 5.1 Hz, 1H), 2.05 (s, 3H), 1.27 (s, 9H), 1.20 (s, 9H) [2]

Spectral Data in accordance with reference 2

#### 4.4.1.4 Synthesis of 2,3,4,6-Tetra-O-acetyl-D-galactopyranosyl trichloroacetimidate (4)

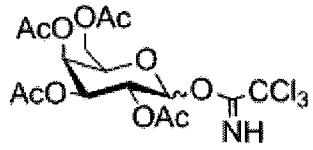


A solution of pentaacetate-D-galactose (3.9 g, 10 mmols) and $BnNH_2$ (1.2 mL, 11 mmols) in THF (45 mL) was stirred at 50 °C for 18 h. The solvent was removed under reduced pressure and the residue was dissolved in $CH_2Cl_2$ and extracted with 10 % (v/v) HCl and water. The organic layer was concentrated and the residue was purified by flash column chromatography (1:1 Ethyl Acetate: Hexanes), to yield the anomerically deprotected tetraacetylated galactose (2.6 g, 75 %). This product was redissolved in $CH_2Cl_2$ (120 mL) and cooled to 0°C, to which $K_2CO_3$ (5.18 g, 37 mmols) and trichloroacetimidate (7.47 mL, 74 mmols) were added and allowed to stir to ambient temperature over 18 h. The solution was filtered through celite and concentrated. The residue was purified by flash column chromatography (1:1 Ethyl Acetate: Hexanes), to yield compound **4** (3.34 g, 91 %) as an α:β mixture.

$^1$H NMR (400 MHz, $CDCl_3$) δ ppm 8.70 (s, 1H), 8.65 (s, 1H), 6.55 (d, *J* = 3.5 Hz, 1H), 5.80 (d, *J* = 8.2 Hz, 1H), 5.51 (dd, *J* = 3.1, 1.2 Hz, 1H), 5.48-5.40 (m, 2H), 5.38 (dd, *J* = 10.9, 3.1 Hz, 1H), 5.31 (dd, *J* = 10.9, 3.5 Hz, 1H), 5.09 (dd, *J* = 10.4, 3.5 Hz, 1H), 4.40 (dt, *J* = 6.6, 6.6, 0.7 Hz, 1H), 4.15-4.01

(m, 6H), 2.14 (s, 3H), 2.12 (s, 3H), 2.00 (s, 3H), 1.98 (s, 3H), 1.98 (s, 3H), 1.97 (s, 3H), 1.97 (s, 3H), 1.96 (s, 3H). [3]

Spectral Data in accordance with reference 3

**4.4.1.5 Synthesis of Allyl 2,3,4,6-tetra-*O*-acetyl- $\beta$ -D-galactopyranosyl-(1→3)-2-acetamido-2-deoxy-4,6-di- *O*-pivaloyl- $\beta$ -D-galactopyranoside (5)**

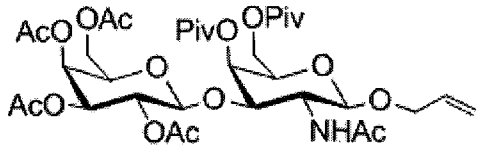


A solution of **4** (0.52 g, 1.1 mmols) in $CH_2Cl_2$ (5 mL) and hexanes (5 mL) was added dropwise to a solution of **3** (458 mg, 1.1 mmols), $BF_3 \cdot OEt_2$ (0.53 mL, 4.4 mmols) and 4 Å molecular sieves in $CH_2Cl_2$ (5 mL) and hexanes (5 mL) at -25 °C, under $N_2$. After an hour a second equivalent of **4** (0.52 g, 1.1 mmols) was added, and the reaction was monitored for completion by thin layer chromatography (8:2 Ethyl Acetate: Hexanes). The reaction was quenched with TEA, filtered through a pad of silica gel (Ethyl Acetate), and concentrated. The residue was purified by flash column chromatography (1:1 Ethyl Acetate: Hexanes), to yield compound **4** (450 mg, 54 %).

$^1$H NMR (400 MHz, $CDCl_3$) δ ppm 5.87 (dddd, *J* = 15.9, 10.4, 6.3, 5.5 Hz, 1H), 5.66 (d, *J* = 6.9 Hz, 1H), 5.39 (d, *J* = 3.3 Hz, 1H), 5.32 (dd, *J* = 3.3, 0.8 Hz, 1H), 5.26 (m,1H), 5.20 (m, 1H), 5.07 (m, 2H), 4.95 (dd, *J* = 10.4, 3.4 Hz, 1H), 4.73 (dd, *J* = 10.8, 3.6 Hz, 1H), 4.59 (d, *J* = 7.8 Hz, 1H), 4.34-4.29 (m, 1H), 4.16-4.04 (m, 4H), 4.00-3.95 (m,1H), 3.89-3.83 (m, 2H), 3.26-3.20 (m,2H), 2.11, 2.05, 2.03, 1.96, 1.95 (5 s, 15H), 1.23 (s, 9H), 1.19 (s, 9H). [2]

Spectral Data in accordance with reference 2

### 4.4.1.6 Synthesis of Allyl-β-D-galactopyranosyl-(1→3)-2-acetamido-2-deoxy-β-D-galactopyranoside (6)

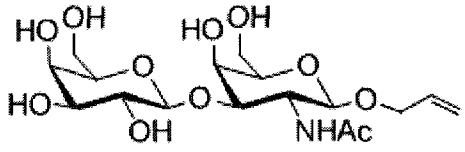


To a solution of **5** (300 mgs, 0.40 mmol) in MeOH (5 mL) cooled to 0 °C, 1 M solution of methanolic NaOMe was added to a pH of 9. The reaction was stirred to ambient temperatures for 24 hours, or until complete by thin layer chromatography. The solution was neutralized using Dowex 50 ($H^+$) resin, and the methanol was removed under reduced pressure. The product was isolated by recrystalization with methanol: ethyl acetate mixtures. The final product **6** (64 mg, 37 %) was isolated as white crystals.

$^1$H NMR (400 MHz, $D_2O$) δ ppm 5.90 (dddd, *J* = 17.0, 10.5, 6.3, 5.2 Hz, 1H), 5.30 (ddd, *J* = 17.4, 3.2, 1.6 Hz, 1H), 5.27-5.24 (m, 1H), 4.54 (d, *J* = 8.6 Hz, 1H), 4.42 (d, *J* = 7.7 Hz, 1H), 4.34 (tdd, *J* = 13.3, 5.1, 1.4, 1.4 Hz, 1H), 4.20-4.11 (m, 2H), 4.01 (dd, *J* = 10.9, 8.5 Hz, 1H), 3.90-3.55 (m, 9H), 3.51 (dd, 1H), 2.01 (s, 3H). [2]

HRMS (ESI): Calcd for $C_{17}H_{29}NO_{11}$ $[M+NH_4]^+$ 446.164, found 446.160

Spectral Data in accordance with reference 2

### 4.4.2 Reaction Scheme 2, Synthesis of Allyl-β-D-galactopyranosyl-(1→4)-2-acetamido-2-deoxy-β-D-galactopyranoside

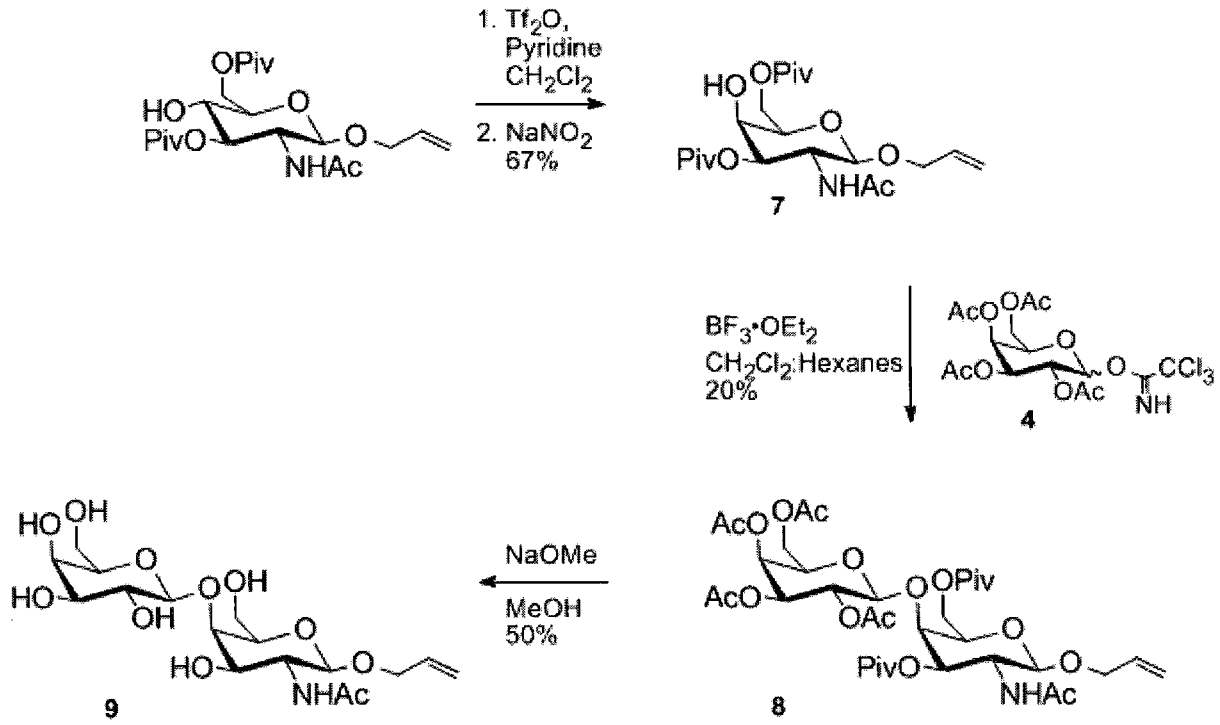


**4.4.2.1 Synthesis of allyl 2-acetamido-2-deoxy-3,6-di-O-pivaloyl- $\beta$ -D-galacopyranoside (7)**

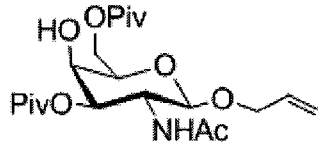


Trifluoromethanesulfonic anhydride (0.28 mL, 1.6 mmol) was added dropwise at -15 °C under $N_2$ to a solution of **2** (0.50 g, 1.2 mmol) in dry $CH_2Cl_2$ (5 mL) and pyridine (0.5 mL). The solution was stirred and allowed to warm to ambient temperature over a period of 2 h. After which crushed ice was added and the solution was diluted with $CH_2Cl_2$ (25 mL). The solution was extracted with brine, water, dried with $MgSO_4$, and concentrated under reduced pressure, to obtain the crude triflated intermediate. The residue was then dissolved in DMF (10 mL) and

$NaNO_2$ (0.29 g, 4.3 mmol) was added and allowed to stir at ambient temperature for 3 h. The solution was then poured into ice cold water and extracted with ethyl acetate. The combined organic layers were then washed with 10 % (v/v) HCl solution, and water, dried ($MgSO_4$), and concentrate. The residue was purified by flash column chromatography (1:1 Ethyl Acetate: Hexanes), to yield compound **4** (335 mg, 67 %).

$^1$H NMR (400 MHz, $CDCl_3$) δ ppm 5.90-5.79 (m, 2H), 5.24 (ddd, *J* = 17.4, 3.2, 1.6 Hz, 1H), 5.19-5.13 (m, 1H), 5.08 (dd, *J* = 11.2, 3.2 Hz, 1H), 4.58 (d, *J* = 8.4 Hz, 1H), 4.35-4.27 (m, 3H), 4.22 (td, *J* = 11.1, 8.8, 8.8 Hz, 1H), 4.11- 4.04 (m, 1H), 3.96-3.92 (m, 1H), 3.77 (t, *J* = 6.3, 6.3 Hz, 1H), 1.92 (s, 3H), 1.20 (s, 18H)

$^{13}$C NMR (100 MHz, $CDCl_3$) δ ppm 178.5, 178.3, 171.1, 133.9, 117.4, 100.4, 72.6, 72.3, 69.9, 66.9, 62.9, 50.6, 39.0, 38.7, 27.1, 27.0, 23.0

**4.4.2.2 Synthesis of Allyl 2,3,4,6-tetra-*O*-acetyl- β -D-galactopyranosyl-(1→4)-2-acetamido-2-deoxy-4,6-di- *O*-pivaloyl- β -D-galactopyranoside (8)**

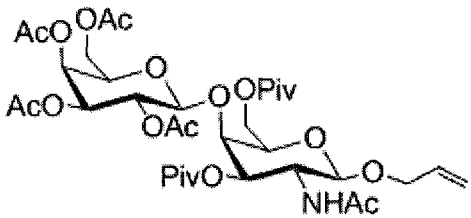


A solution of **4** (0.11 g, 0.22 mmols) in $CH_2Cl_2$ (2 mL) and hexanes (2 mL) was added dropwise to a solution of **3** (100 mg, 0.22 mmols), $BF_3$•$OEt_2$ (0.12 mL, 0.88 mmols) and 4 Å molecular sieves in $CH_2Cl_2$ (2 mL) and hexanes (2 mL) at -25 °C, under $N_2$. After an hour a second equivalent of **4** (0.11 g, 0.22 mmols) was added, and the reaction was monitored for completion by thin layer

chromatography (8:2 Ethyl Acetate: Hexanes). The reaction was quenched with TEA, filtered through a pad of silica gel (Ethyl Acetate), and concentrated. The residue was purified by flash column chromatography (1:1 Ethyl Acetate: Hexanes), to yield compound **8** (33 mg, 20 %).

$^1$H NMR (400 MHz, $CDCl_3$) δ ppm 5.85 (dddd, *J* = 17.0, 10.4, 6.6, 4.8 Hz, 1H), 5.38 (dd, *J* = 3.4, 1.0 Hz, 1H), 5.31 (dd, *J* = 10.6, 7.9 Hz, 1H), 5.24 (ddd, *J* = 17.2, 3.2, 1.6 Hz, 1H), 5.21-5.15 (m, 2H), 5.00 (dd, *J* = 11.2, 2.8 Hz, 1H), 4.90 (dd, *J* = 10.6, 3.4 Hz, 1H), 4.63 (d, *J* = 8.0 Hz, 1H), 4.39 (d, *J* = 8.4 Hz, 1H), 4.36-4.05 (m, 7H), 4.02 (d, *J* = 2.4 Hz, 1H), 3.82 (dt, *J* = 6.9, 6.7, 1.0 Hz, 1H), 3.69 (m, 1H), 2.23 (s, 3H), 2.16 (s, 3H), 2.04 (s, 3H), 1.98 (s, 3H), 1.91 (s, 3H), 1.23 (s, 9H), 1.21 (s, 9H)

### 4.4.2.3 Synthesis of Allyl-β-D-galactopyranosyl-(1→4)-2-acetamido-2-deoxy-β-D-galactopyranoside (9)

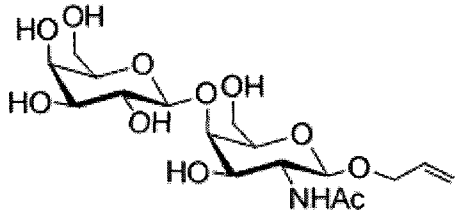


To a solution of **8** (20 mgs, 0.03 mmol) in MeOH (5 mL) cooled to 0 °C, 1 M solution of methanolic NaOMe was added to a pH of 9. The reaction was stirred to ambient temperatures for 24 hours, or until complete by thin layer chromatography. The solution was neutralized using Dowex 50 ($H^+$) resin, and the methanol was removed under reduced pressure. The product was isolated by recrystalization with methanol: ethyl acetate mixtures. The final product **9** (6 mg, 50 %) was isolated as white crystals.

$^1$H NMR (500 MHz, $CDCl_3$) δ ppm 5.79-5.70 (m, 1H), 5.17-5.12 (m, 1H), 5.12-5.03 (m, 1H), 4.42 (d, *J* = 7.2 Hz, 1H), 4.38 (d, *J* = 8.6 Hz, 1H), 4.20-4.15 (m, 1H), 4.04-3.97 (m, 2H), 3.84 (dd, *J* = 10.8, 8.6 Hz, 1H), 3.74 (d, *J* = 2.9 Hz, 1H), 3.71 (dd, *J* = 11.8, 6.1 Hz, 1H), 3.68-3.44 (m, 9H), 1.88 (s, 3H)

$^{13}$C NMR (126 MHz, $D_2O$) δ ppm 174.9, 133.3, 118.1, 104.3, 100.2, 76.31, 75.0, 74.1, 72.6, 71.5, 71.2, 70.2, 68.5, 60.9, 60.4, 52.8, 22.1

HRMS (ESI): Calcd for $C_{17}H_{29}NO_{11}$ $[M+NH_4]^+$ 446.164, found 446.177

**4.4.2.4 Synthesis of allyl 2-acetamido-2-deoxy-β-D-galactopyranoside (10)**

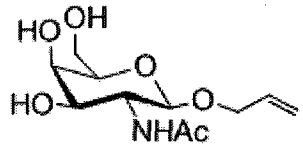


To a solution of **7** (1.61 g, 3.75 mmol) in MeOH (50 mL) cooled to 0 °C, 1M solution of methanolic NaOMe was added to a pH of 9. The reaction was stirred at ambient temperatures for 24 hours, or until complete by thin layer chromatography. The solution was neutralized using Dowex 50 ($H^+$) resin, and the methanol was removed under reduced pressure. The residue was purified by flash column chromatography (8:2 Ethyl Acetate: Methanol), to yield compound **10** (550 mgs, 56 %) as a white solid.

$^1$H NMR (400 MHz, $D_2O$) δ ppm 5.90 (dddd, *J* = 16.9, 10.5, 6.3, 5.2 Hz, 1H), 5.30 (ddd, *J* = 17.4, 3.2, 1.6 Hz, 1H), 5.27-5.23 (m, 1H), 4.49 (d, *J* = 8.5 Hz, 1H), 4.34 (tdd, *J* = 13.2, 5.2, 1.4, 1.4 Hz, 1H), 4.16 (tdd, *J* = 13.3, 6.3, 1.2, 1.2 Hz, 1H), 3.95-3.86 (m, 1H), 3.84-3.65 (m, 4H), 2.03 (s, 3H) [4]

Spectral data in accordance with reference 4

### 4.4.3 Reaction Scheme 3 Synthesis of Glycosyl Acceptor: 2-Azide-4,6-O-benzylidene-2-deoxy-D-galactopyranosyl fluoride

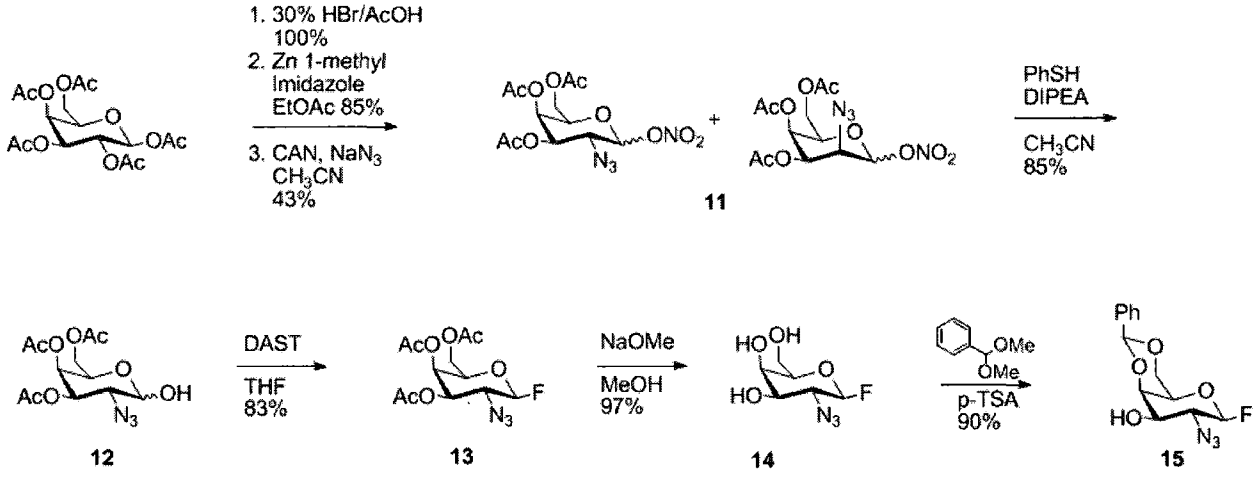


### 4.4.3.1 Synthesis of 3,4,6-tri-O-Acetyl-2-azido-2-deoxy-β/α-D-galactopyranosyl nitrate and , 3,4,6-tri-O-Acetyl-2-azido-2-deoxy-β/α-D-talopyranosyl (11)

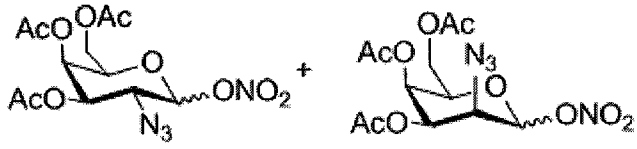

To a solution of 30 % HBr in Acetic acid (60 mL) cooled to 0°C, commercially available pentaacetylated-β-galactopyranoside (20.0 g, 0.051mol), was added. The solution was stirred for 45 min, then diluted with $CH_2Cl_2$ and extracted several times with water until the organic layer was a neutral pH, then dried with $MgSO_4$, and concentrated. The α-bromo galactopyranoside (20.9 g, quantitative yield) was achieved without purification, and carried forward to the next step.

A mixture of 1-methyl imidazole (1.03 mL, 12.9 mmol), zinc (5.06 g, 77.4 mmol) and ethyl acetate (50 mL) was heated to reflux, to which a solution of α-bromo galactopyranoside (5.3 g, 13 mmol) dissolved in ethyl acetate (20 mL) as added dropwise over a period of 30 min. The reaction was refluxed for 3 h, or until deemed complete by thin layer chromatography. The reaction was extracted with 10 % HCl, saturated sodium bicarbonate solution, water and then dried with $MgSO_4$. The organic layers were concentrated and purified by flash column chromatography (7:3 Ethyl Acetate: Hexanes), to obtain galactal (3.0 g, 85 %).

Galactal (2.26 g, 9.2 mmols) was then dissolved in acetonitrile (70 mL) and cooled to -20°C, to which Cerium Ammonium Nitrate (19.0 g, 34.6 mmols) and sodium azide (0.93g, 14.4 mmol) were added. The solution was stirred at -20°C for 1 h and allowed to warm to room temperature and stirred at room temperature for 1 h. The organic later was diluted with ethyl acetate (150 mL) and extracted with water and dried with $MgSO_4$. The organic layers were concentrated and crudely purified with flash column chromatograph (7:3 Ethyl Acetate: Hexanes) to achieve an inseparable mixture of 3,4,6-tri-O-Acetyl-2-azido-2-deoxy-β/α-D-galactopyranosyl nitrate and 14 % of 3,4,6-tri-O-Acetyl-2-azido-2-deoxy-β/α-D-talopyranosyl **11** (1.56 g, 43 %). [5]

Spectral data in accordance with Reference 5

**4.4.3.2 Synthesis of 3,4,6-Tri-O-acetyl-2-azide-2-deoxy-D-galactopyranosyl fluoride (13)**

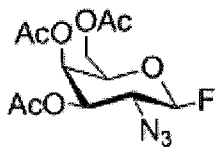

The mixture of compounds **11** (1.8 g, 4.8 mmol), was dissolved in acetonitrile (13.2 mL) and cooled to 0°C, to which diisopropyl ethyl amine (0.83 mL, 4.8 mmol) and thiophenol (1.45 mL, 14.4 mmol) and stirred to ambient temperature over a period of 2 h, or until the reaction was deemed complete by thin layer chromatography (3:7 Ethyl Acetate: Hexanes). The reaction concentration and purified by flash column chromatography (3:7 Ethyl Acetate: Hexanes) to yield the anomerically deprotected intermediate **12** (1.35 g, 85 %).

The intermediate **12** (0.500 g, 1.15 mmol) was then dissolved in THF (6 mL) and cooled to -20°C. Diethyl amino sulphur trifluoride, DAST, (0.41 mL, 1.2 mmol) was added and the solution was stirred at -20°C for 1 hour. The reaction was quenched by the addition of MeOH (2 mL). The solution was diluted with $CH_2Cl_2$ (50 mL) and extracted with water, saturated sodium bicarbonate solution, and brine, then dried with $MgSO_4$ and concentrated. The residue was purified with flash column chromatography (8:2 Toluene: Ethyl Acetate) to yield **13** (0.42 g, 83 %).

$^1$H NMR (400 MHz, $CDCl_3$) δ ppm 5.38-5.35 (m,1H), 5.11 (dd, *J* = 51.7, 7.5 Hz, 1H), 4.85 (ddd, *J* = 10.9, 3.3, 0.9 Hz, 1H), 4.18 (dd, *J* = 6.5, 1.6 Hz, 2H), 4.00-4.94 (m, 1H), 3.82 (ddd, *J* = 12.8, 11.1, 7.5 Hz, 1H). [6]

Spectral data in accordance with reference 6

**4.4.3.3 Synthesis of 2-Azide-4,6-O-benzylidene-2-deoxy-D-galactopyranosylfluoride (15)**

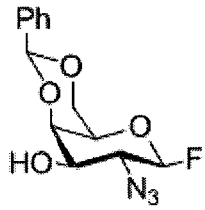


To a solution of **13** (1.24 g, 3.7 mmol) in MeOH (50 mL) cooled to 0 °C, 1 M solution of methanolic NaOMe was added to a pH of 9. The reaction was stirred to ambient temperatures for 24 hours, or until complete by thin layer chromatography. The solution was neutralized using Dowex 50 ($H^+$) resin, and the methanol was removed under reduced pressure. The residue was purified by flash column chromatography (8:2 Ethyl Acetate: Methanol), to yield compound **14** (70 g, 97 %) as a white solid.

To a solution of compound **14** (0.70 g, 3.6 mmol) in DMF (20 mL) camphor sulphonic acid (0.42 g, 1.8 mmol), benzaldehyde dimethylacetal (1.1 mL, 7.2 mmol) were added. The solution was stirred at 50 °C for 2 hours. The solution was diluted with ethyl actetate (100 mL) and extracted three times with water, then dried with $MgSO_4$, and concentrated. The residue was purified by flash column chromatography (7:3 Ethyl Acetate: Hexanes), to yield compound **15** (0.67 g, 62 %).

$^1$H NMR (400 MHz, $CDCl_3$) δ ppm 7.55-7.35 (m, 5H), 5.59 (s, 1H), 5.06 (dd, *J* = 52.2, 7.5 Hz, 1H), 4.39 (dd, *J* = 12.7, 1.6 Hz, 1H), 4.21 (ddd, *J* = 3.7, 2.7, 1.1 Hz, 1H), 4.10 (td, *J* = 12.6, 1.8, 1.8 Hz, 1H), 3.75 (ddd, *J* = 11.9, 10.2, 7.5 Hz, 1H), 3.66 (br s, 1H), 3.58-3.56 (m, 1H), 2.62 (d, *J* = 7.5 Hz, 1H) [6]

Spectral data in accordance with reference 6

### 4.4.4 Reaction Scheme 4, 2,3,4,6-Tetra-O-Acetyl-β-D-galactopyranosyl-(1→3)-2-azide-4,6-di-O-Acetyl-2-deoxy-β-D-galactopyranosyl fluoride (20)

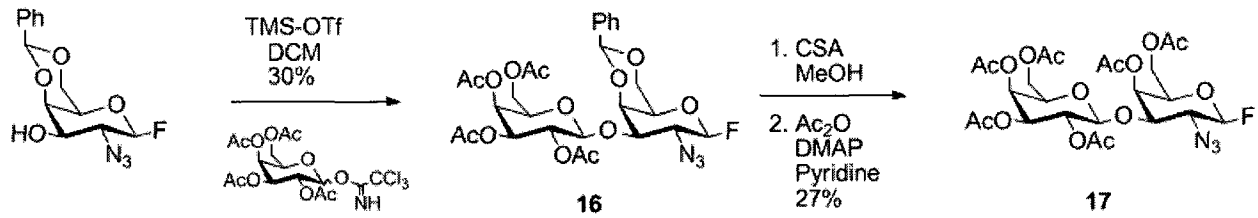


### 4.4.4.1 2,3,4,6-Tetra-O-acetyl-β-D-galactopyranosyl)-(1→3)-2-azide-4,6-O-benzylidene-2-deoxy-β-D-galactopyranosyl fluoride (16)

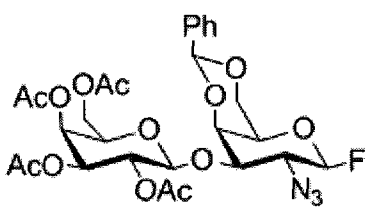

Under an inert atmosphere ($N_2$) glycosyl acceptor **18** (100 mgs, 0.34 mmol) in dry $CH_2Cl_2$ (5 mL) was transferred to a dry flask containing activated 4 Å molecular sieves. The solution was cooled to -78°C to which TMSOTf (0.01 mL, 0.034 mmol) and galactosyl imidate (335 mg, 0.68mmol) in dry $CH_2Cl_2$ (5 mL) were added dropwise. The reaction was monitored by thin layer chromatography (1 % MeOH in $CH_2Cl_2$), and upon completion quenched with triethyl amine. The solution was concentrated and purified by flash column chromatography (1 % MeOH in $CH_2Cl_2$), to yield **19** (98 mg, 46 %).

$^1$H NMR (400 MHz, $CDCl_3$) δ ppm 7.55-7.30 (m, 5H), 5.54 (s, 1H), 5.37 (dd, *J* = 3.4, 0.9 Hz, 1H), 5.24 (dd, *J* = 10.4, 7.9 Hz, 1H), 5.12-4.96 (m, 2H), 4.77 (d, *J* = 7.9 Hz, 1H), 4.77 (d, *J* = 7.9 Hz, 1H),

4.12-4.00 (m, 2H), 3.98-8.86 (m, 2H), 3.51 (dd, *J* = 10.6, 2.9 Hz, 1H), 3.48-3.44 (m, 1H), 2.14 (s, 3H), 2.04 (s, 3H), 2.02 (s, 3H), 1.96 (s, 3H) [6]

Spectral data in accordance with reference 6

**4.4.4.2 2,3,4,6-Tetra-O-Acetyl-β-D-galactopyranosyl-(1→3)-2-azide-4,6-di-O-Acetyl-2-deoxy-β-D-galactopyranosyl fluoride (17)**

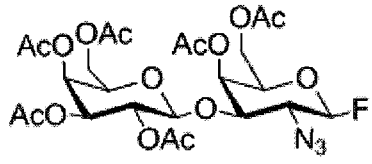


Camphor sulfonic acid (197 mg, 0.13 mmol) was added to a solution of **19** (810 mg, 1.3 mmol) in methanol (6 mL) and was allowed to stir at ambient temperature for 24 h. The solution was neutralized with triethylamine and concentrated. The residue was purified by flash column chromatography (3 % methanol in $CH_2Cl_2$) to obtain the benzylidene deprotected compound (150 mg, 22 %) which was dissolved in acetic anhydride (0.5 mL) and pyridine (0.5 mL) at 0 °C. DMAP (10 mg) was added and the reaction was allowed to warm to ambient temperature over a period of 18h. The solution was diluted with $CH_2Cl_2$ (50 mL), and extracted with saturated $CuSO_4$ solution, water, and dried with $MgSO_4$. The solution was concentrated and purified by flash column chromatography (3 % methanol in $CH_2Cl_2$), to yield **20** (120 mg, 68 %).

$^1$H NMR (400 MHz, $CDCl_3$) δ ppm 5.40-5.35 (m, 2H), 5.16 (dd, *J* = 10.5, 7.8 Hz, 1H), 5.12-4.94 (m, 2H), 4.70 (d, *J* = 7.8 Hz, 1H), 4.23 (dd, *J* = 11.8, 4.3 Hz, 1H), 4.19-4.01 (m, 3H), 3.92-3.83 (m, 2H),

3.74 (ddd, *J* = 13.1, 10.4, 7.5 Hz, 1H), 3.62-3.57 (m, 1H), 2.16 (s, 3H), 2.15 (s, 3H), 2.08 (s, 3H), 2.08 (s, 3H), 2.06 (s, 3H), 1.98 (s, 3H) [7]

LRMS (ESI): Calcd for $C_{24}H_{32}N_3O_5F$ $[M+K]^+$ 660.1 found 660.0

*Spectral data in accordance with Reference 7*

### 4.5. Assessing Antifreeze Activity

#### 4.5.1 Recrystallization Inhibition (RI)

Recrystallization-inhibition (RI) activity was assessed using the splat cooling technique previously described by Knight and co-workers.[8] Briefly, the technique involves generating a frozen wafer from the analyte which is dissolved in phosphate buffered saline (PBS) solution; a 10 uL drop of this solution is then dropped from a pipette through a two metre high plastic tube (10 cm in diameter) onto a block of polished aluminum pre-cooled to approximately -80 °C. The droplet freezes instantly on the polished aluminum block and is approximately 1 cm in diameter and 20 μm thick. This wafer is then carefully removed from the surface of the block and transferred to a cryostage (refrigerated microscope stage) held at -6.4 °C. The wafer is left to anneal at this temperature for a period of 30 min and then photographed between crossed polarizing filters using a digital camera (Nikon CoolPix 5000) fitted to the microscrope. During flash freezing, ice crystals spontaneously nucleated from the super-cooled solution. These initial crystals were relatively homogenous in size and quite small. During the annealing cycle recrystallization occurred, resulting in a dramatic increase in ice crystal size. A quantitative

measure of the difference in recrystallization inhibition of two compounds X and Y is the difference in the dynamics of the ice crystal size distribution.

RI analysis via mean elliptical method:

A total of six different images are taken from each wafer; three from the middle and three from the edge. The images are then analyzed using the mean elliptical method. In this method, the ten largest ice crystals were chosen from the field of view (FOV) in each image. Selection of these crystals was arbitrary in that they were chosen after a visual inspection of the image.[9], [10] The two dimensional surface area of each of these ten crystals was then calculated via approximation of the crystal as an elliptical area. The major and minor elliptical axes were defined by the two largest orthogonal dimensions across the ice grain surface. The surface area of each ice grain was then calculated based on the formula: $A = \pi ab$, in which A represented area; a and b represented the length of the major and minor elliptical axes. Totalling all individual measurements for each FOV produces a value for the average grain surface area referred to as the mean largest grain size (MLGS). Error was calculated using standard error of the mean (SEM). T-tests were performed to a 95 % confidence level.

Analysis via domain recognition software program :

For each sample including PBS, three drops were performed and three images were taken from the middle of each wafer. Image analysis of the ice wafers was performed using a novel

domain recognition software (DRS) program that was developed at the Steacie Institute for Molecular Sciences (SIMS) of the National Research Council of Canada (NRCC).[11] The software was written in C using Microsoft Visual Studio 6.0 on a Pentium class personal computer running Microsoft Windows 2000 or XP. This processing employed the Microsoft Windows Graphical User Interface to allow a user to visually demarcate and store the vertices of ice crystal domains in a digital micrograph. These data were then used to calculate the domain areas. To eliminate the need to fully process each micrograph, an algorithm was developed to randomly display a number of x/y locations. The algorithm made use of a built-in pseudo random number generator [rand(x)] and was written so that no two locations were closer than 1/10th the field of view of the micrograph. The formula for the area of a polygon that is not self-intersecting and contains no holes is then given by:

$$A = \frac{1}{2}\sum_{i=0}^{N-1}\left(x_i y_{i+1} - x_{i+1} y_i\right)$$

where N is the number of vertices, and $x_0, y_0$ to $x_{N-1}, y_{N-1}$ are the vertices circumventing the polygon in a clockwise direction. The point $x_0, y_0$ is assumed to be equivalent to the point $x_N, y_N$. In the FOV of each image, twelve locations (ice crystal domains) were randomly chosen and analyzed. All data was compiled, further analyzed and plotted using Microsoft Excel.

### 4.5.2 Thermal Hysteresis (TH)

Nanoliter osmometry was performed using a nanoliter osmometer (Clifton Technical Physics, Hartford, NY) as described by Chakrabartty and Hew.[12] All measurements were made in doubly distilled water. Ice crystal morphology was observed through a Leitz compound microscope equipped with an Olympus 20X (infinity corrected) objective, Leitz Periplan 32X photo eyepiece and a Hitachi KP-M2U CCD camera connected to a Toshiba MV13K1 TV/VCR system. Still images were captured directly using a Nikon CoolPix digital camera.

## 4.6 References


1. Huang, G.L. et. al, *Journal Bioorganic and Medicinal Chemistry Letters*, **2006,** *16*, 2042.

2. Amer, H. et al., *Carbohydrate Research,* **2003**, *338*, 35.

3. Ross, A. J.; Sizova, O.; Nikolaev, A. V., *Carbohydrate Research*, **2006**, *341*,1954.

4. Wong, T. C.; Townsend, R. R.; Lee, Y. C, *Carbohydrate Research*, **1987**, *170*, 27.

5. Lemieux, R. U.; Ratcliffe, R. M, *Canadian Journal of Chemistry*, **1979**, *57*, 1244.

6. Tachibana, Y.; Matsubara, N.; Nakajima, F.; Tsuda, T.; Tsudo, S.; Monde, K.; Nishimura, S., *Tetrahedron*, **2002**, *58*, 10213.

7. Shao, N.; Guo, Z., *Organic Letters*, **2005**, *7*, 3589.

8. Knight, C. A.; Hallett, J.; DeVries, A. L. *Cryobiology*, **1988,** *25*, 55.

9. Eniade, A.; Purushotham, M.; Ben, R.N.; Wang, J.B.; Horwath, K., *Cell Biochem. Biophys.* **2003**, 38, 115.

10. Liu, S.; Ben, R.N., *Org. Lett.* **2005**, 7, 2385

11. Jackmann, J.; Noestheden, M.; Moffat, D.; Pezacki, J.; Findlay, S.; Ben, R. N., *Biochem. Biophys. Res. Commun.* **2007**, 354, 340.

12. Chakrabartty, A., Hew, C.L., *Eur. J. Biochem.* **1991**, 202, 1057.

## 4.6 Spectra

1.

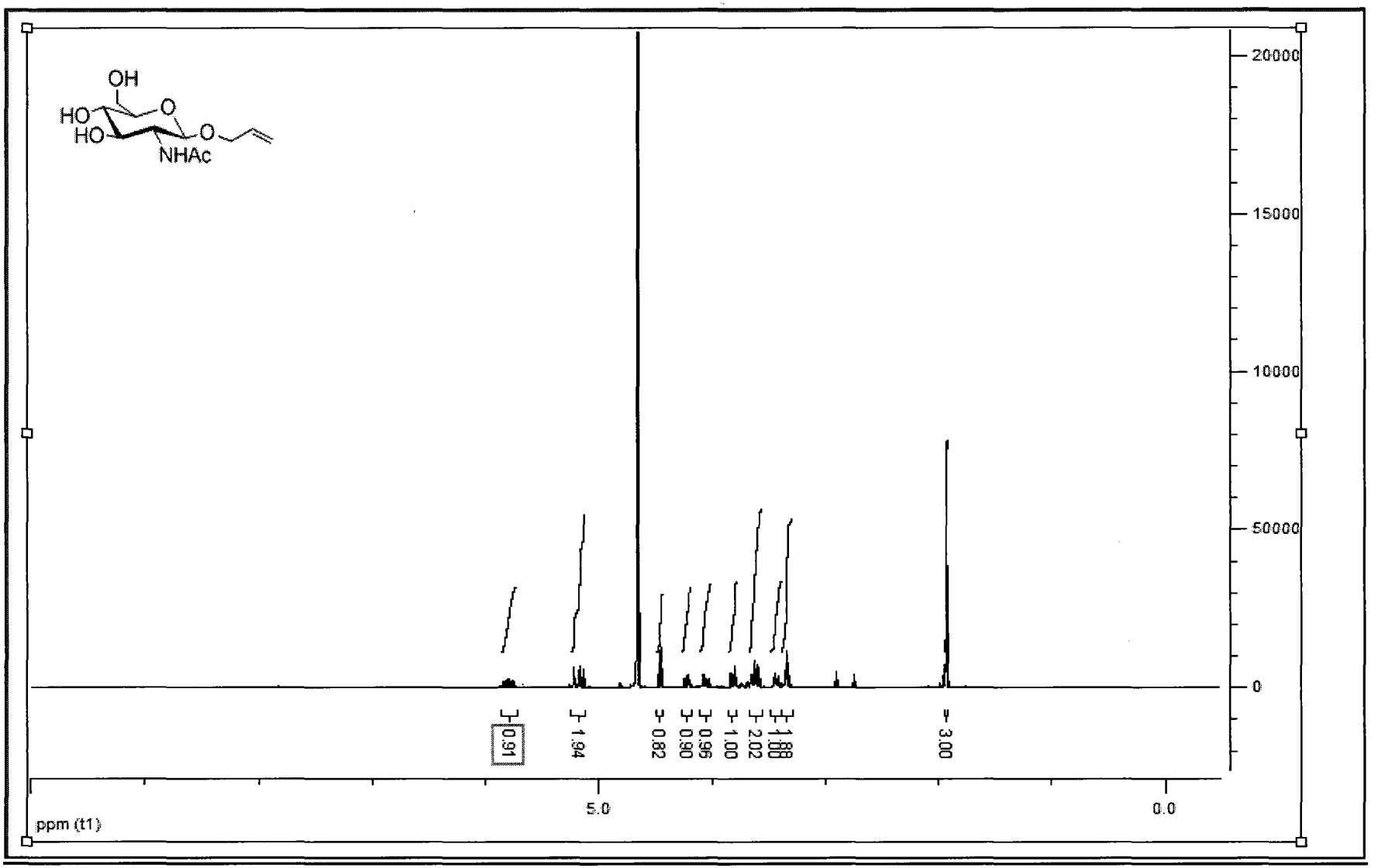
OH
HO
HO
O
O
NHAc
20000
15000
10000
50000
0
0.91
1.94
0.82
0.90
0.96
1.00
2.02
3.00
5.0
0.0
ppm (t1)

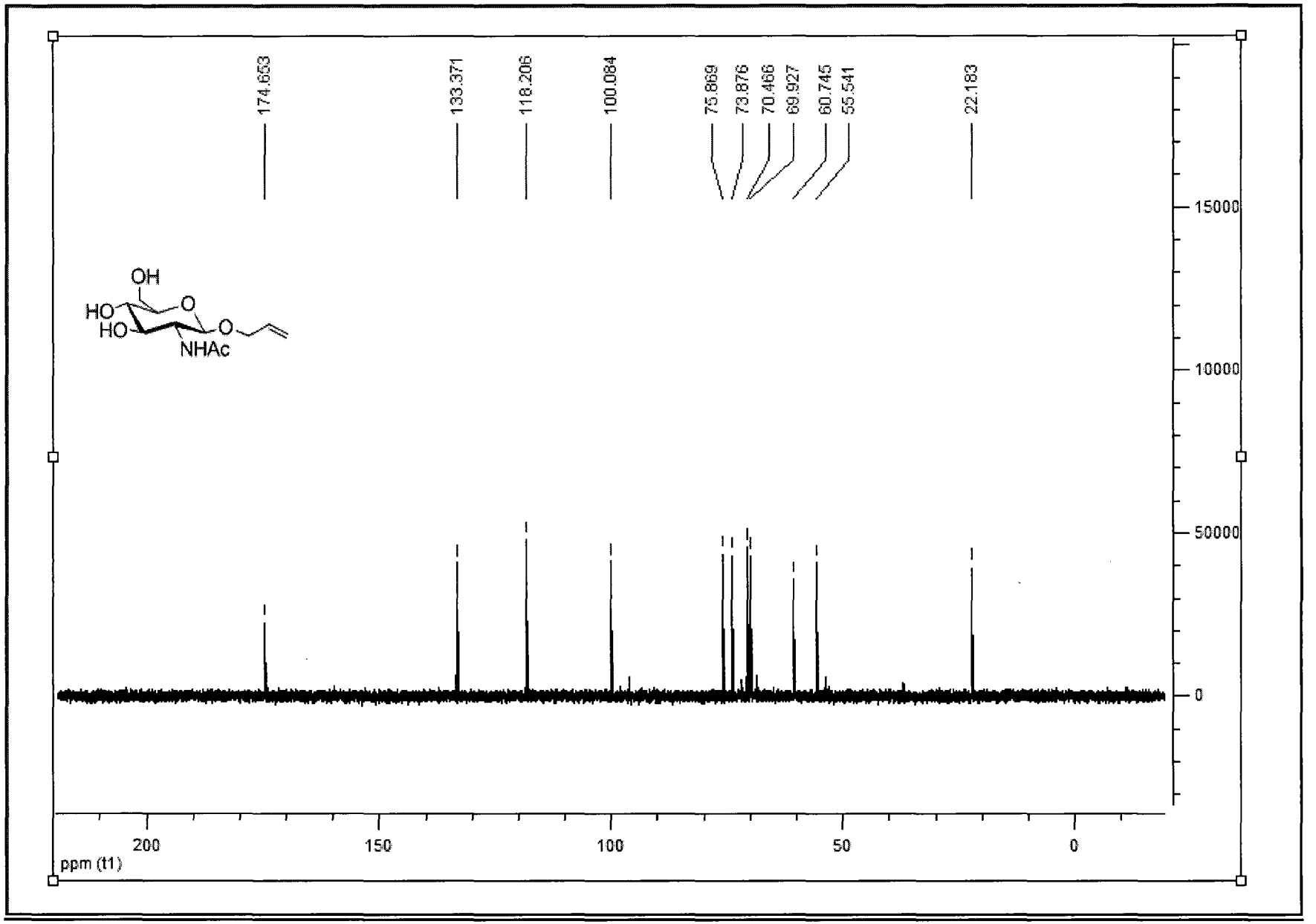
174.653
133.371
118.206
100.084
75.869
73.876
70.466
69.927
60.745
55.541
22.183
OH
HO
HO
O
O
NHAc
15000
10000
50000
0
200
150
100
50
0
ppm (t1)

2.

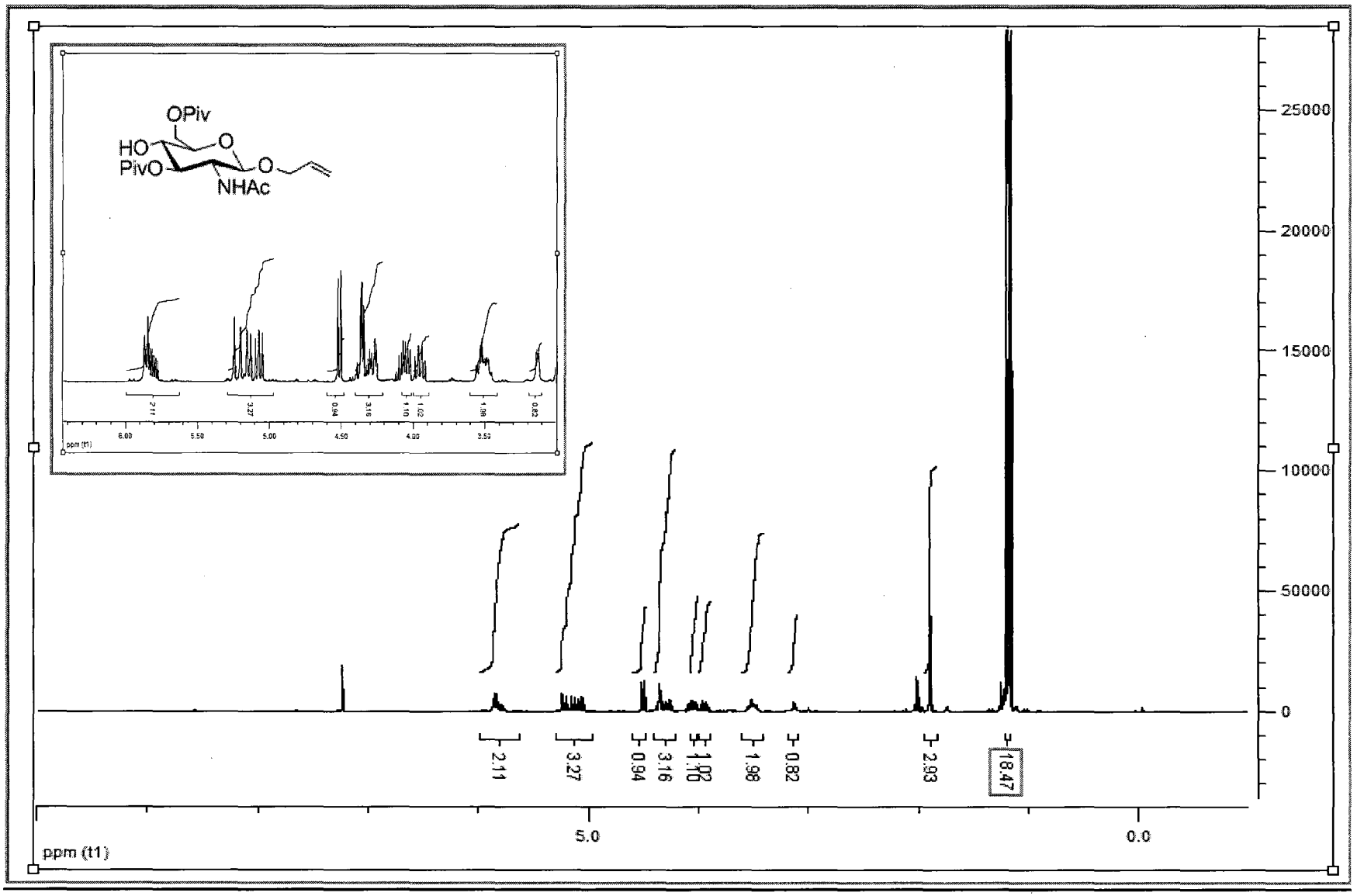
OPiv
HO
PivO
O
O
NHAc
25000
20000
15000
10000
50000
0
2.11
3.27
0.94
3.16
1.10
1.02
1.98
0.82
2.93
18.47
5.0
0.0
ppm (t1)

3.

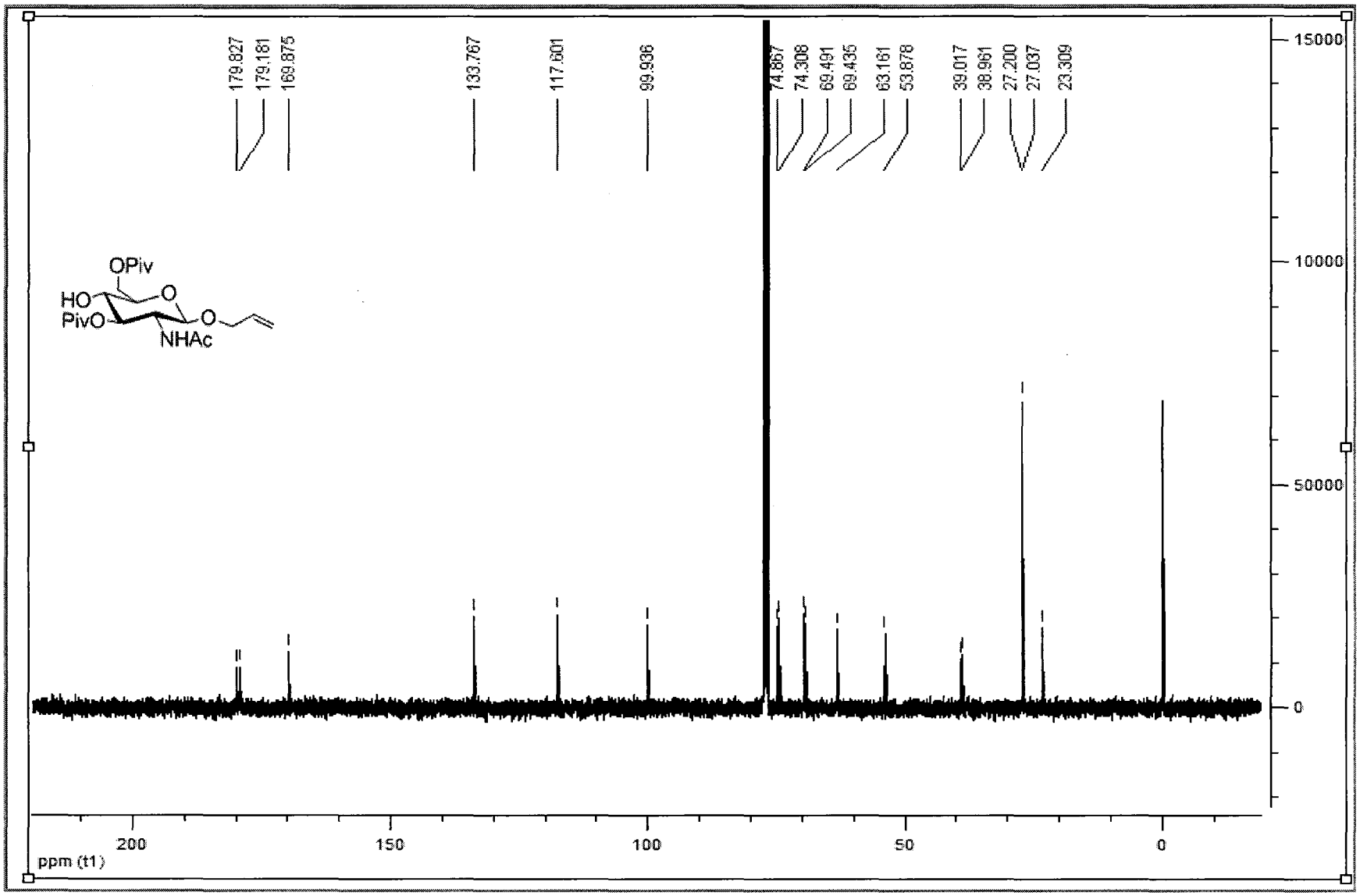
179.827
179.181
169.875
133.767
117.601
99.936
74.867
74.308
69.491
69.435
63.161
53.878
39.017
38.961
27.200
27.037
23.309
OPiv
HO
PivO
O
O
NHAc
15000
10000
50000
0
200
150
100
50
0
ppm (t1)

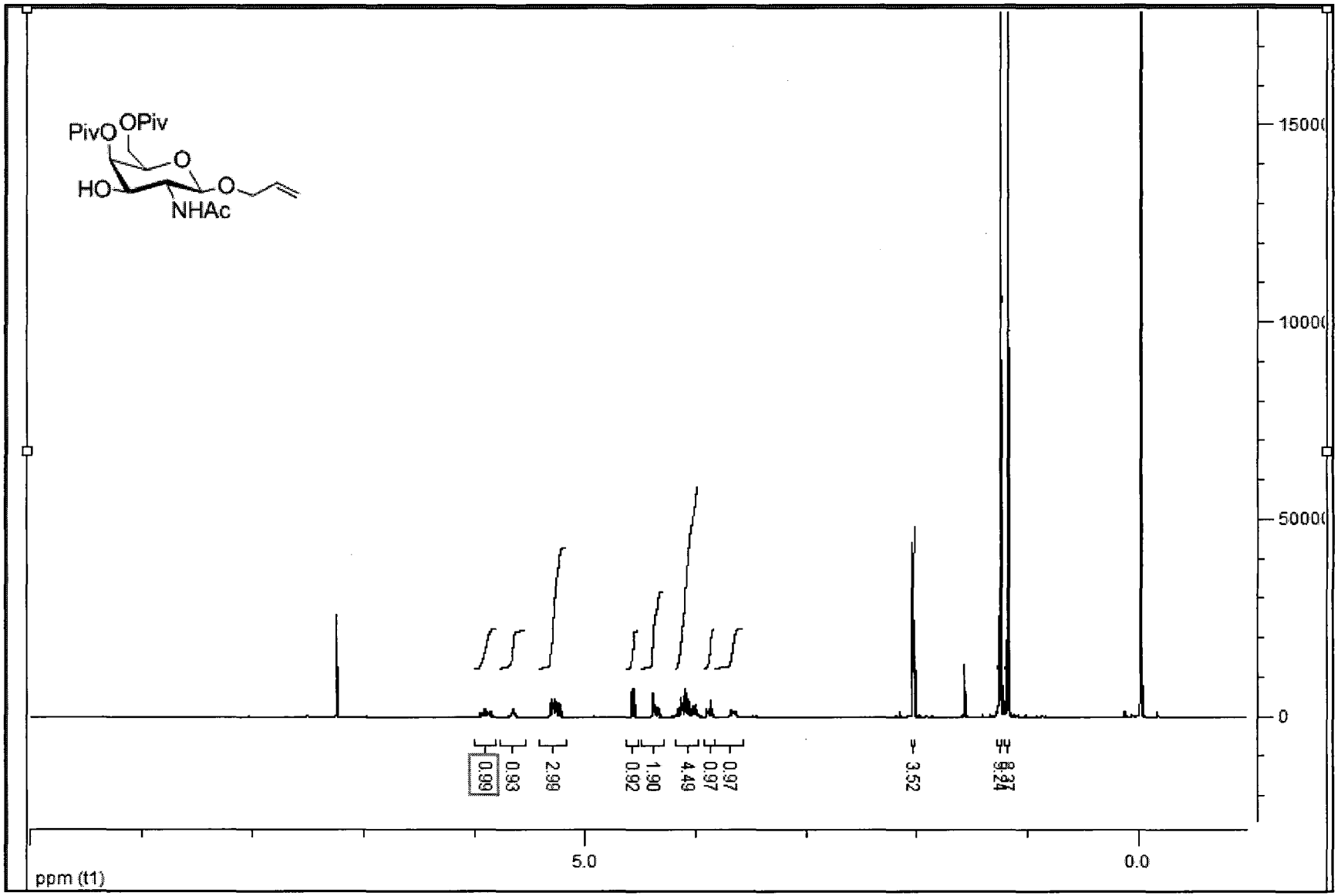
PivO
OPiv
O
HO
O
NHAc
15000
10000
50000
0
0.99
0.93
2.99
0.92
1.90
4.49
0.97
0.97
3.52
8.37
5.0
0.0
ppm (t1)

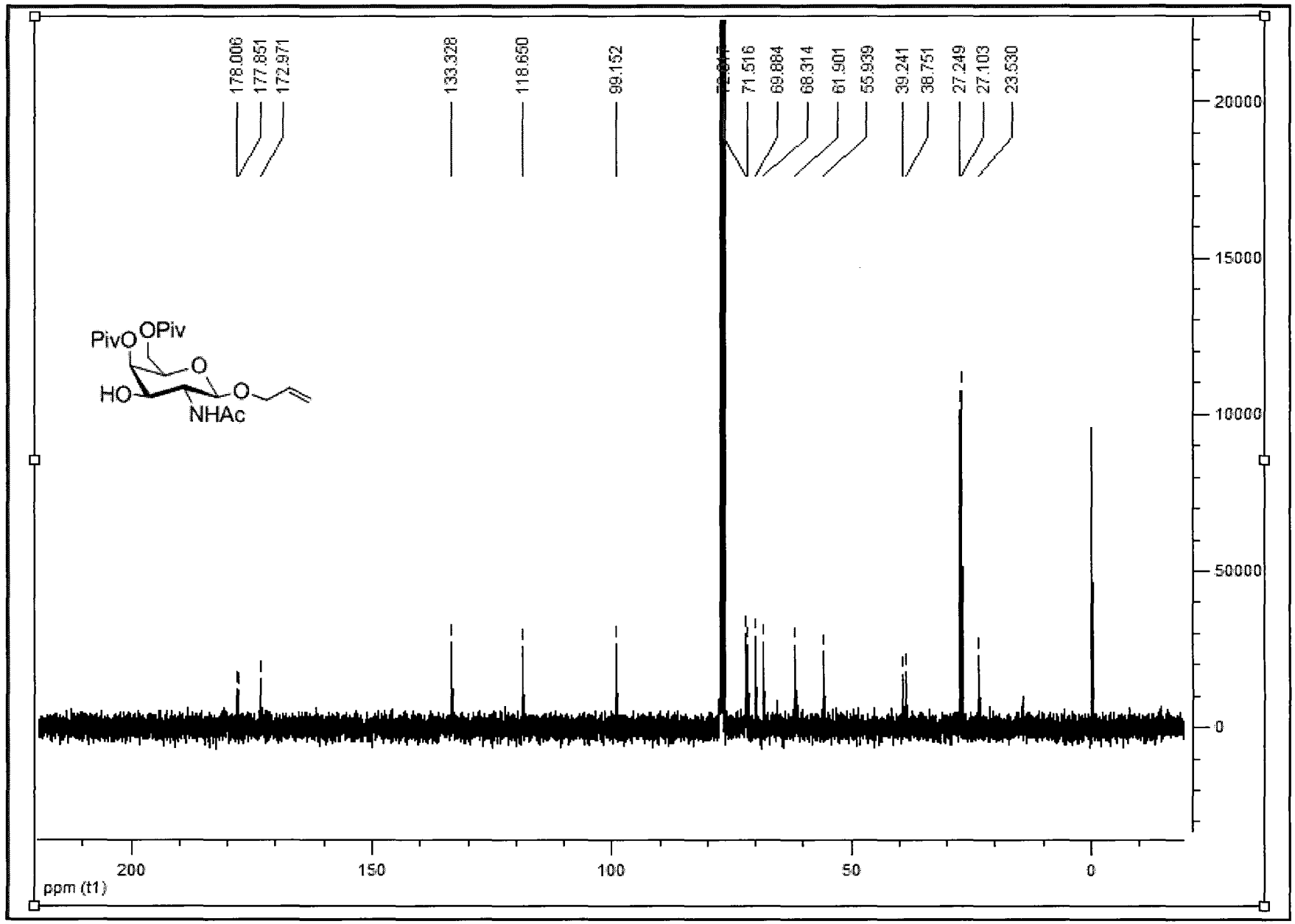
178.006
177.851
172.971
133.328
118.650
99.152
71.516
69.884
68.314
61.901
55.939
39.241
38.751
27.249
27.103
23.530
PivO
OPiv
O
HO
O
NHAc
20000
15000
10000
50000
0
200
150
100
50
0
ppm (t1)

4.

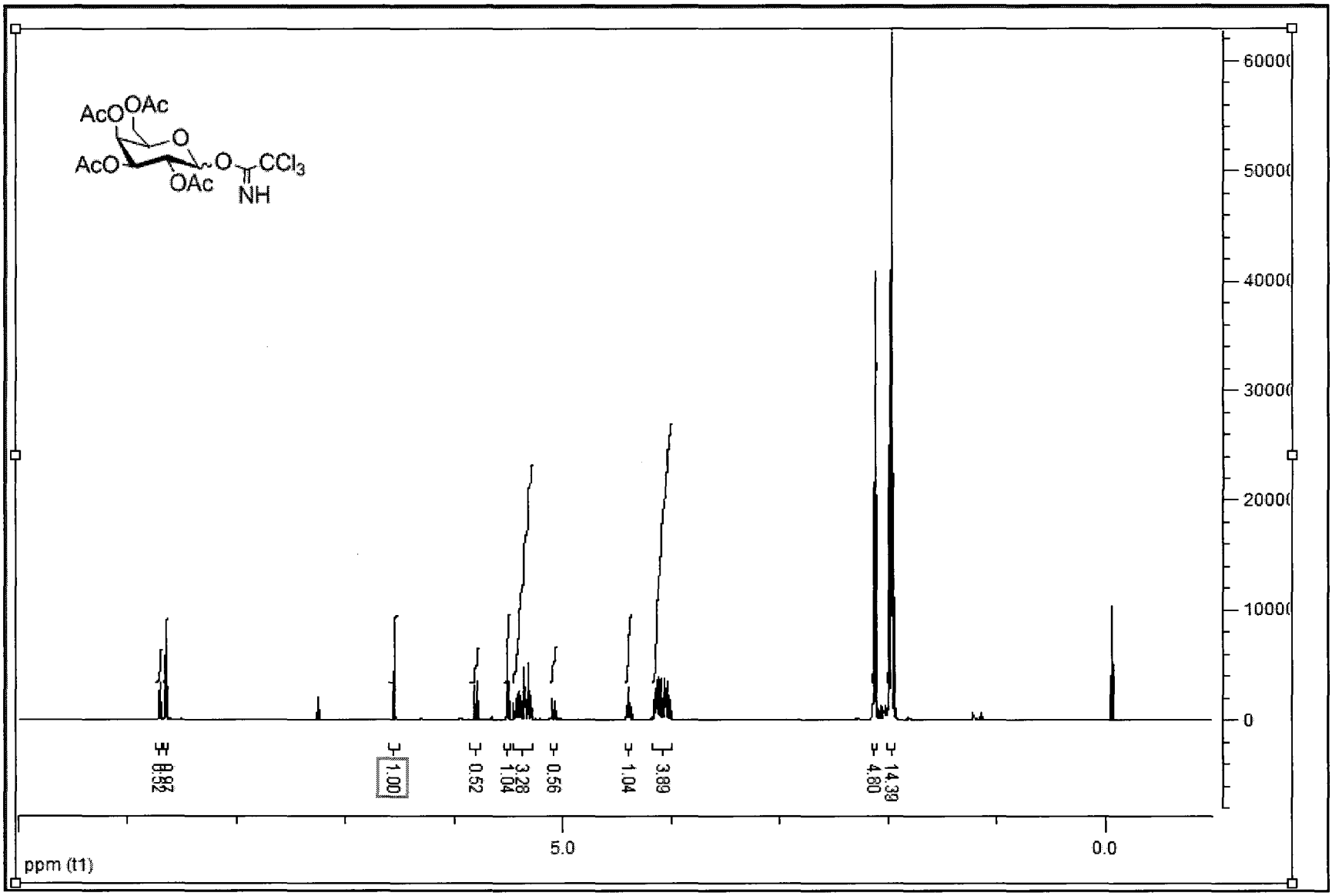
AcO
OAc
O
AcO
O
CCl3
OAc
NH
60000
50000
40000
30000
20000
10000
0
0.87
1.00
0.52
1.04
3.28
0.56
1.04
3.89
4.80
14.39
5.0
0.0
ppm (t1)

5.

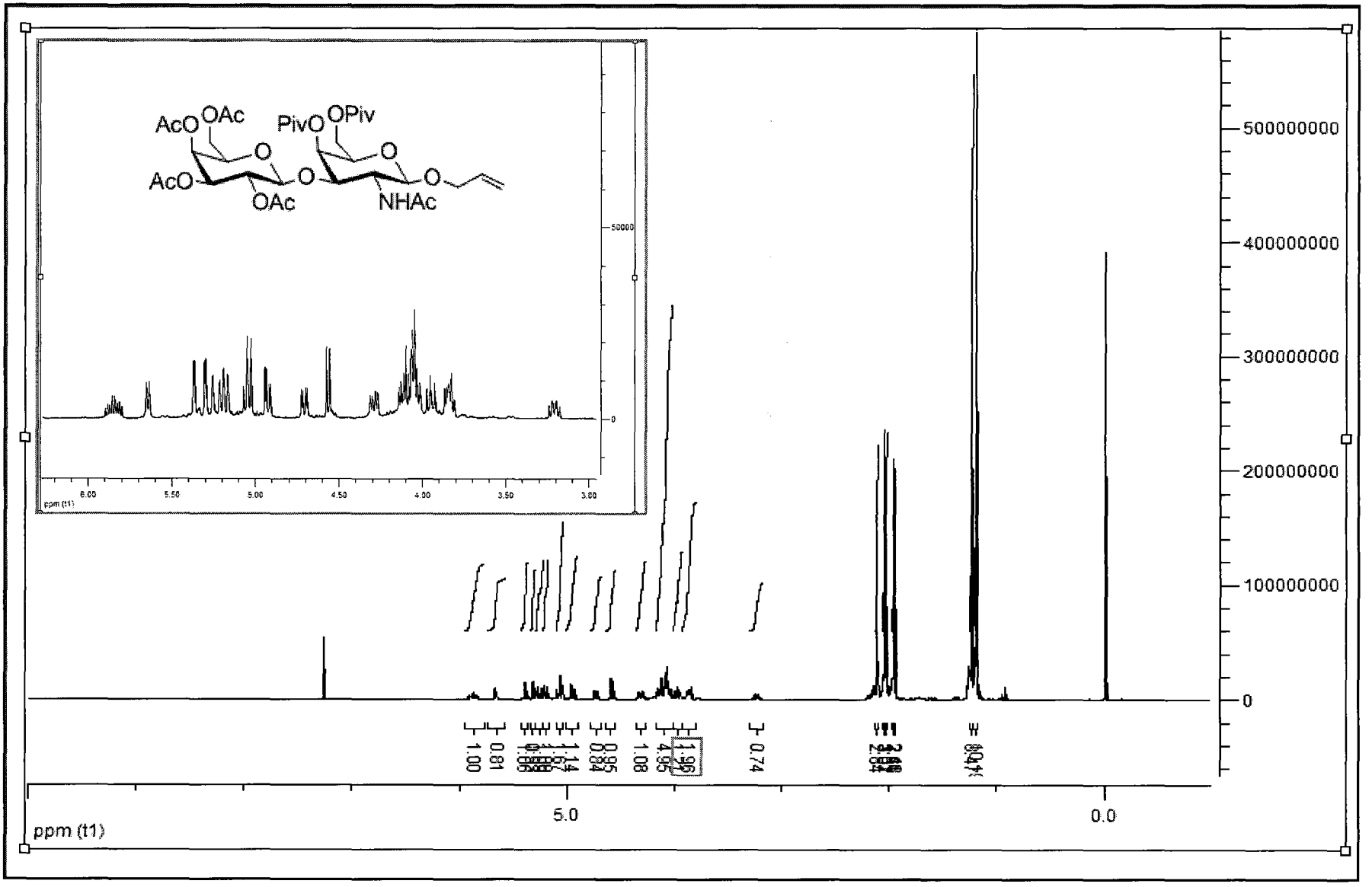

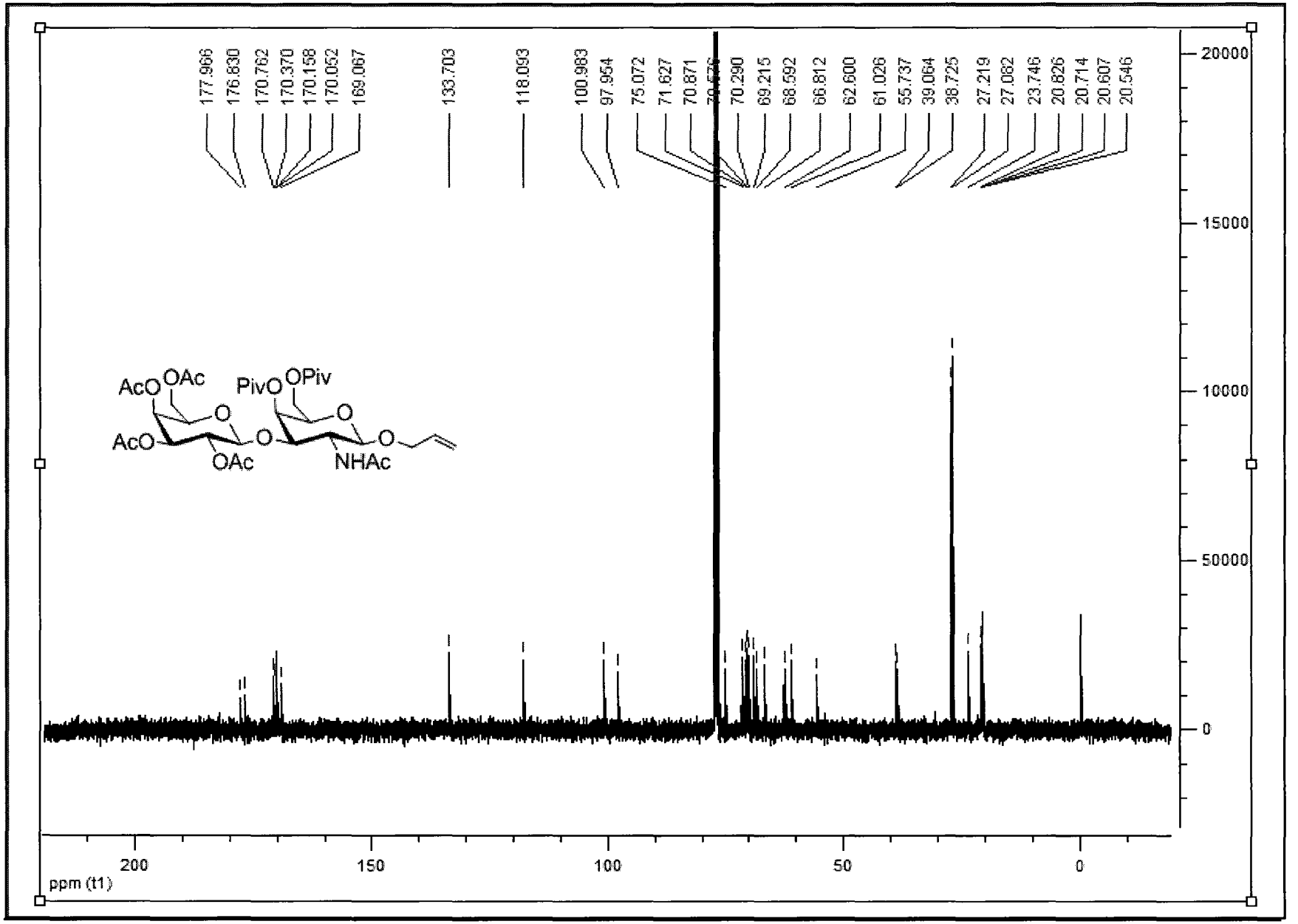
177.966
176.830
170.762
170.370
170.158
170.052
169.067
133.703
118.093
100.983
97.954
75.072
71.627
70.871
70.290
69.215
68.592
66.812
62.600
61.026
55.737
39.064
38.725
27.219
27.062
23.746
20.826
20.714
20.607
20.546
AcO
OAc
AcO
OAc
PivO
OPiv
O
O
O
O
NHAc
20000
15000
10000
50000
0
200
150
100
50
0
ppm (t1)

**6.**

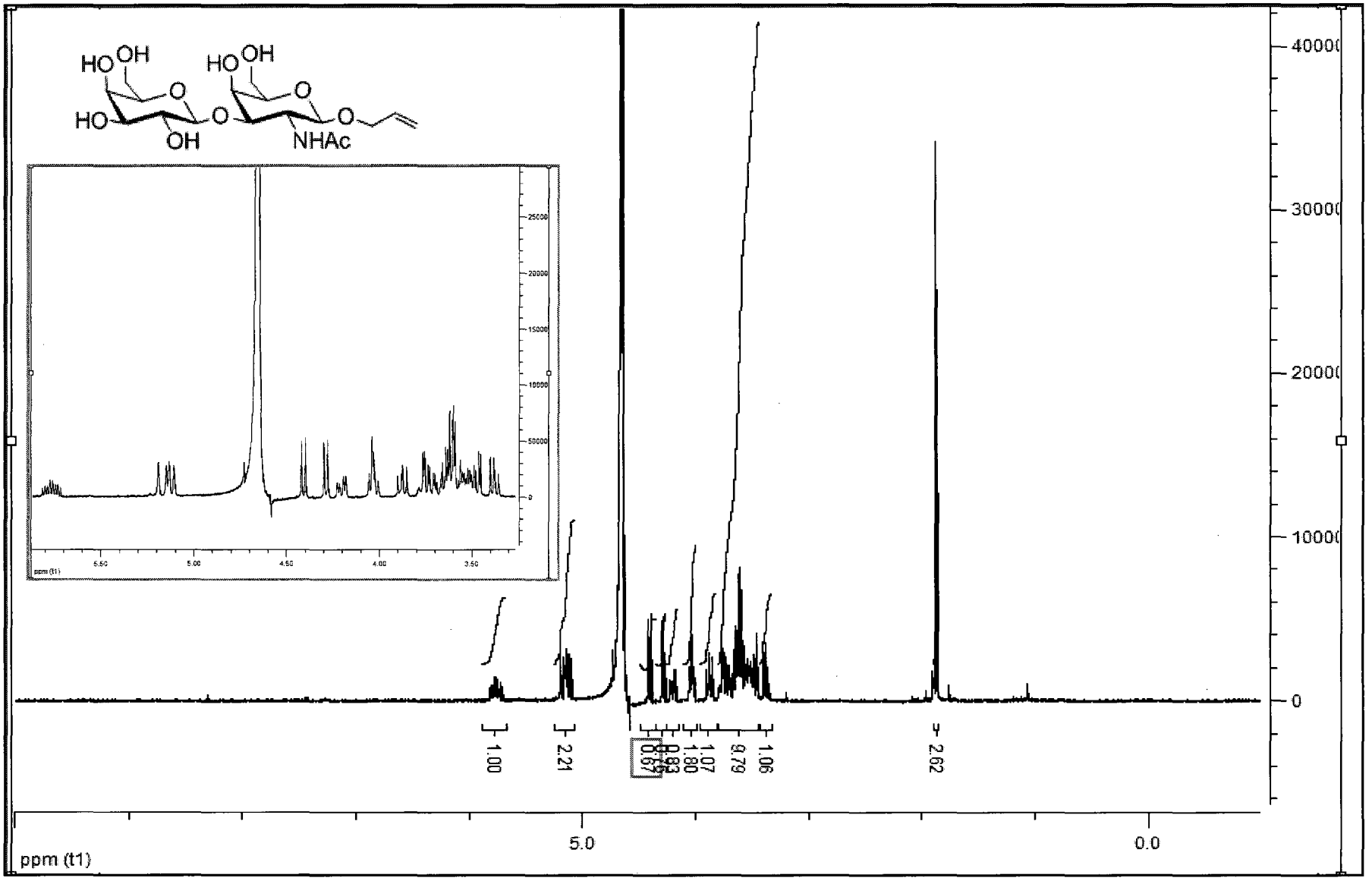
HO
OH
HO
O
HO
OH
O
HO
OH
O
O
NHAc
1.00
2.21
1.07
1.80
9.79
1.06
2.62
5.0
0.0
ppm (t1)

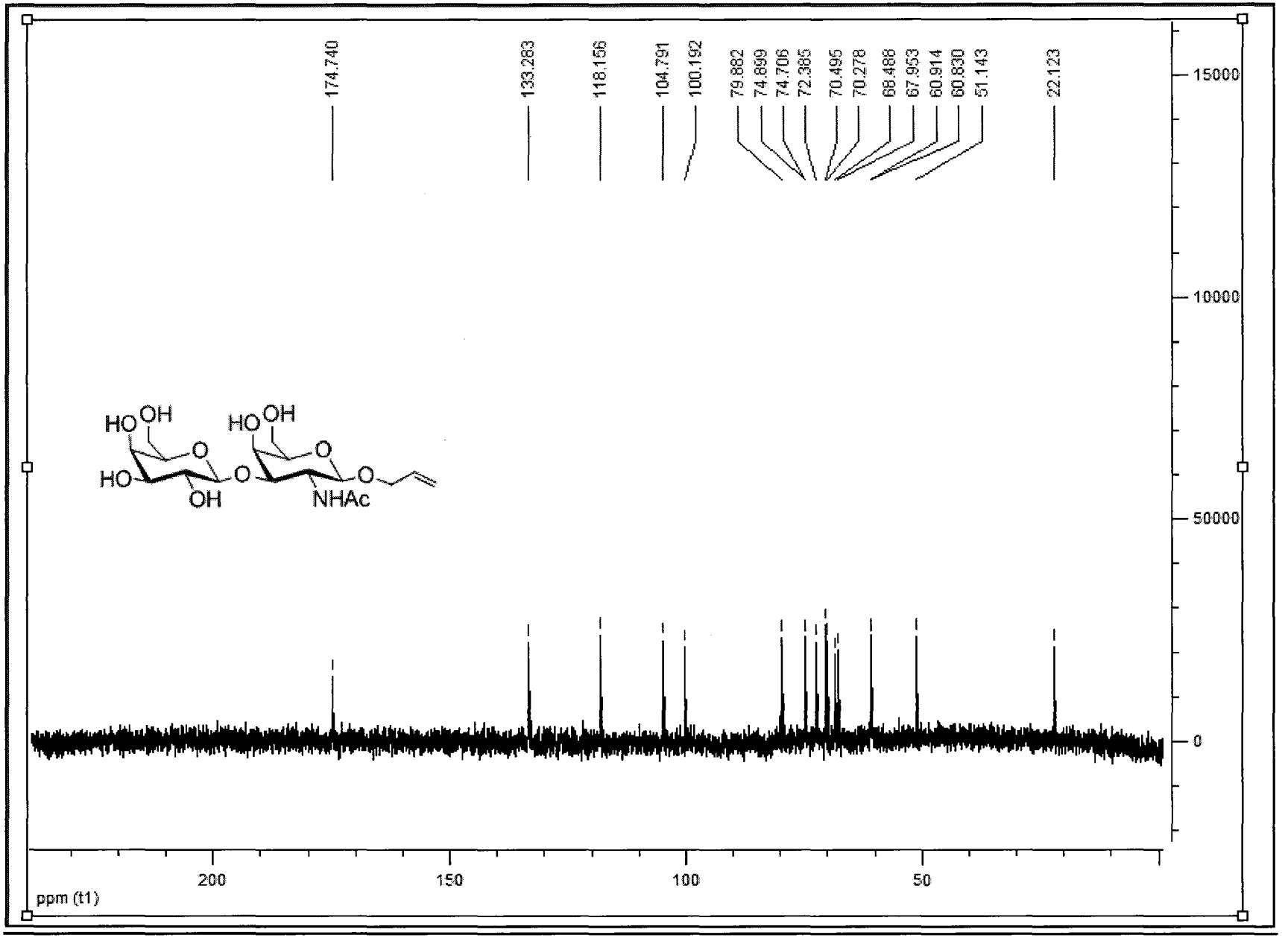
174.740
133.283
118.156
104.791
100.192
79.882
74.899
74.706
72.385
70.495
70.278
68.488
67.953
60.914
60.830
51.143
22.123
15000
10000
50000
0
HO
OH
HO
OH
O
O
HO
O
O
OH
NHAc
200
150
100
50
ppm (t1)

**7.**

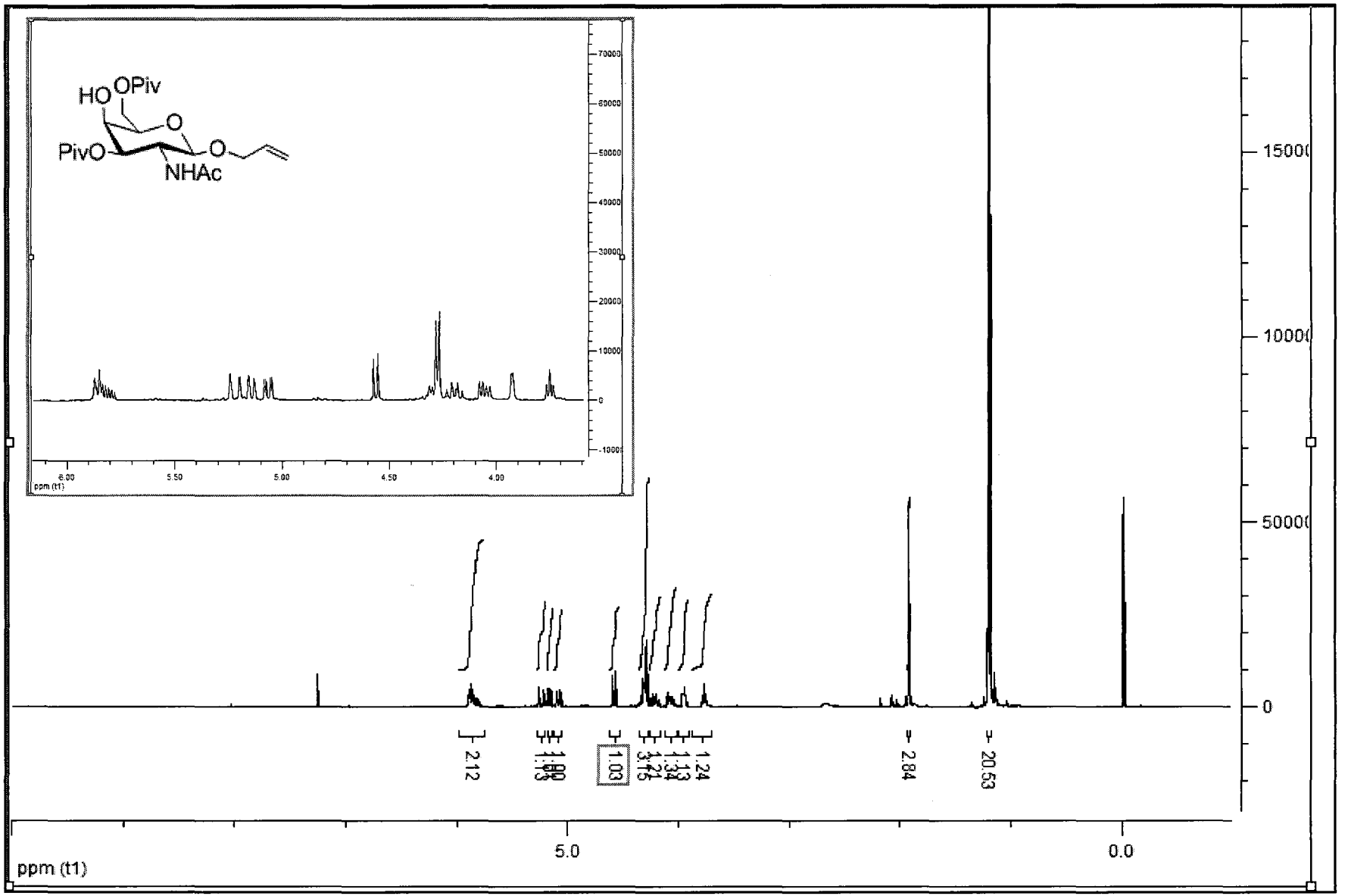

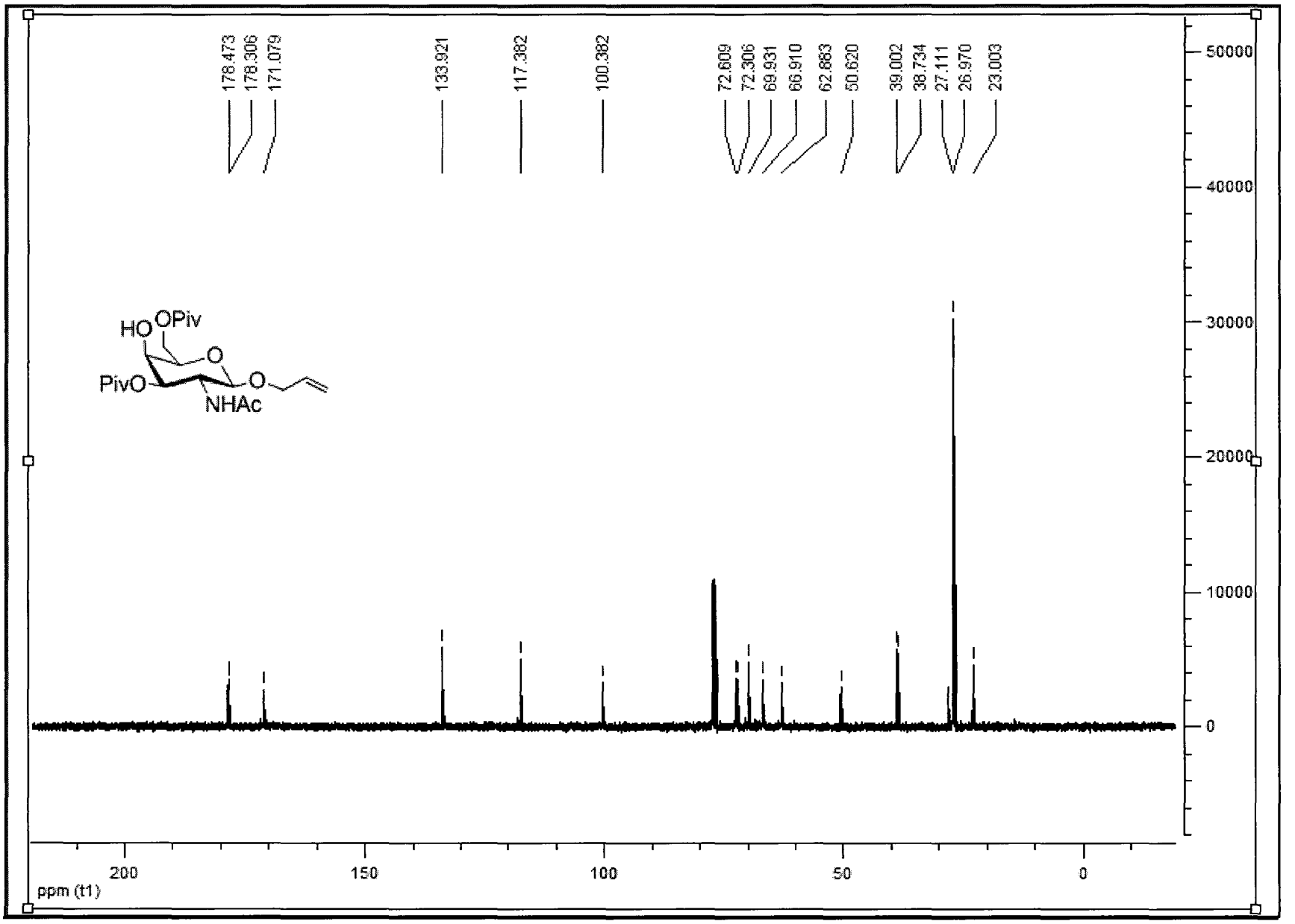
178.473
178.306
171.079
133.921
117.382
100.382
72.609
72.306
69.931
66.910
62.883
50.620
39.002
38.734
27.111
26.970
23.003
HO
OPiv
O
PivO
O
NHAc
50000
40000
30000
20000
10000
0
200
150
100
50
0
ppm (t1)

**8.**

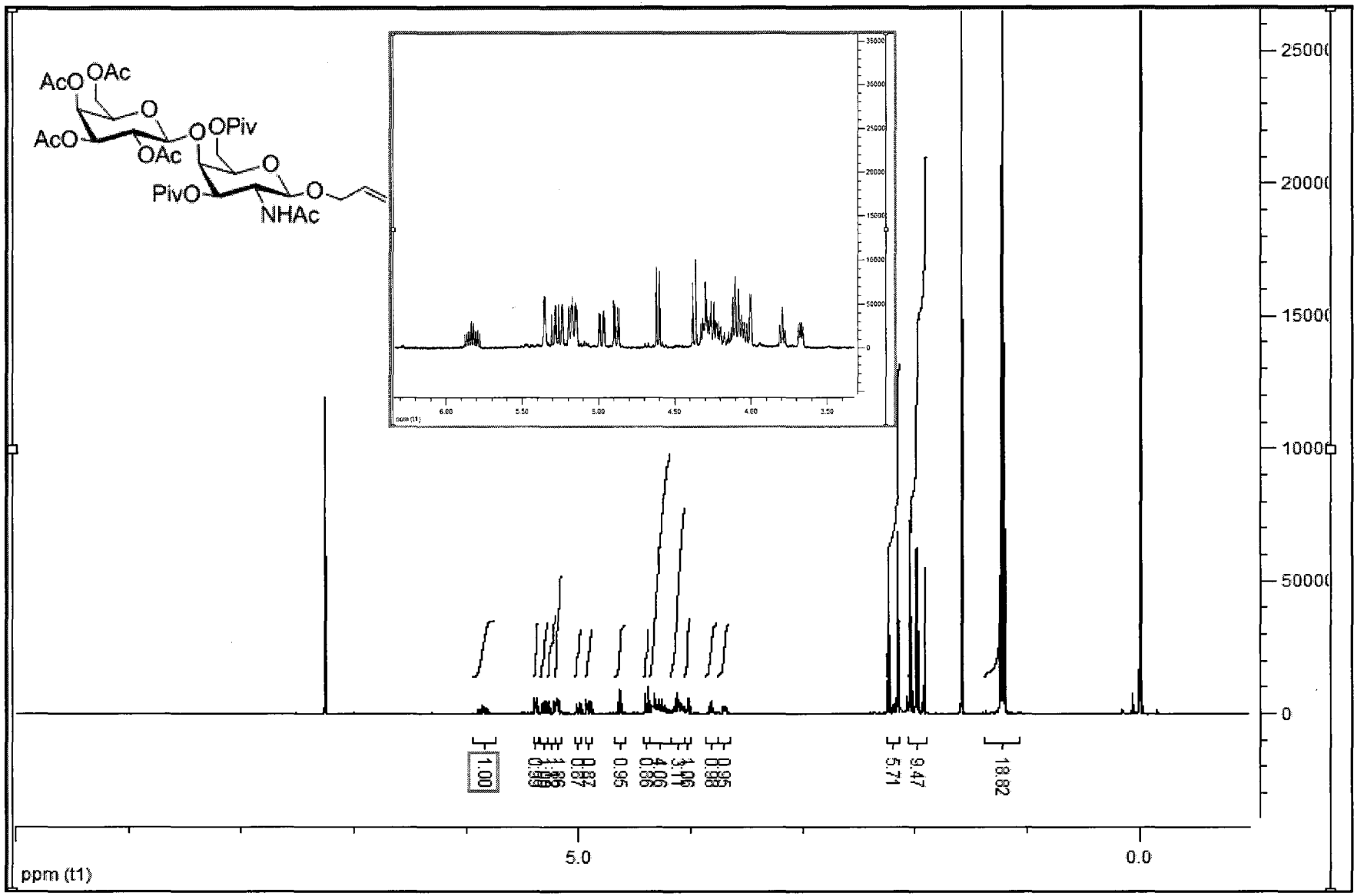
AcO
OAc
O
AcO
OAc
O
OPiv
O
PivO
O
NHAc
25000
20000
15000
10000
50000
0
1.00
0.95
5.71
9.47
18.82
5.0
0.0
ppm (t1)

**9.**

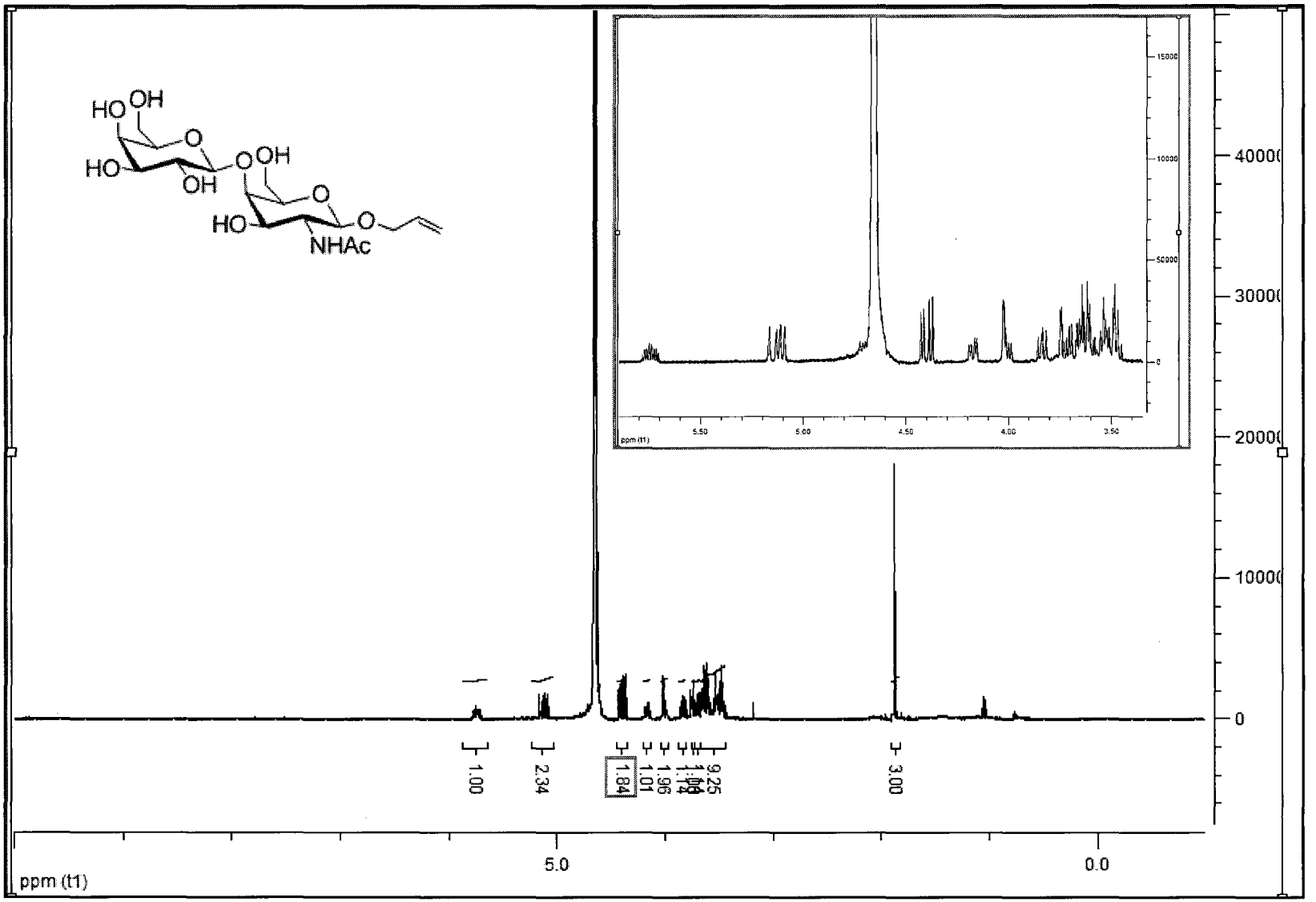

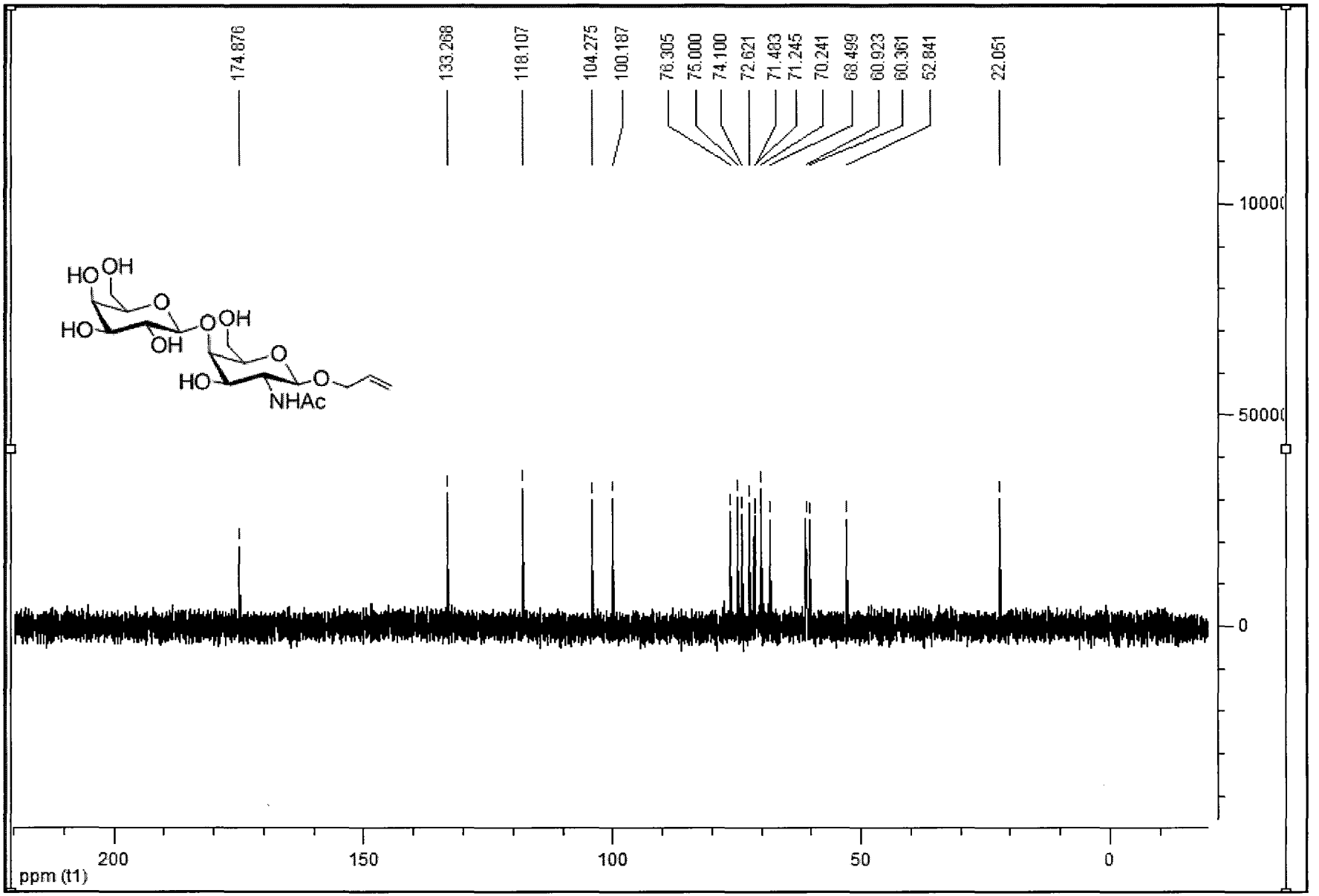
174.876
133.268
118.107
104.275
100.187
76.305
75.000
74.100
72.621
71.483
71.245
70.241
68.499
60.923
60.361
52.841
22.051
HO
OH
O
HO
OH
O
OH
O
HO
O
NHAc
10000
5000
0
200
150
100
50
0
ppm (t1)

10.

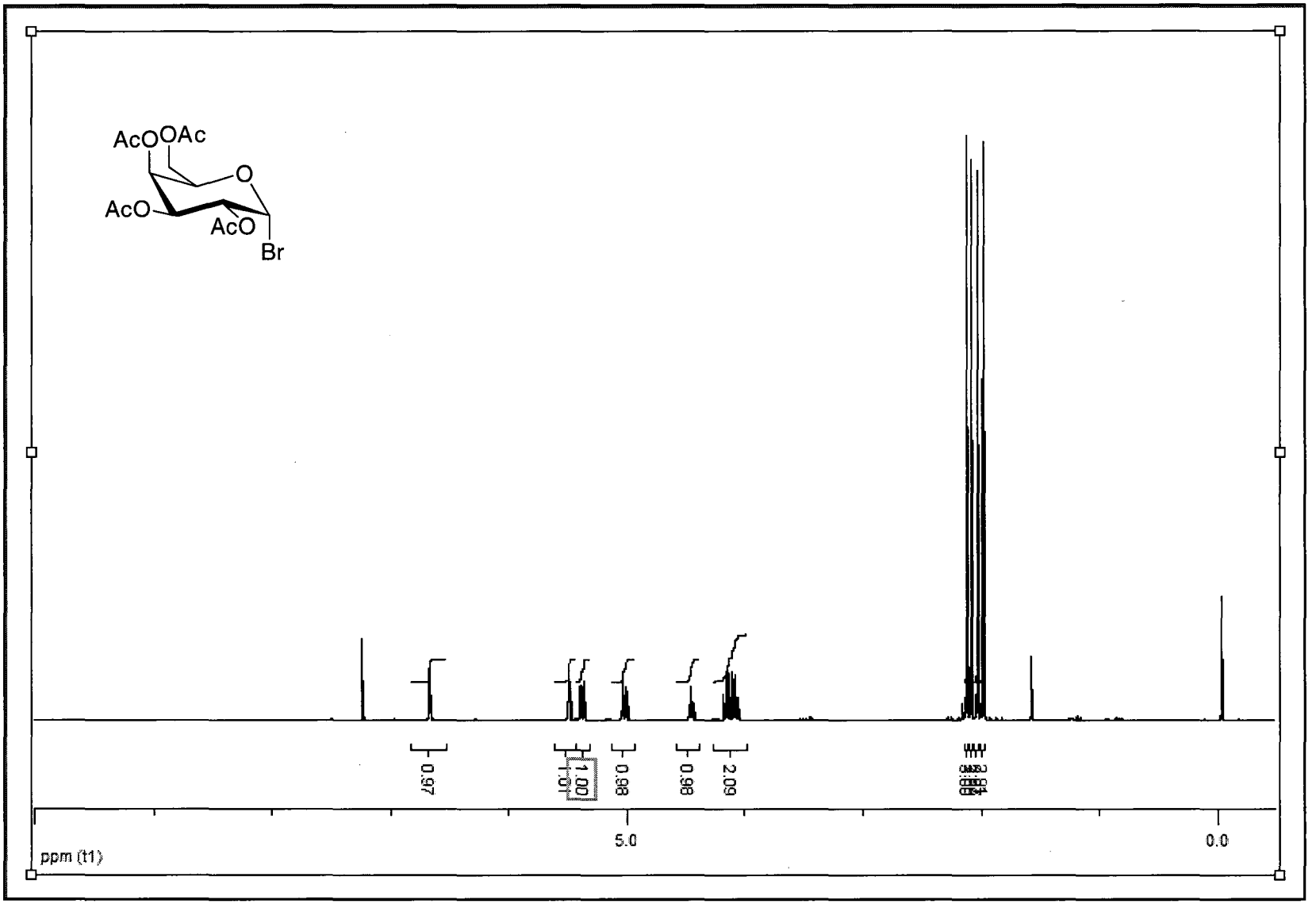

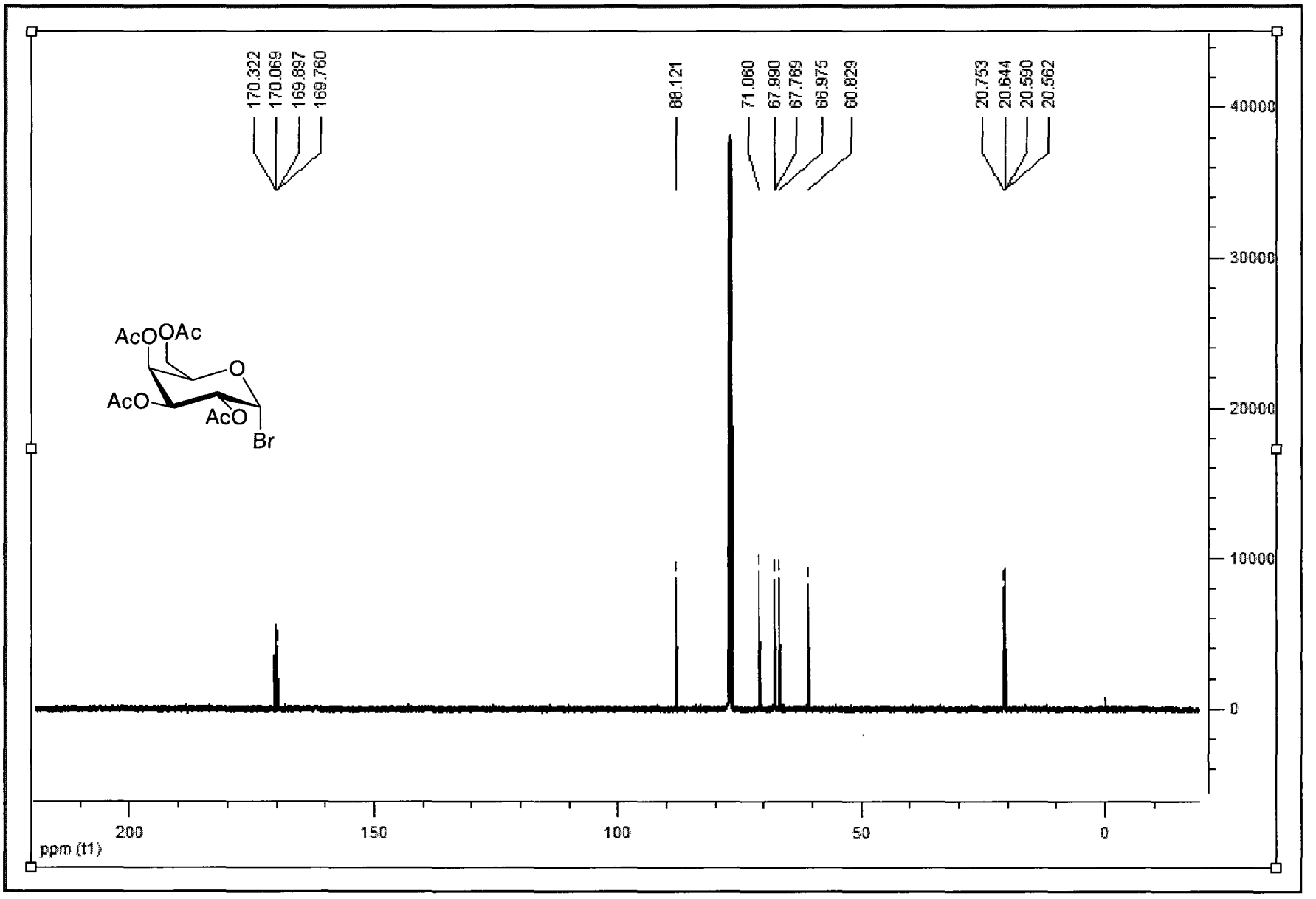
170.322
170.069
169.897
169.760
88.121
71.060
67.990
67.769
66.975
60.829
20.753
20.644
20.590
20.562
AcO
OAc
O
AcO
AcO
Br
40000
30000
20000
10000
0
200
150
100
50
0
ppm (t1)

11.

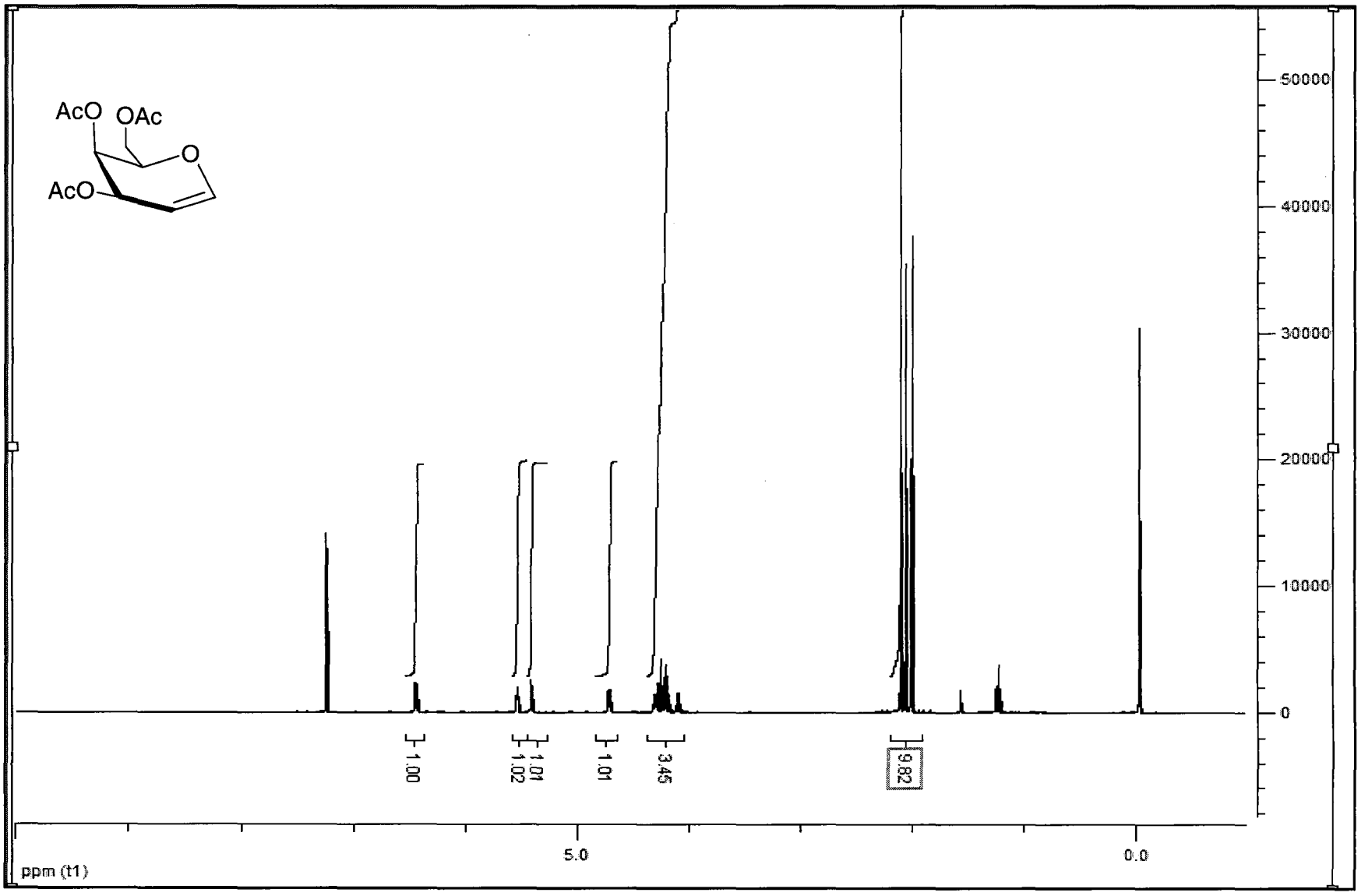
AcO
OAc
O
AcO
50000
40000
30000
20000
10000
0
1.00
1.02
1.01
1.01
3.45
9.82
5.0
0.0
ppm (t1)

12.

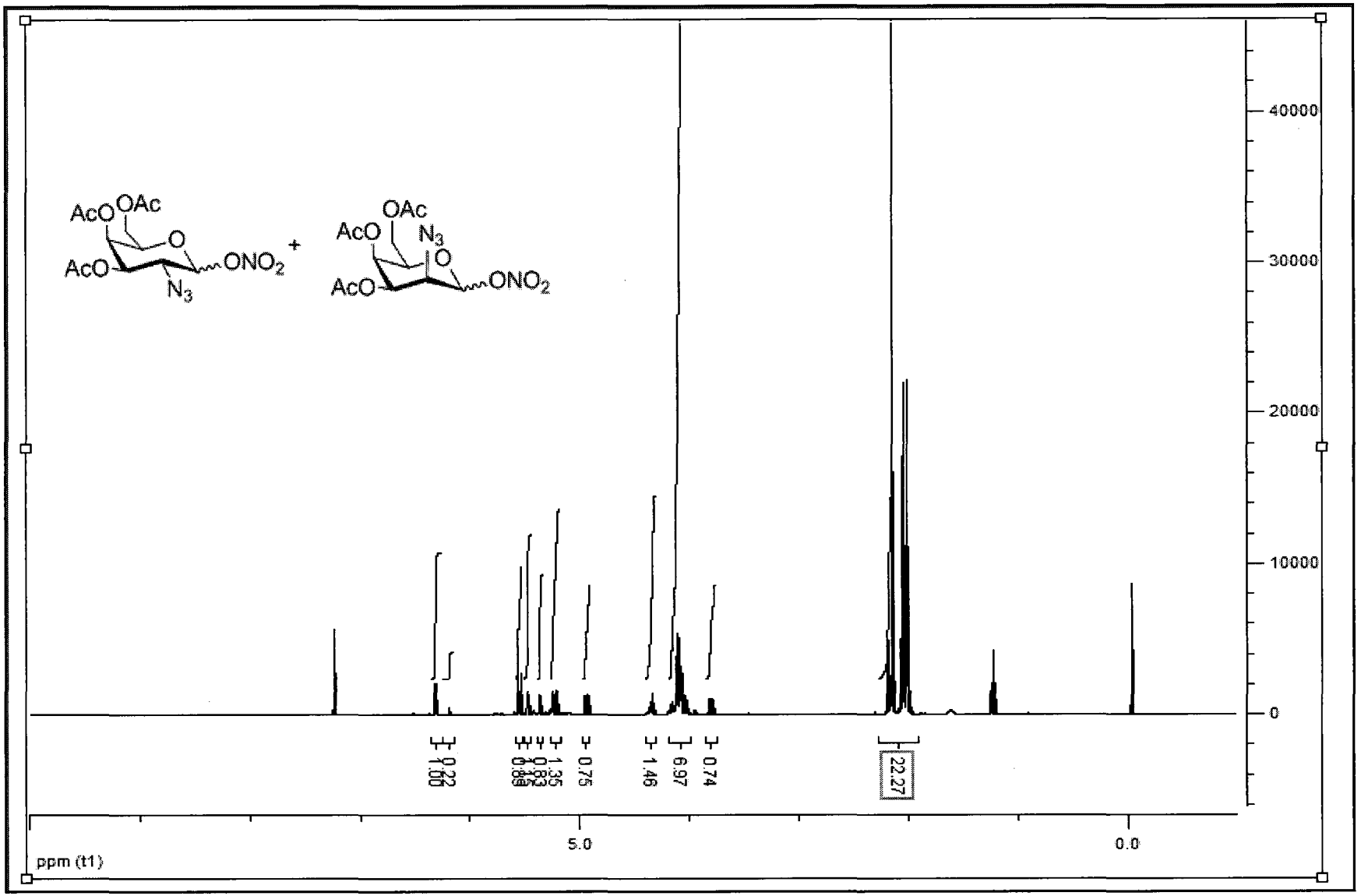
AcO
OAc
O
AcO
ONO2
N3
+
AcO
OAc
N3
O
AcO
ONO2
40000
30000
20000
10000
0
1.00
0.22
0.75
1.46
6.97
0.74
22.27
5.0
0.0
ppm (t1)

13.

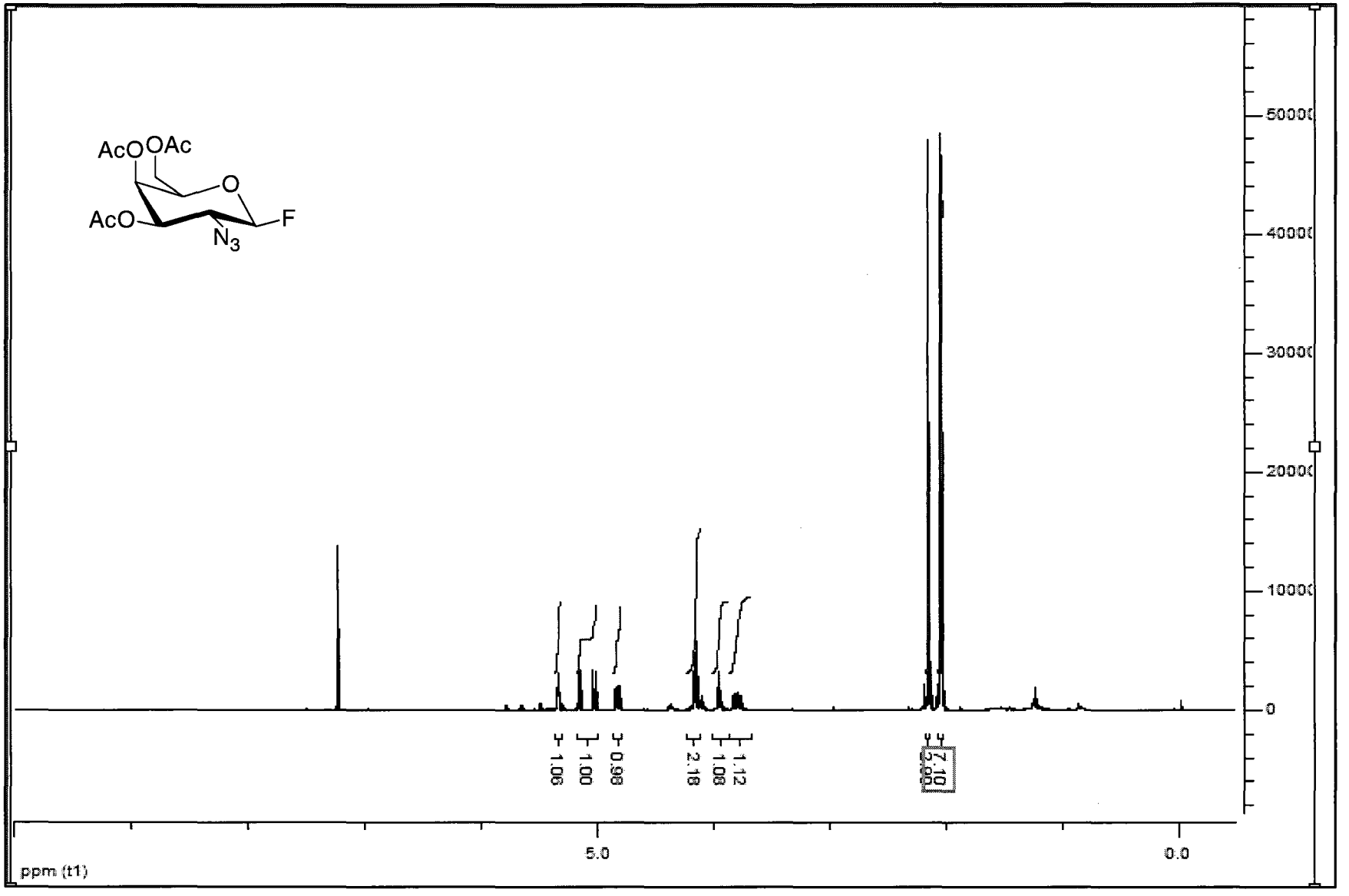
AcO
OAc
O
AcO
F
N3
50000
40000
30000
20000
10000
0
1.06
1.00
0.98
2.18
1.08
1.12
7.10
2.00
5.0
0.0
ppm (t1)

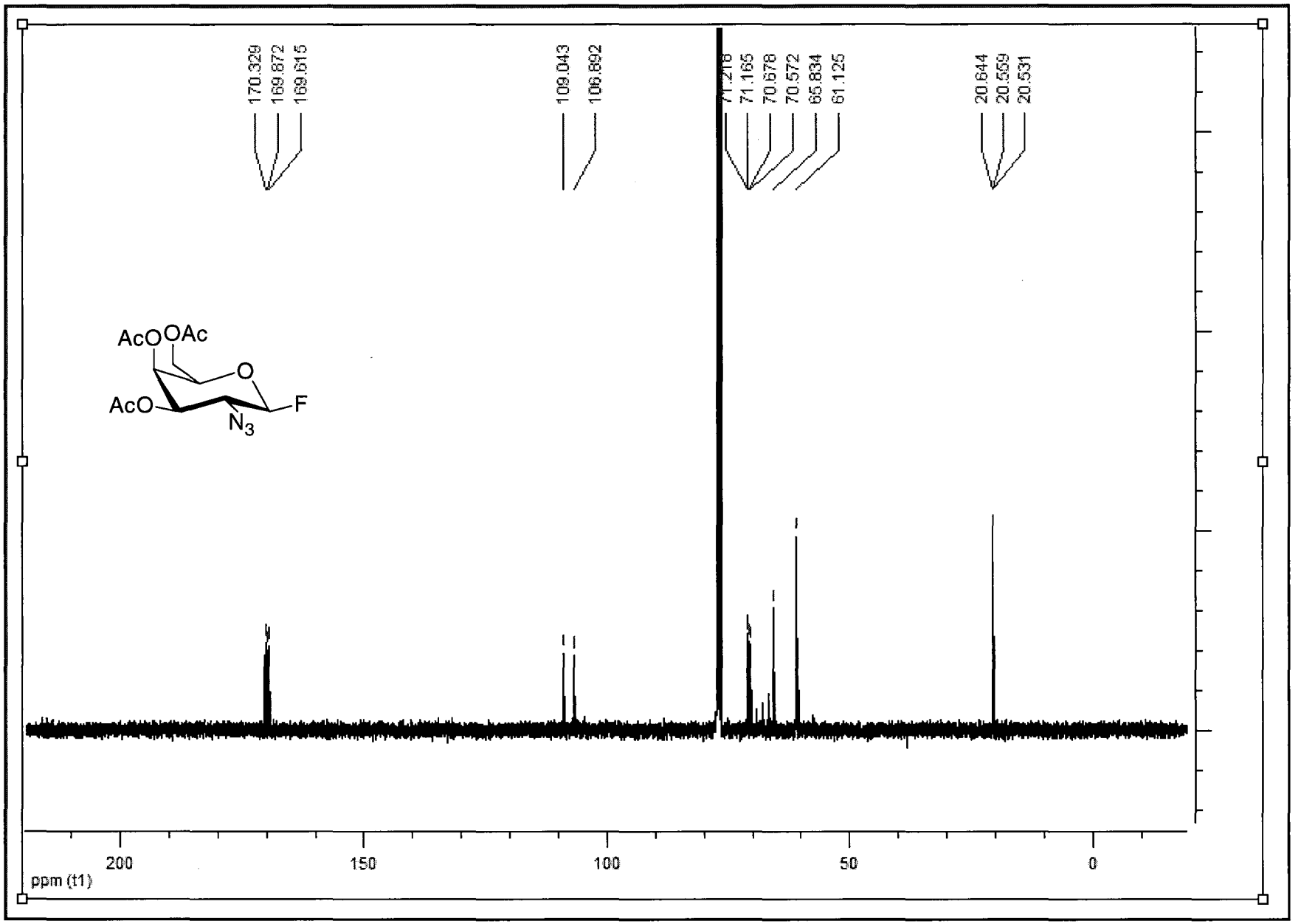
170.329
169.872
169.615
109.043
106.892
71.218
71.165
70.678
70.572
65.834
61.125
20.644
20.559
20.531
AcO
OAc
O
AcO
F
N3
200
150
100
50
0
ppm (t1)

14.

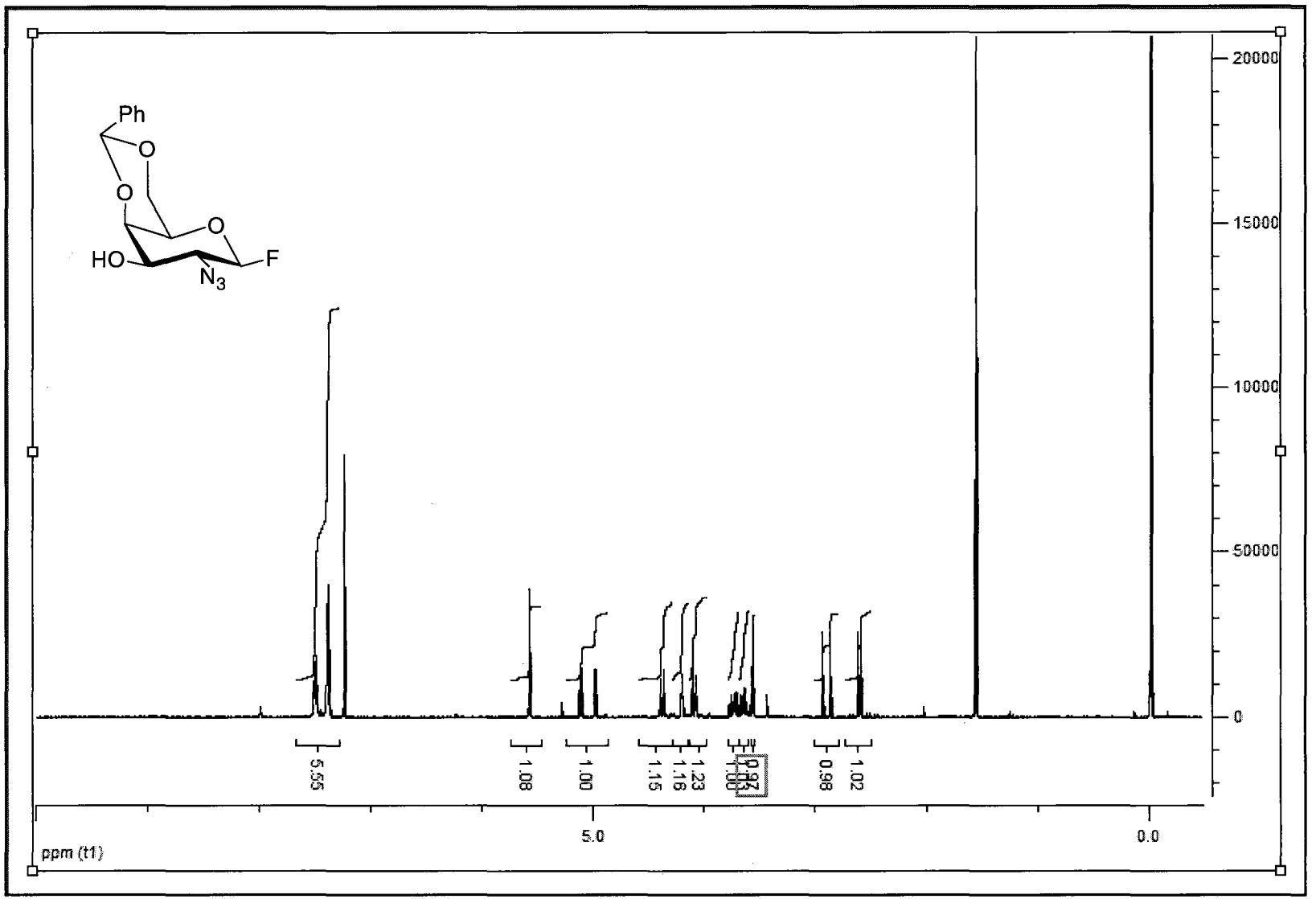
Ph
O
O
O
HO
F
N3
20000
15000
10000
50000
0
5.55
1.08
1.00
1.15
1.16
1.23
0.98
1.02
5.0
0.0
ppm (t1)

15.

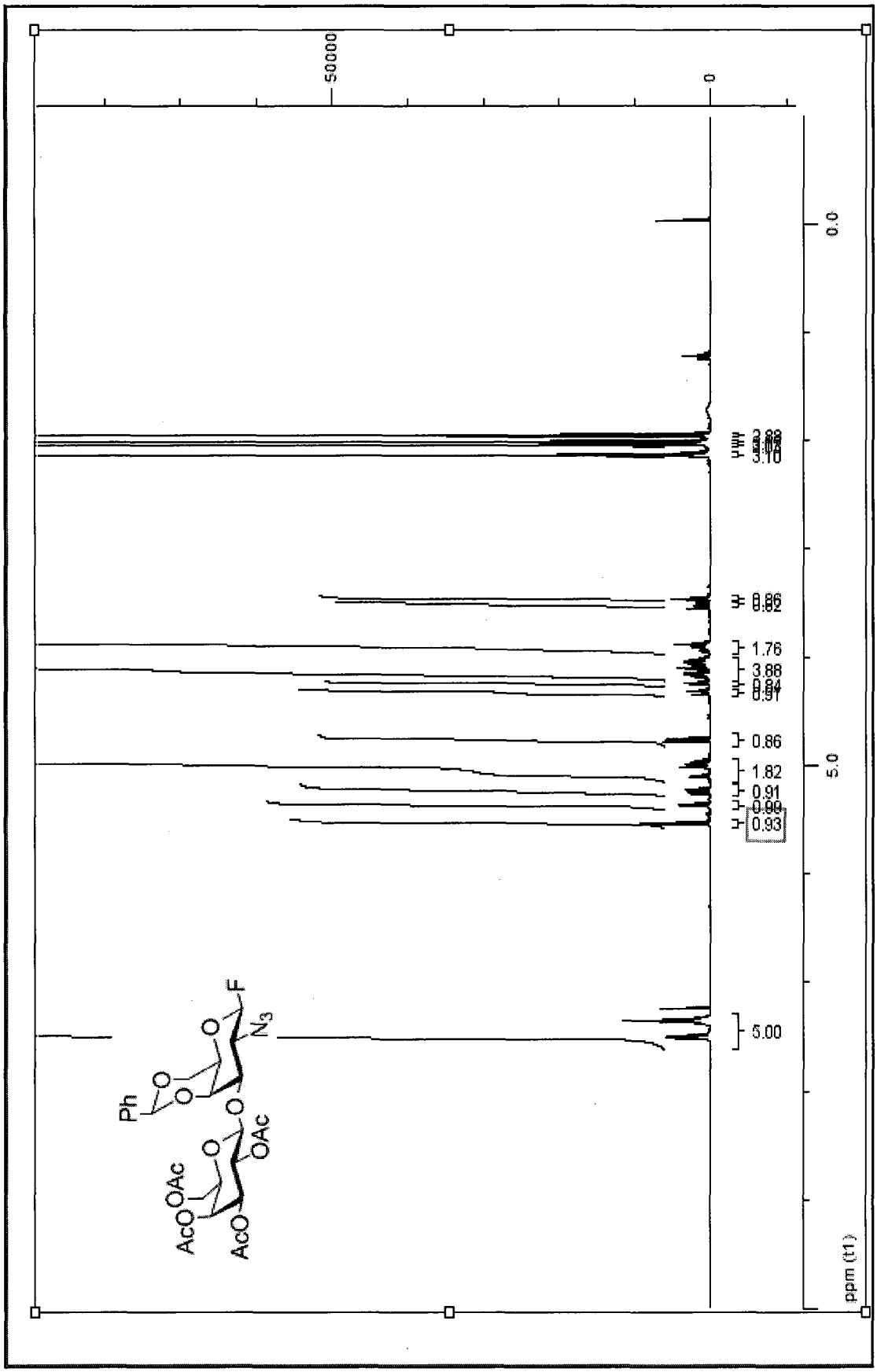
50000
0
0.0
5.0
ppm (t1)
5.00
0.93
1.82
0.86
1.76
3.10
F
N3
Ph
OAc
AcO
AcO
OAc

16.

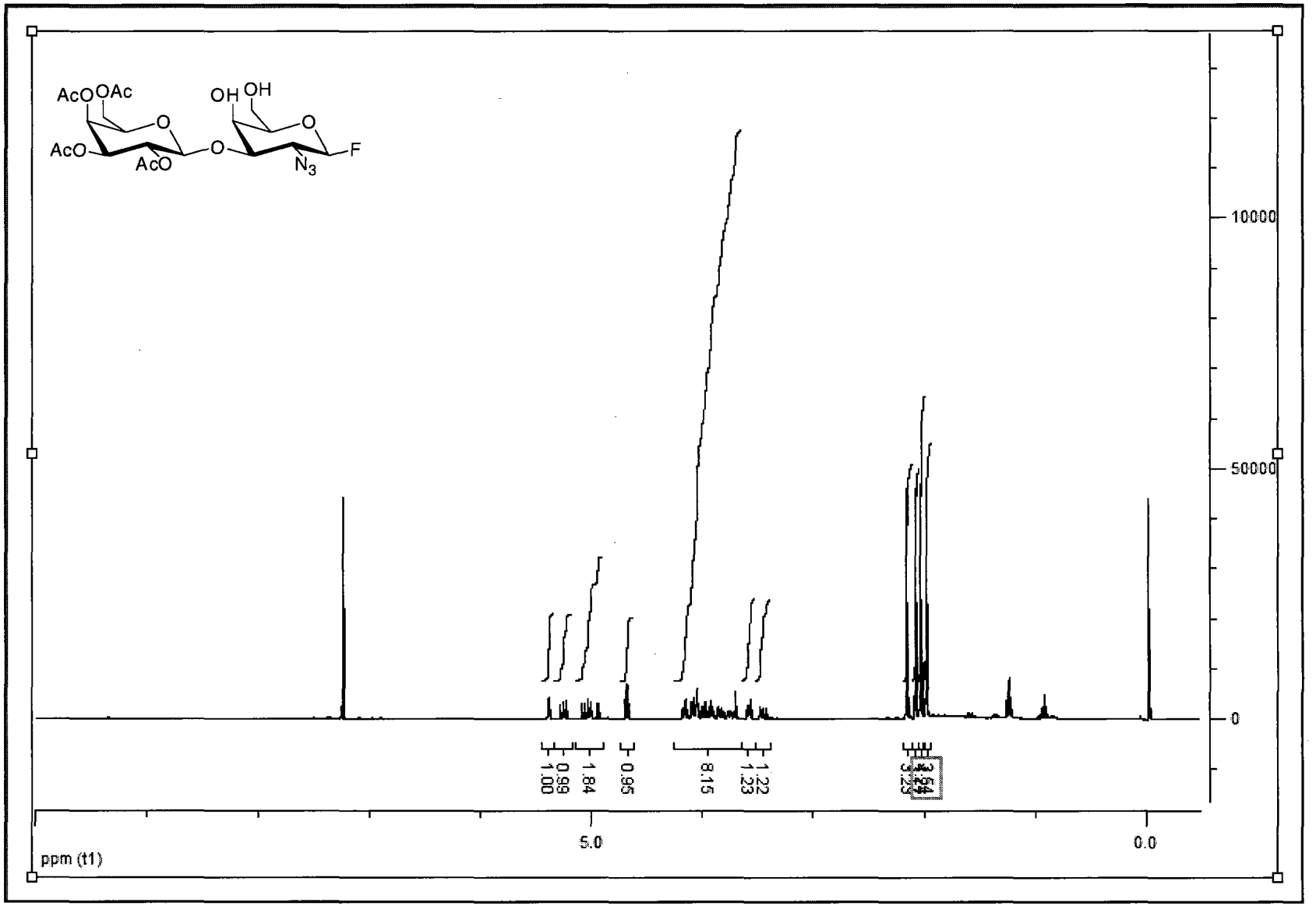
AcO
OAc
AcO
AcO
O
O
OH
OH
O
F
$N_3$
10000
50000
0
1.00
0.99
1.84
0.95
8.15
1.23
1.22
3.29
5.0
0.0
ppm (t1)

17.

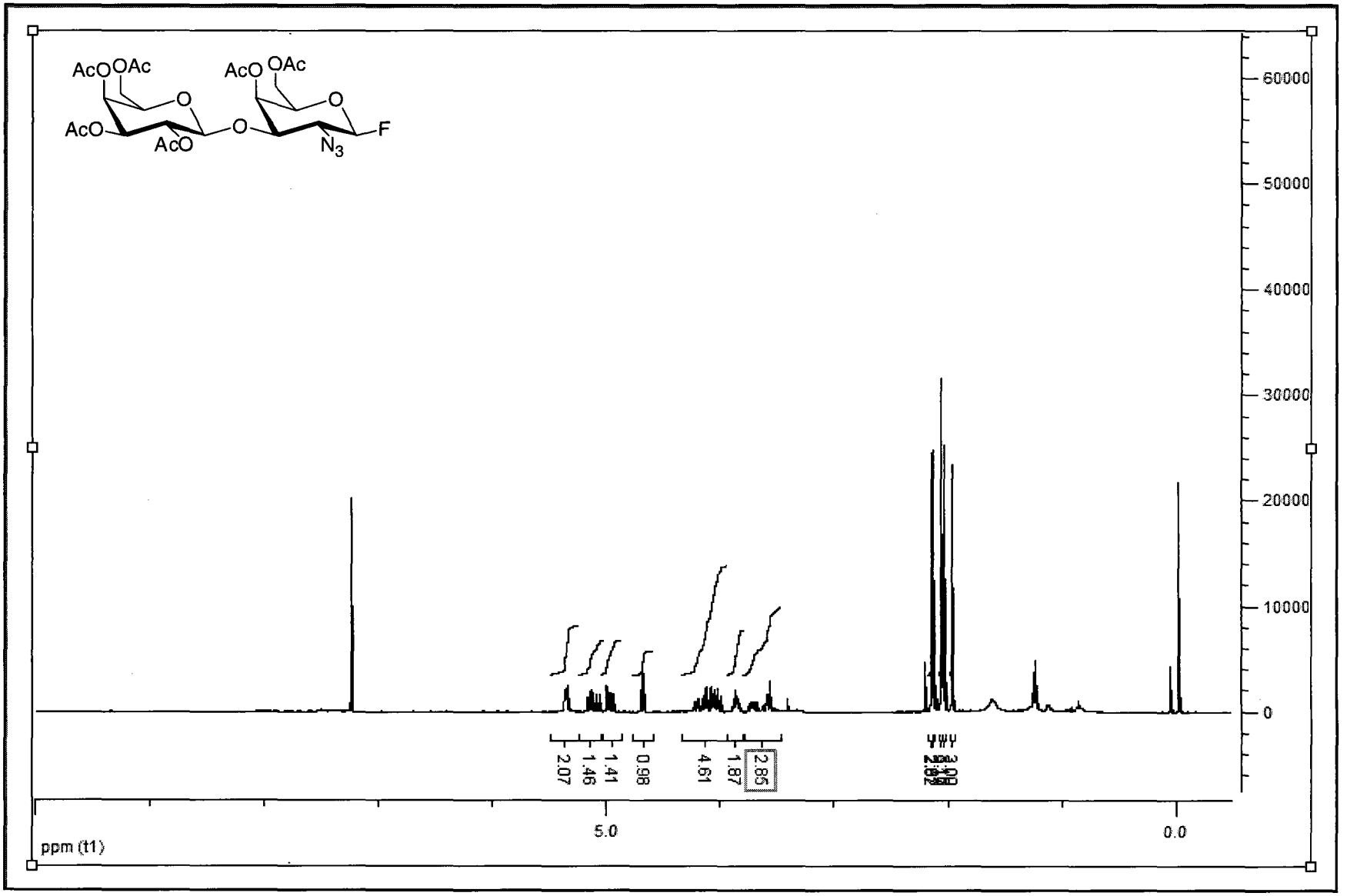
AcO
OAc
AcO
OAc
O
AcO
AcO
O
O
F
$N_3$
60000
50000
40000
30000
20000
10000
0
2.07
1.46
1.41
0.98
4.61
1.87
2.85
5.0
0.0
ppm (t1)